Development and Application of Emerging Engine Exhaust Aerosol Measurement Technologies

A DISSERTATION
SUBMITTED TO THE FACULTY OF THE GRADUATE SCHOOL
OF THE UNIVERSITY OF MINNESOTA
BY

Jacob John Swanson

IN PARTIAL FULFILLMENT OF THE REQUIREMENTS
FOR THE DEGREE OF
DOCTOR OF PHILOSOPHY

Dr. David B. Kittelson, Dr. David Y.H. Pui

August, 2010

Acknowledgements

Many individuals are deserving of my gratitude for their support of my work at the University of Minnesota. Foremost, I thank my advisors, Dr. David Kittelson and Dr. David Pui for allowing me the opportunity to research under their guidance. Their technical knowledge, innovative ideas, and continuous encouragement provided the framework necessary for this research to succeed. Dr. Winthrop Watts served as a mentor, editor and an additional source of perspective. A non-exhaustive list of undergraduate and graduate students who provided a professional and social environment to work in includes Anil Bika, Grace Chan, Aaron Collins, Luke Franklin, David Gladis, Zhun Liu, André Olson, Coty Jen, Adam Ragatz, Lei Tian, Matt Schumacher, Weon-Gyu Shin, Jing Wang, and Darrick Zarling.

Without the financial support of Donaldson Company, Inc., this research would not have been possible. I graciously thank Eivind Stenersen (formally of Donaldson Company) for initiating research at the University of Minnesota and for his many encouraging conversations along the way.

Additionally, the following centers and companies have supported my research.

- University of Minnesota Center for Filtration Research
- University of Minnesota Center for Diesel Research
- Johnson Matthey
- NIOSH

My Dad assisted throughout the process by reading initial drafts and commenting critically while always being supportive and I thank him sincerely.

Abstract

To force the development and use of the best available emission technologies needed to significantly reduce Diesel particulate matter (DPM) mass, the 2007 United States Environmental Protection Agency DPM standards for on-road trucks were reduced by 90% to 0.01 g/hp-hr. On-road Diesel engines manufactured after 2007 emit low levels of DPM. The gravimetric method used for certification differentiates between compliant and noncompliant engines at the 0.01 g/hp-hr level. At concentrations below ~10 $\mu g/m^3$ the method lacks sensitivity, making it difficult to evaluate alternative engine designs, emission control devices, alternative fuels, and modified lubricants that reduce DPM even further. Alternative methods and metrics like the particle size and number concentration measurements extend this lower limit of detection and may enable engine manufacturers and others to make better decisions on what future technologies are required for meeting a zero emission goal. The objectives of this research are to improve the understanding of variables like dilution and sampling conditions that contribute to particle-based emission measurements, to identify and improve current and emerging methods, and to use alternative methods to make measurements of engine exhaust to further elucidate the impact of fuels, emission control and engine state-of-maintenance on emissions. Additional background information is found in **Chapter 1.**

Chapter 2 is a synthesis and evaluation of ideas and perspectives that were presented at a series of workshops sponsored by the Coordinating Research Council that aimed to evaluate the current and future status of DPM measurement. Measurement of DPM is a complex issue with many stakeholders, including air quality management and enforcement agencies, engine manufacturers, health experts, and climatologists.

Adoption of the U.S. Environmental Protection Agency 2007 heavy-duty engine DPM standards posed a unique challenge to engine manufacturers. The new standards reduced DPM emissions to the point that improvements to the gravimetric method were required to increase the accuracy and the sensitivity of the measurement. Despite these improvements, the method still has shortcomings. The objectives of this chapter are to

review the physical and chemical properties of DPM that make gravimetric measurement difficult at very low concentrations and to review alternative metrics and methods that are potentially more accurate, sensitive, and specific. Particle volatility, size, surface area, and number metrics and methods to quantify them are considered. Although an alternative method is required to meet the needs of engine manufacturers, the methods reviewed are applicable to other areas where the gravimetric method detection limit is approached and greater accuracy and sensitivity are required. The review suggests that a method to measure active surface area, combined with a method to separate semi-volatile and solid fractions to further increase the specificity of the measurement, has potential for reducing the lower detection limit of DPM and enabling engine manufacturers to reduce DPM emissions in the future.

Chapter 3 improves the understanding of variables like dilution and sampling conditions that contribute to particle-based emission measurements by assessing and comparing the nucleation tendency of Diesel aerosols when diluted with a porous wall dilutor or an air ejector in a laboratory setting. A de facto standard air-ejector dilutor and typical dilution conditions were used to establish the baseline sensitivity to dilution conditions for the given engine operating condition. A porous tube dilutor was designed and special attention was given to integrating the dilutor with the exhaust pipe and residence time chamber. Results from this system were compared with the ejector dilutor. Exhaust aerosols were generated by a Deere 4045 Diesel engine running at low speed (1400 rpm) and low load (50 Nm, ~10% of rated). Primary dilution parameters that were varied included dilution air temperature (25 and 47 °C) and dilution ratio (5, 14, and 55). Particle measurements were made at 0.3, 0.75, and 1.0 s to evaluate particle growth in the residence time chamber.

Exhaust size distribution measurements made using the ejector dilutor were bimodal with high concentrations of nucleation mode particles. Varying the dilution ratio from 5 to 55:1 (with a dilution air temperature of 25 ºC and residence time of 1 s) caused the greatest change in the particle number concentration (4×10^8 to 4×10^{10} particles/cm^3)

compared to changes in the other variables. Particle concentration was lower with higher dilution air temperatures and particles were larger in size. Size distributions downstream of the porous tube and ejector dilutor were qualitatively similar in shape. Using a simple dilution model and equations for particle growth in the free molecular regime, particle growth in the two residence time chambers was compared. Model results suggest that dilution in the porous tube dilution system occurs more slowly than in the ejector dilutor. This is consistent with the findings that the particle number concentrations were consistently higher and the geometric mean diameter was generally 1 to 5 nm larger downstream of the porous tube dilutor.

Chapter 4 describes the comparison of two methods that are used to separate the solid and volatile components of an aerosol: the thermal denuder (TD) and catalytic stripper (CS). The TD and CS were challenged with atmospheric and laboratory generated aerosols. Laboratory generated particles were composed of tetracosane, tetracosane and sulfuric acid, and dioctyl sebacate and sulfuric acid. These compositions were chosen because they roughly simulate the composition of nanoparticles found in Diesel exhaust. The TD method produced semi-volatile particle artifacts due to the incomplete removal of evaporated compounds that nucleated and formed particles and solid particle artifacts that formed during treatment of the aerosol by the TD. Fundamental differences in the performance of the two methods lead to different conclusions regarding the presence or absence, size, and concentration of solid particles in Diesel exhaust.

In **Chapter 5** the physical and chemical nature of the engine exhaust from a Formula SAE spark ignition engine was evaluated using two competition fuels, 100 octane race fuel and E85. Three engine conditions were evaluated: 6000 RPM 75% throttle, 8000 RPM 50% throttle, and 8000 RPM 100% throttle. Diluted emissions were characterized using a Scanning Mobility Particle Sizer (SMPS) and a Condensation Particle Counter (CPC). E85 fuel produced more power and produced less particulate matter emissions at all test conditions, but more fuel was consumed.

Chapter 6 demonstrates how exhaust aerosol measurements can be used to diagnose an engine fault in a Diesel engine. A cyclic variation in total particle number concentration was observed while making routine exhaust emission measurements. Many dilution and engine operating conditions were examined and by sequentially shutting down individual cylinders the problem was traced to cylinder 2. The engine was disassembled and piston 2's oil control ring was found to be fractured. Replacement of the ring eliminated the particle concentration fluctuation. This chapter presents the results of experimental measurements made to determine the cause of the irregular emissions.

Chapter 7 describes the results of three experiments performed with Continuously Regenerating Traps (CRTs) in a controlled laboratory setting to elucidate the effects of fuel sulfur content, filter age, and storage and release effects on particle concentration. In the first experiment, a new CRT was evaluated using near zero sulfur Fischer Tropsch fuel and low sulfur lubricating oil (420 ppm). The objective was to measure particle emissions from an emission control device that had not previously been exposed to sulfur under a variety of operating and dilution conditions. Next, a used CRT was evaluated using the same fuel and lubricating oil. Finally, the used uncatalyzed Diesel particulate filter (DPF) from the used CRT was replaced with a new, uncatalyzed DPF. The emissions from the used Diesel oxidation catalyst (DOC) + new DPF configuration were evaluated and compared to those of the used CRT.

Results show that particle number emissions from the new CRTs are 99.9% lower than equivalent used CRT data collected on-road at an exhaust temperature of 370°C. Even as the new CRT temperature was increased to almost 400°C, emissions levels were still at background levels for roadway aerosol and no nucleation mode was observed. At an exhaust temperature of about 380°C, the nucleation mode particle number concentration increased sharply and remained high for the duration of the used CRT test. Mass emissions were estimated and found to exceed U.S. EPA on-road standards. The particle number concentration at the start of the used DOC + new DPF evaluation was equal to that measured at the end of the used CRT experiment, suggesting that only sulfates

released from the DOC and not the uncatalyzed DPF significantly contribute to nanoparticle formation.

Contents of this thesis have been or will be published in the following peer-reviewed journals. Reprint copyright permissions are found in Appendix A.

Chapter 2: *Swanson, J.*, Kittelson, D., Pui, D., Watts, W. "Alternatives to the Gravimetric Method for Quantification of Diesel Particulate Matter Near the Lower Level Of Detection." In press, *J. Air Waste Management Association*, 2010.

Chapter 3: *Swanson, J.*, Watts, W., Kittelson, D. "Diesel Exhaust Aerosol Measurements Using Air-Ejector and Porous Wall Dilution Techniques." *SAE Tech. Pap. Ser.* 111PFL-0658.

Chapter 4: *Swanson, J.*, Kittelson, D. "Evaluation of Thermal Denuder and Catalytic Stripper Methods for Solid Particle Measurements." In review, *J. Aerosol Science*, 2010.

Chapter 5: Ragatz, A., *Swanson, J.*, Watts, W., Kittelson, D. "Particle and Gaseous Emissions Characteristics of a Formula SAE Race Car Engine." *SAE Tech. Pap. Ser.* 2009, 2009-01-1400.

Chapter 6: *Swanson, J.*, Ragatz, A., Kittelson, D., Watts, W., Winsor, R. "Nanoparticle Measurements Used to Detect an Engine Fault." *Proc. IMechE Part D: J. Automotive Engineering*, 2009, 8, 1071 – 1076.

Chapter 7: *Swanson, J.*, Kittelson, D., Watts, W., Gladis, D., Twigg, M. "Influence of Storage and Release on Particle Emissions from New and Used CRTs." *Atmospheric Environment*, 2009, 43, 3998 – 4004.

Table of Contents

List of Tables

List of Figures

Chapter 1: Introduction

Background

Diesel emission standards

Recent changes to the heavy-duty Diesel emissions standards are shown in Table 1 (40 CFR 86, EU Commission regulation 851). For comparison, EU standards are also shown. Emission reductions reflect the growing concern and understanding that DPM, NOx, and HC emissions reduce air quality. The particle number standard will be discussed in more detail in a subsequent section.

Table 1: U.S. and European Union emission standards for heavy duty Diesel engines

Standards (mg/kWh)	U.S.			European Union
	1998	2007/2010	% Reduction	Euro V 2008
Particulate matter	134	13	90	20
Oxides of nitrogen	5364	268	95	2000
Hydrocarbons	1743	188	89	460
Solid particle number	-	-	-	6×10^{11}/km*

*The particle number standard is designated Euro 5.5 and takes effect after the Euro 5 phase-in,, 2011 and is initially applied to passenger and light duty commercial vehicles.

The following section describes the properties of Diesel particulate matter. DPM standards are based on studies that link particulate matter with adverse health effects. These links are discussed in the health effects section. Methods used to measure particle size, concentration, and composition are discussed next. Fuel and emission control technology used to meet the current DPM standard and their impact on particle properties are described. Chapter 1 ends with a description of the organization of the body chapters and the motivation and significance of this thesis.

Diesel particulate matter

Diesel exhaust contains a complex mixture of particles and gases that are regulated by current DPM, HC, and NOx emission standards. Gaseous emissions such as hydrocarbons, oxides of nitrogen, and carbon dioxide (CO_2) are characterized by their concentration and composition. HCs form from incomplete combustion and range in volatilities. Consequently, they may be found in the vapor (Siegl et al. 1999, Schauer at al., 1999, Schmitz et al., 2000, Zielinska et al., 2004) or in the particulate phase (Schauer at al., 1999, Tobias et al., 2001, Sakurai et al., 2003, Ristimäki et al., 2007). Figure 1 (Kittelson, 1998, Whitby et al., 1972) shows an idealized engine-out lognormal, trimodal Diesel aerosol particle size distribution consisting of nucleation, accumulation, and coarse modes. The boundaries of these modes are not rigid but depend considerably on sampling conditions, engine operating conditions, and emission control devices. Nevertheless, these modes possess physical and chemical characteristics that allow them to be distinctly separated.

Coarse mode particles are typically crankcase fumes or reentrained agglomerates, and typically contain less than 1% of the number and 5-20% of the mass.

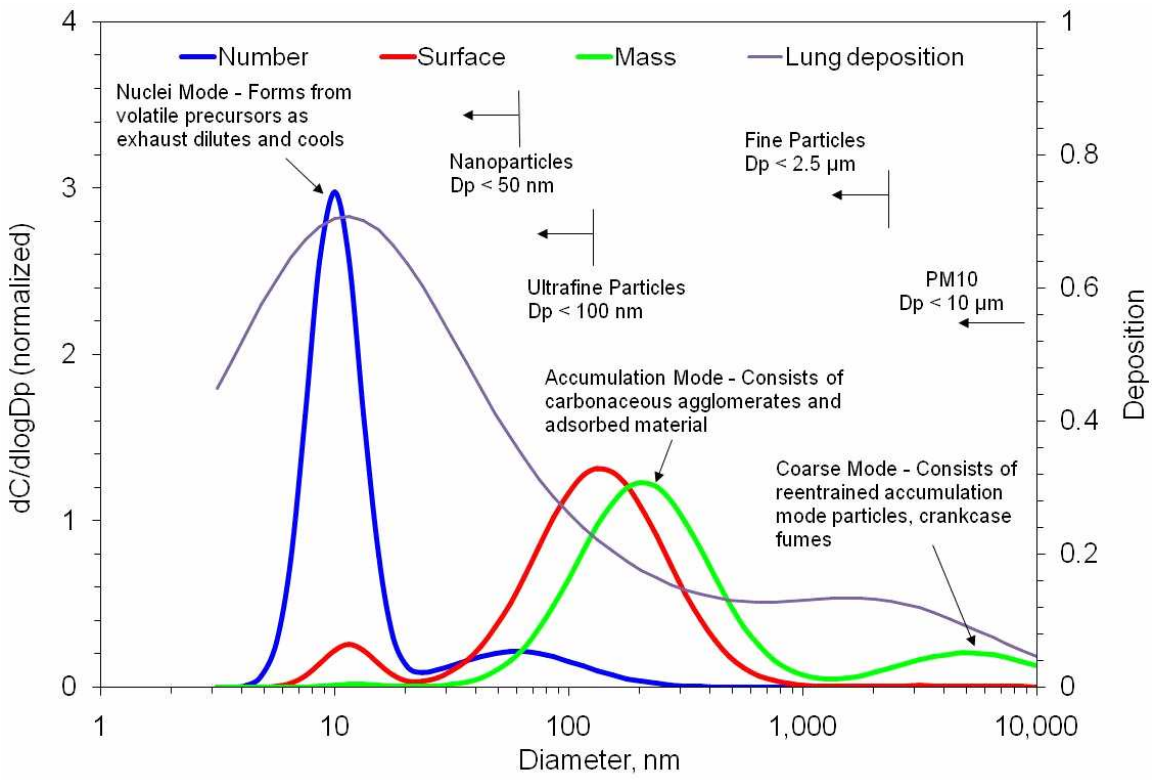

Figure 1. Typical Diesel engine exhaust particle size distribution (as modified by Kittelson, 1998, adapted from Whitby et al., 1972) and corresponding lung deposition curve.

Nucleation mode particles are primarily volatile and consist of HC or sulfur compounds that condense to the particle phase as their temperature decreases following release from the combustion process, cooling, and dilution with ambient air. The formation and growth of nucleation mode particles depends on the rates of nucleation, condensation, and adsorption, which are nonlinear functions of the saturation ratio (Friedlander, 2000). In a modern, low emissions engine there is little carbonaceous surface area available to adsorb or condense vapors, making nucleation more likely (McMurry and Friendlander, 1979, Bagley et al., 1996, Johnson et al., 1996, Kittelson et al., 2006). A small fraction of the sulfur in the fuel is oxidized to sulfate (SO_3) that leads to sulfuric acid and sulfate particles (Laresgoiti et al., 1977, Truex, 1980, Schneider et al., 2005). Some nucleation mode particles contain solid ash from lube oil or wear metals (Kittelson et al., 1978,

Abdul-Khalek et al., 1998, Lee et al., 2006). Typically, 85% of the number and 0.1-10% of the (engine out) DPM mass are found in the nucleation mode.

Accumulation mode particles are composed primarily of carbon agglomerates. Soot primarily results from incomplete combustion which generally occurs when the fuel/air ratio is greater than stoichiometric in some regions of the combustion chamber, thus preventing or inhibiting complete combustion. Tiny unburned HC platelets nucleate in this fuel-rich region to form small crystal-like structures that coagulate and grow by condensation to form carbon spheres inside the cylinder (Smith, 1981). While still inside the cylinder and during their release from the cylinder into the exhaust stream, the spheres agglomerate into chain-like structures that collide to form dendrite-like structures (fractal dimension ~2.3). Some nucleation mode particles are found attached to accumulation mode particles due to the high coagulation coefficient between dissimilarly sized particles. In addition, HC vapors and sulfur compounds condense onto or adsorb to accumulation mode particles and thus contribute to the size and mass of accumulation mode particles. The total mass of organic particulate is called the soluble organic fraction (SOF) and it is primarily found bound to accumulation mode particles (rather than in the nucleation mode). Approximately 15% of the number and 80% to 90% of the total DPM mass is typically contained in the accumulation mode.

The typical time-scales, temperatures, pressures, and dilution ratios (DR) associated with the formation of solid and volatile particles are shown in detail in Figure 2. Figure 2 indicates that while soot particles are formed in the combustion chamber, volatile particles are formed after the pressure and temperature has decreased to roughly ambient values and the exhaust has been diluted by 10:1. Filter samples for 2007 DPM measurements and particle number-based measurements are typically taken or made after ~10:1 dilution and after ~1 second of aging. In both cases, the exhaust is sampled during its physical and chemical transition between two very different states. The specifics of

this transition affect the composition and concentration of the particulate matter in the exhaust and difficulty of sampling in the middle of the particle's lifetimes is an important theme that is addressed continuously throughout this work.

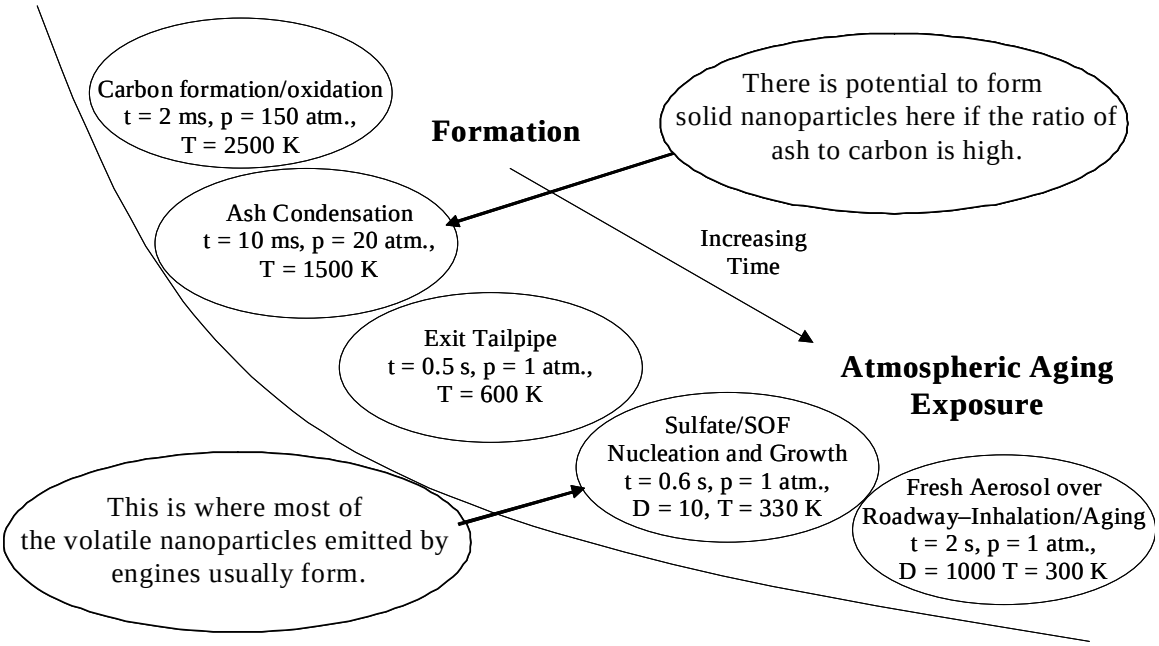

Figure 2. Particle formation history—most nanoparticles form during dilution (Kittelson et al., 2006a)

Health effects

Inhalation of DPM emitted by Diesel engines is associated with acute and chronic health effects in humans (Seaton et al., 1995, Seaton et al., 1996, Liao et al, 1999, Gold et al., 2000, Samet et al., 2000, Peters et al., 2001). The causal mechanisms that lead to adverse responses are largely undefined. Traditional exposure assessment of Diesel combustion aerosols has been based on the measurement of mass concentration. However, adverse health effects have been correlated with particle number, surface area, and particle toxicity. If the recipient is either young, old, or otherwise immunity compromised, the

response to particulate matter may be worse (Pekkanen et al., 1997, Penttinen et al., 2001).

It is the responsibility of EPA to identify pollutants, in this case, particulate matter, that "may reasonably be anticipated to endanger public health and welfare" and to issue criteria for air quality that, "allowing an adequate margin of safety, are requisite to protect the public health." This directive was given to the EPA in 1963 as part of the Clean Air Act (sec. 202a) because of the increasing evidence that particulate matter was harmful. EPA set ambient air particulate matter standards that resulted in a decrease in PM_{10} throughout the United States over the next thirty years. In the late 1990's, in response in part to a growing body of evidence that particles smaller than 2.5 µm in diameter rather than larger particles are more responsible for adverse health effects (Dockery et al., 1993, Pope et al., 1995), the EPA promulgated 24-hour and annual standards for $PM_{2.5}$.

Engine exhaust particulate matter standards for on-road Diesel engines were enacted in 1988. Initially, all sized particles were measured and counted towards the standard. The 2007 Diesel standard regulates all particles that pass through a cyclone or impactor with a 2.5 µm cutpoint. Roughly 99% of particles smaller than 1.0 µm ($PM_{1.0}$) are counted by this approach. The direction of both ambient air quality improvement and Diesel emission reduction trends is to regulate smaller and smaller particles as more is learned about how they affect human heath and the instruments used to measure them improve.

The technology used to measure particulate matter has improved in sensitivity and specificity within the past fifteen years. These advances have allowed researchers to more acutely identify the properties of particulate matter that are responsible for adverse health effects. Recent studies have observed that ultrafine particles (diameter <100 nm) cause adverse health effects similar to $PM_{2.5}$-like particles (Pekkanen et al, 1997, Ibald-Mulli et

al., 2002, Pekkanen et al., 2002). Ultrafine particles efficiently deposited deeply in the alveolar region of the lung (Figure 1) where they cause acute inflammatory reactions because the tissue in this region is not naturally protected. Ultrafine particles deposited in large numbers can be translocated to organs such as the liver, heart, or brain (Oberdörster et al., 2001). Ultrafine particles exhibit higher surface free radical activity than PM_{10}-sized particles (Donaldson et al., 1996). Peters et al. (1997) and Penttinen et al. (2001) showed that when subjects receive mass-equivalent doses of fine and ultrafine particles, the recipients of the ultrafine particles faired much worse. However, the results are not entirely one sided. Osunsanya et al. (2001) concluded that PM_{10} is at least as correlated with health effects as are ultrafine particles. De Hartog et al. (2003) found $PM_{2.5}$ to be more related to cardiorespiratory symptoms than were ultrafine particles.

Particle number, surface area, and mass concentration, particle composition, and crystalline structure are likely confounded variables in many of these studies and some do a better job that others distinguishing between their effects. For example, Oberdörster et al. (2005) reviewed evidence that the surface area of TiO_2 particles, rather than their mass or number concentration, best correlates with adverse biological response in rats. Wittmaack (2007) later argued Oberdörster et al.'s data shows particle number concentration is the best metric.

Simply, there is no consensus amongst experts as to the best metric to measure or regulate exposure to particulate matter but the preponderance of the evidence suggests mass concentration standards alone cannot accurately reflect the full complexity of DPM exposure. However, Diesel particulate matter standards will be mass-based environmental standards until evidence conclusively shows this metric is inappropriate, a better metric and measurement methodology is established, and the Clean Air Act is revised. The Advanced Collaborative Emission Study or ACES (French, 2004) is

currently evaluating the health effects of emissions from a 2007 compliant engine. The results of this study may provide direction for future emission regulations.

Particle measurement methods

Different sampling systems and methods are used to measure particulate matter emitted by Diesel engines. A method is typically specific to why and what is being measured. A method optimized for mass measurement is not necessarily appropriate to measure particle number concentration and often metrics do not often correlate (Mayer et al., 1998, Hall et al., 2001). Vouitsis et al. (2003) reviewed many sampling methods, including those intended for measuring regulated and non-regulated emissions from low-emitting Diesel engines. Burtscher (2005) and Mohr (2005) reviewed many instruments and measurement principles with a focus on non-mass based measurements. All authors concluded that many instruments are available that provide quantitative measurements of DPM, although not one method/instrument combination is satisfactorily without issue.

In this section, three mainstream experimental methods are compared: U.S. particulate matter mass measurement (40 CFR 86), European Union solid particle number measurement (Andersson et al., 2004) and a method of particle size and number measurement using a two-state micro dilution tunnel, fully described by Khalek et al. (1999), that is similar to the system evaluated in Chapter 3 and used throughout this thesis. The advantages and limitations of each are described. Figure 3 schematically compares these measurements.

The gravimetric method used to determine compliance with the engine emission DPM standard is specified by EPA. This method was first specified when engine exhaust contained > 50 times more DPM than is found in current technology engines but has since been improved only incrementally. During an emission measurement, all of the vehicle’s exhaust is routed into a large stainless steel dilution tunnel where it is mixed

with filtered, ambient air while the engine performs a driving cycle called the Federal Test Procedure (FTP). The chemical composition and concentration of exhaust pollutants are functions of the engine speed and load (Heywood, 1988). The concentration and composition of the exhaust is a rapidly varying function of time during the FTP cycle, characterized by high temperature segments of soot and sulfate emissions and low temperature segments of semi-volatile hydrocarbon emissions. The exhaust + dilution flowrate is kept constant and is termed constant volume sampling (CVS). The exhaust must be diluted enough so that the temperature of the exhaust and dilution air mixture is less than 191°C. A consequence of this method is that the dilution ratio varies with engine speed and load in a manner that does not simulate atmospheric dilution. Regardless, from this "full flow" dilution, a small sample is taken, in proportion to the total flow, and diluted again in the secondary dilution tunnel. This dilution must further cool the exhaust mixture to 47 ± 5°C. Particles in the dilute mixture must pass through a cyclone or impactor with a 2.5 µm cutpoint. Roughly 99% of particles smaller than 1.0 µm ($PM_{1.0}$) are counted by this approach. The exhaust is then filtered through a pre-weighed 47 mm filter and DPM collects on the filter. After conditioning in a temperature and humidity controlled weighing room, the filter is weighed to determine the mass gained. This process provides a definition of DPM: the mass of 47°C Diesel exhaust collected on filter during a specified driving cycle. For very low emitting engines, roughly 10% or less of the collected mass is suspended particulate matter and 90% is adsorbed hydrocarbon vapor (Khalek, 2005, 2006, 2007). The method lacks reproducibility due to imprecisely defined sampling conditions (Swanson and Kittelson, 2009a) although it adequately differentiates between compliant and noncompliant engines.

The U.S. and EU mass measurement methods are similar. In addition to the EU PM mass standard, a particle number standard is enforced for EURO VI vehicles. The method was developed by the Particulate Measurement Programme (PMP). Similar to the mass

measurement, all exhaust is diluted in a CVS tunnel. A small fraction of exhaust is taken from the tunnel; the sample is diluted and passed through a heated tube in which semi-volatile compounds evaporate called a volatile particle remover (VPR). The particles exit the VPR; are diluted again so that the total concentration is $<10^4$ part/cm^3; and a condensation particle counter counts remaining solid particles sized between 23 and 1000 nm in diameter. This method precisely measures the concentration of suspended particles - condensation particle counting is accurate and fundamental (Agarwal et al., 1980). A potential challenge in the solid particle measurement is in controlling the coagulation of the aerosol. The mass concentration is conserved in a coagulating aerosol but the particle number concentration is not. However, coagulation negligibly changes the total number concentration when the concentration is $<10^4$ particles/cm^3 and the time scale is seconds (Hinds, 1999).

In the method descibed by Khalek et al. (1999) only a small fraction of the total exhaust flow is diluted. The dilute exhaust flows through an aging chamber where particles nucleate and grow before being diluted again to reduce number concentration and to quench growth processes. Particle sizing and counting instruments measure the size distribution of particles based on characteristic diameters. Surface area and mass distributions and total concentrations can be estimated from the size distributions. The typical particle size range is 5 to 500 nm. This method differs from the EU particle number method in that only a fraction of exhaust is diluted and the sample is not typically proportional to the exhaust flow, semi-volatile particles are considered, and particles are sized in addition to being counted. Because the formation of semi-volatile particles strongly depends on the sampling conditions, results from this method depend on many variables and the result can be tuned to more or less particle formation or for larger or smaller particles.

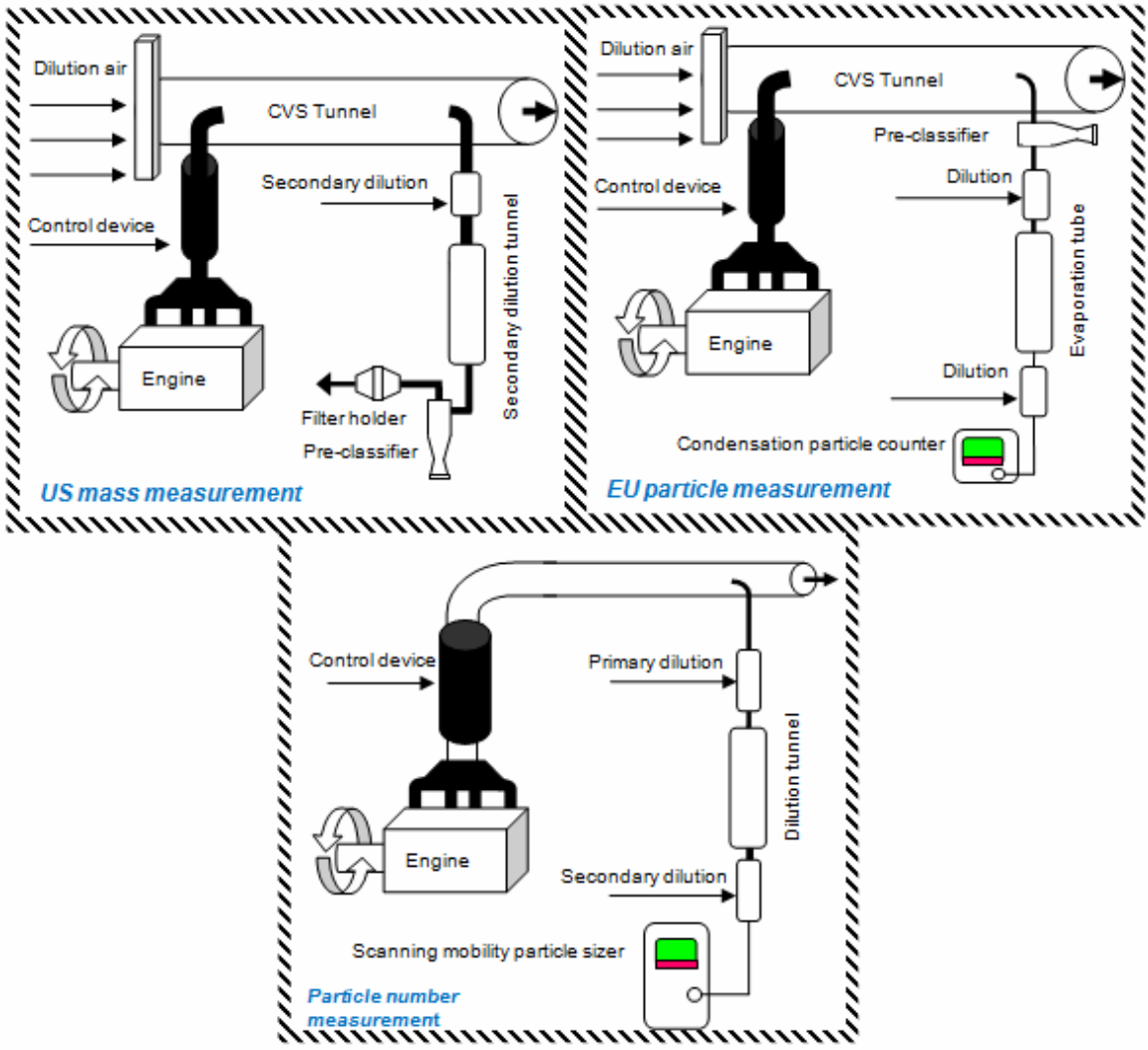

Figure 3. A comparison between methods used to measure Diesel particulate matter. (Top left) The United State's mass measurement protocol—all engine exhaust is diluted in tunnel, a small fraction is diluted again and a 1.5 m^3 sample is taken for gravimetric analysis. (Top right) The European Union's particle number measurement—exhaust is diluted similarly to the U.S. mass measurement but the sample is heated in evaporation tube to remove volatile compounds. The exhaust is diluted again to reduce number concentration to $<10^4$ part/cm^3. A condensation particle counter counts remaining non-volatile particles sized between 23 and 1000 nm. (Bottom) The proposed particle measurement setup—only a small fraction of exhaust is diluted. Particles nucleate and grow in the aging chamber before being diluted again to quench the growth processes

Emission control strategies

Figure 1 illustrates that typically 90% of DPM mass in raw exhaust is found in the accumulation mode. Reducing the majority of soot particles that comprise this mode is required to meet the current DPM standard and many reduction strategies exist. The strategy may reduce DPM emissions by preventing soot formation in the combustion chamber or by eliminating the soot post-combustion or both. Methods to reduce soot formation include modifying the combustion chamber geometry (Hill et al., 2007), increasing the fuel injection pressure, timing, or number of injections (Morgan et al., 2003), using alternative fuels like biodiesel (EPA, 2002, 2006), and turbocharging and intercooling (Heywood, 1988). Eliminating soot post combustion can be accomplished through cyclonic separation (Leonhard and Projahn, 1991), electrostatic precipitation (Ludecke and Dimick, 1983, Kittelson et al., 1986), and flow-through thermal and/or catalytic oxidation systems (van Setten et al., 2001). All are proven methods to reduce soot, but they alone cannot typically reduce soot to 2007 levels; thus, engine manufacturers rely on Diesel particulate filters (DPF) to meet the standard.

Wall-flow Diesel particulate filters (DPF) are used by every major U.S. heavy-duty Diesel engine manufacturer to reduce the soot emissions of 2007 U.S. engines (Johnson, 2008). The basic geometry of a DPF is seen in Figure 4. Exhaust flows through a core of alternatively plugged channels, with the soot being captured on the channel walls and clean exhaust passing through. The soot capture efficiency depends, among other things, on particle size (Mayer et al., 1996). The captured soot must be removed to prevent excessive engine backpressure. Bulk soot removal events are termed “filter regenerations,” and are accomplished without removing the DPF from the vehicle through oxidation.

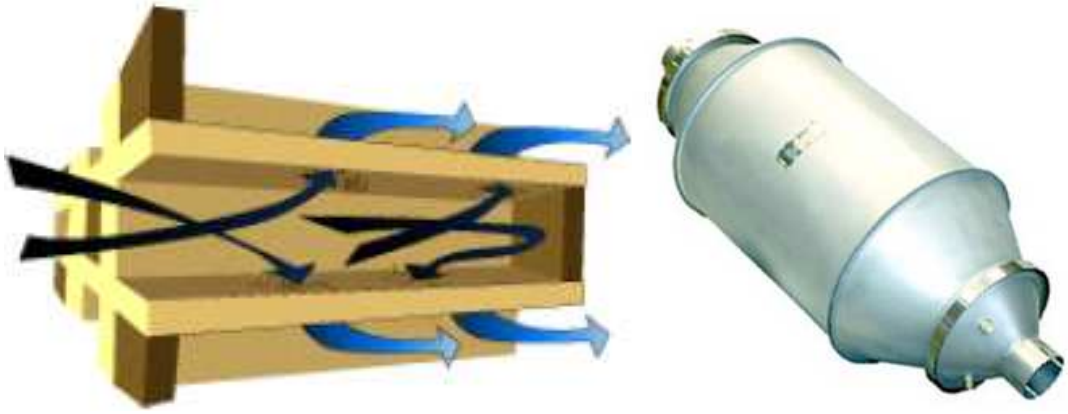

Figure 4. Inside and outside views of a wall-flow Diesel particulate filter. The brown squares represent solid, impermeable surfaces, while the tan channels areas are permeable to gas molecules (airflow), but not to solid carbonaceous particles

Many DPF regeneration techniques have been investigated. “Active” methods use some type of control to start (and sometimes stop) the regeneration process by increasing the temperature in the DPF. Some of these methods include electrically heating the filter (Hüthwohl et al., 1987), injecting extra gaseous hydrocarbons in the cylinder (during the exhaust stroke) or in the exhaust upstream of the filter (Rao et al., 1985), and by manually increasing the load or speed or by throttling the intake to increase the exhaust temperature (Salvat et al., 2000). Van Setten et al. (2001) reviewed additional methods. Hydrocarbon injection is the most used active method in on-road vehicle applications.

The effect of adding unburned hydrocarbons to the exhaust stream is to increase the temperature of the exhaust downstream of the oxidation catalyst due to the heat of oxidation of the fuel. The increased temperature allows the oxidation of soot that is trapped on the filter. Salvat et al. (2000) explained how active systems are integrated into passenger cars and their effect on regulated emissions (large reductions) and fuel consumption (~5% increase). Hiranuma et al. (2003) showed that closed-loop temperature feedback controls improved the reliability of this process. Joshi et al. (2006) found that optimum regeneration times are 10 min where ~30 g of soot is burned. For

example, a fully loaded semi truck cruising at 100 kph (100 kW) and emitting PM (engine-out) at 0.067 g/kWh would require 10 min filter regenerations every 4 hr. Carefully controlling the length and amount of regeneration is necessary to prevent excessive heat release that leads to thermal stresses in the filter and ultimately, its destruction.

A “passive” system is designed so that regeneration occurs without any outside intervention, thus eliminating the controls and complexity found in active systems. The most common passive system exploits the fact that soot oxidation in the presence of nitrogen dioxide (NO_2) occurs at a much lower temperature than it does in the presence of O_2 (Cooper and Thoss, 1989). The NO produced during combustion is oxidized to NO_2 and a DPF is placed downstream of the NO_2 production site, allowing the NO_2 to contact the soot. As a result, the self-regeneration oxidation temperature is decreased to ~250°C (compared to ~550°C), which is closer to the typical operating exhaust temperature of many Diesel vehicles. These systems require a NOx/PM ratio of ~25 to combust all soot. The Johnson Matthey Continuously Regenerating Trap (CRT^{TM}) is a commercial product utilizing this technology.

The average life of a heavy-duty Diesel engine is ~1,600,000 km (1,000,000 mi) or 15 – 20 yr (Mayer et al., 2008) so there is sufficient motivation to equip old polluting vehicles with technology enabling them to comply with current standards, termed “retrofitting.” Either active or passive filtration systems can be used to retrofit. Retrofit PM systems are verified by the CARB for use in the *Diesel Risk Reduction Program* and are typically classified as Level 3 devices that remove 85% or more Diesel particulate matter when engine out emissions are less than 0.134 g/kWh.

Fuel composition

Current United States' on-road, ultra-low sulfur Diesel fuel is a fractional distillate of crude oil containing less than 15 ppm sulfur that has a volumetric energy density of 38 MJ/l. Diesel fuel contains many differently sized molecules (roughly 70% alkanes and 30% aromatic compounds) with $C_{16}H_{28}$ representing the average molecule (Heywood, 1988). The maximum permissible sulfur content in Diesel fuel was reduced from 500 to 15 ppm in 2006. This reduction enables the use of catalyzed particle filters and NOx control devices (discussed previously) and reduces particulate sulfate emissions (Wall et al., 1987, Allansson et al., 2002, Bardasz et al., 2004).

Recent efforts have been made to replace traditional Diesel fuel (a fossil fuel) with alternative renewable fuels like biodiesel to reduce greenhouse gas emissions and to reduce reliance on petroleum based fuels (Knothe et al., 2006, Tilman et al., 2006). Biodiesel is composed of mono-alkyl esters of long chain fatty acids derived from vegetable oils or animal fats that meet the requirements of ASTM (American Society for Testing and Materials) D 6751. Biodiesel is made from vegetable oils (soy beans in Minnesota), animal fats, or recycled fats/oils through a process called transesterification. Biodiesel contains less than 15 ppm sulfur, no aromatic hydrocarbons, has high lubricity, is biodegradable, and is non-toxic (Bickel, 2006). For these and other economic and political reasons, B20 or 20% biodiesel and 80% Diesel may be mandated for use in Minnesota by 2015.

Ethanol is a gasoline alternative oxygenated fuel that has a stoichiometric fuel-air ratio higher than regular gasoline and contains roughly 2/3rds the amount of energy per unit volume. A typical engine consumes almost 40% more E85 than gasoline, but E85 fuels typically reduce particulate matter emissions. E10 or 10% ethanol and 80% gasoline is mandated for use in Minnesota and future increases in the ethanol fraction are planned.

Sampling conditions and nanoparticles

The nucleation of nanoparticle precursors and their subsequent growth depends strongly on the sampling conditions and these conditions are not standardized. Many studies have experimentally investigated the effects of dilution air temperature, dilution ratio and rate, relative humidity, residence time, and dilution air chemistry on particle formation and growth in the nucleation mode. This section reviews recent studies that explicitly evaluated the impact of sampling conditions on nanoparticle formation and emissions.

The results from these studies are tabulated in Table 2. Except in a few instances, the results apply to the behavior of engine-out emissions that may or may not be characteristic of emissions downstream of emission control systems. The results show that nanoparticle formation and growth is favored by low dilution air temperatures and high relative humidity. Particles appear larger as the residence time is increased due to growth via adsorption of gaseous compounds and coagulation. The primary dilution ratio is a complicated but important variable. The exact origin of the nucleation mode and the concentrations of precursor species are not often known so sensitivity analyses are needed to determine how strongly the dilution ratio influences particle formation. This summary shows that a primary dilution ratio between 5 and 50 typically maximizes particle formation. For a given engine condition, the dilution ratio that produces peak particle formation will depend on the sampling conditions and the concentration of gas phase species that contribute to nucleation and growth. Secondary dilution is used to quench nucleation and growth so a stable aerosol can be transported to instrument. Particle size and concentration do not typically depend on the exact value of the secondary dilution; a value between 5 and 50 is commonly used. In addition, these results apply to steady-state sampling conditions. Few researchers have evaluated particle size and number emissions during transient operating conditions in the laboratory and those that do use variable sampling conditions, like the dilution ratio, (Khalek et al., 2003, Ntziachristos et al., 2004, Liu et al., 2007).

Table 2. Effect of sampling conditions on nucleation mode particles

	Author	Year	Values	Results
Temperature, °C				
	Khalek et al.	1999	13-48	Order of magnitude reduction in nucleation mode for temp 13→48
	Khalek et al.	**2000**	**32-68**	**Shows strong particle surface area concentration sensitivity to temperature**
	Mathis et al.	2004	15-55	Concluded nanoparticle formation is most sensitive to temperature
	Wei et al.	**2005**	**15-43**	**2 order of magnitude increase in nucleation mode when temperature is lowered, effect is less pronounced when fuel sulfur is lower**
Relative humidity, %				
	Khalek et al.	**1999**	**15-40**	**Small sensitivity to RH at dilution temperature of 48°C**
	Shi and Harrison	1999	5-65	Nucleation mode w/ humid air is gone with dry air. Calculated nucleation rate as function of RH (and vs. temp and time)
	Mathis et al.	**2004**	**5-90**	**Particles get larger, increase in concentration, distribution shape unchanged**
Dilution ratio				
	Khalek et al.	**1998**	**4-85**	**Growth quenched for primary DR >60**
	Shi and Harrison	1999	4-900	Total number concentration increased with DR up to DR=900 for low and high loads
	Kittelson et al.	**1999**	**12-25**	**Modest decrease in nucleation mode for 12→25**
	Mathis et al.	2004	8-45	Number concentration peak at DR= 23
	Kawai et al.	**2004**	**14, 50**	**Nucleation mode at DR=14 disappears at DR=50 when air temperature is also increased from 15 to 150°C**
	Giechaskiel et al.	2005	2000, 7000	On-road results—3 order of magnitude increase in concentration of 10 nm particles when dilution ratio increased from 2000 to 7000:1 and RT decreased (results are coupled with effect of load + catalyst)
	Rönkkö et al.	**2006**	**12-30**	**Largest nucleation mode at DR=12, less in magnitude than observed on-road**
	Casati et al.	2007	7-61	Largest nucleation mode at DR=7, 2 orders of magnitude difference from 7 to 61
Residence time, s				
	Khalek et al.	**1999**	**0.1-1.0**	**Order of magnitude increase in nucleation mode between 0.1 and 1 s; more pronounced when dilution temperature is lower**
	Mathis et al.	2004	0.5-4.0	Change of 0.6 to 3.1 increases size 2-3 nm
	Wei et al.	**2005**	**0.5-1.5**	**Modest increase in nucleation mode particles with increase in residence time**
	Rönkkö et al.	2006	0.45-0.9	No effect of increasing residence time on size distribution for variety of operating conditions→ growth quenched at 0.45 s

Fuel composition and nanoparticles

The objective of this section is to summarize recent studies that have evaluated nanoparticle emissions downstream of Diesel engines equipped with emission control devices and fueled with <15 ppm sulfur Diesel fuel and to briefly discuss the impact of biodiesel on emissions. A summary of nanoparticle emissions measurements made using conventional Diesel fuel is shown in Table 2. The table indicates whether a nucleation mode was observed given the test conditions. To aid in understanding the analysis, Figure 5 shows an example of three "nucleation modes" measured at dilution ratios. While distinctly different in shape due to sampling conditions, any of three would be identified as a nucleation mode in Table 2.

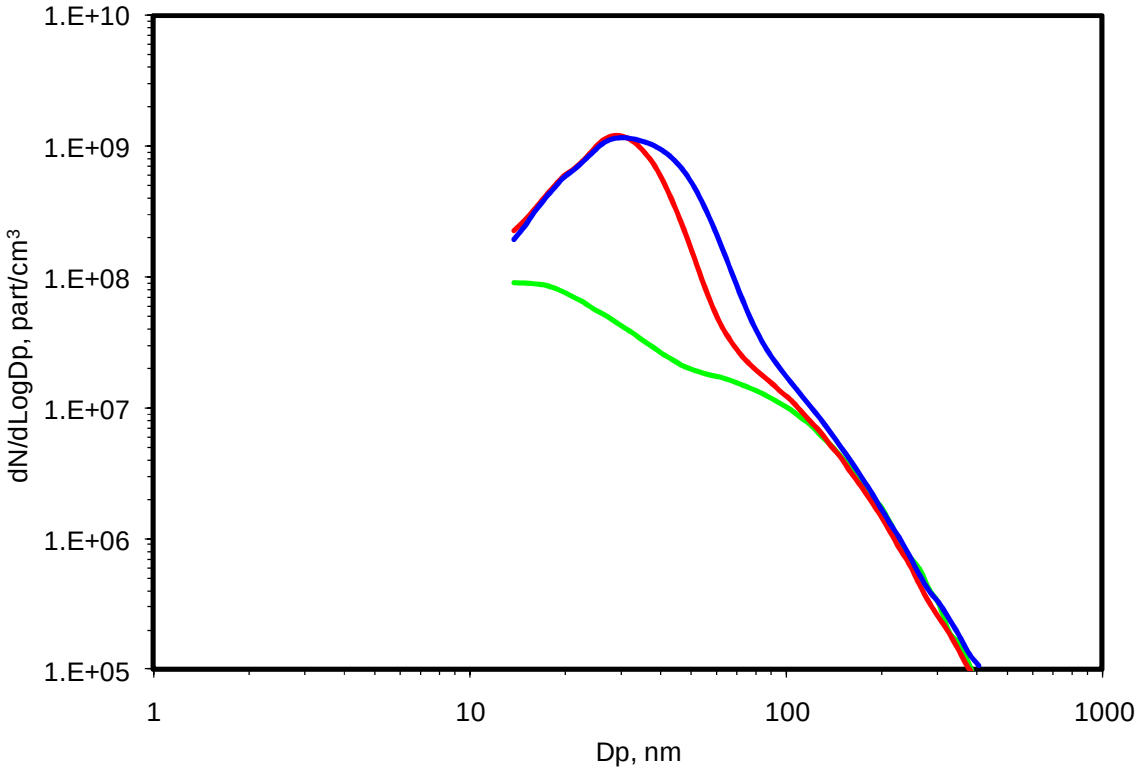

Figure 5. Influence of dilution ratio on particle size in the nucleation mode. DR = 55 (green), 14 (red), 5 (blue)

For engines without emissions control systems, there is generally a strong correlation between mass emissions and fuel sulfur content for fuel sulfur levels between 300 and 500 ppm. The reduction of fuel sulfur to <15 ppm enables the use of emission control devices but does not influence mass emissions greatly (Laresgoiti et al., 1977, Liang et al., 2000, CARB, 2000, Allansson et al., 2002). On the other hand, particle number emissions depend on fuel sulfur between 100 and 5 ppm (Kittelson et al., 2008). The summary results in Table 3 suggest that there is little to no correlation between nanoparticle formation and fuel sulfur content when the fuel sulfur is < 15 ppm. Because neither sampling conditions nor storage and release effects are standardized or fully understood, it is difficult to arrive at a conclusion regarding the influence of fuel sulfur when it is <15 ppm. Additionally, the focus in the following table is fuel sulfur but when fuel sulfur levels are <15 ppm the contribution of lubricating oil sulfur to nanoparticle formation is significant (Vaaraslahti et al., 2005, Kittelson et al., 2008).

Table 3. Influence of fuel sulfur on nucleation mode particles

Author	Year	Fuel sulfur	Comments
Hawker et al.	**1998**	**7**	**No nucleation mode with CRT for range of steady-state operating conditions**
Salvat et al.	2000	<10	Nucleation mode with active, fuel injected DOC + DPF system
Khalek et al.	**2003**	**1**	**Small nucleation mode attributed to lubricating oil or volatile hydrocarbon material from fuel**
Holmén and Ayala	2002	15	Nucleation mode with a CRT-equipped bus fueled with ECD1 fuel and CVS tunnel dilution.
Maricq et al.	**2002**	**4**	**No nucleation mode observed with light duty Diesel vehicle**
Hall and Dickens	2003	10	No nucleation mode observed with CRT—was observed with 50 ppm sulfur fuel
Ntziachristos et al.	**2004**	**10**	**Nucleation mode observed with light duty aftertreatment-equipped Diesel vehicles.**
Vaaraslahti et al.	2004	2	Nucleation mode present at 100% load
Vogt et al.	**2003**	**10**	**On-road results—no nucleation mode downstream of oxidation catalyst**
Ntziachristos et al.	2005	8	No nucleation mode with passenger Diesel, DOC + DPF
Kittelson et al.	2006a	15	On-road results, significant nucleation mode with CRT, particles increase with increasing exhaust temperature
Kittelson et al.	**2006a**	**15**	**On-road results, no nucleation mode with CCRT**
Rönkkö et al.	2007	<10	On-road results, nucleation mode when ~3000 ppm sulfur lubricating oil was used
Casati et al.	**2007**	**<10**	**No nucleation mode with oxidation catalyst, EURO III engine**
Swanson et al.	2009b	2	Nucleation mode at low exhaust temperature but not at high temperature
Swanson et al.	**2009b**	**<1**	**Nucleation mode dominated number *and* mass emissions**

Motivation and significance

The U.S. Environmental Protection Agency (EPA) and European Union (EU) specific DPM as the mass collected on a filter at 47 ± ºC that is quantified gravimetrically. For low-emitting engines, very little mass is collected. Swanson and Kittelson (2009) and Swanson et al. (2009a) quantified the factors that influence the measurement of DPM at the ultra-low 2007 levels. The gravimetric method used for certification differentiates between compliant and noncompliant engines; however, it lacks the sensitivity to evaluate alternative engine designs, emission control devices, alternative fuels, and modified lubricants that reduce DPM emissions to very low levels. The adsorption of semi-volatile gas molecules on a DPM sampling filter leads to an overestimation of the suspended particle mass. Small errors due to low emissions levels, laboratory test procedures, filter requirements, and the gravimetric method are magnified by the semi-volatile nature of the aerosol, and these errors may lead to flawed conclusions. If the measurement goal is to evaluate human exposure then different methods are required to measure exhaust particulate matter, especially nanoparticles, to simulate the effect of atmospheric dilution as described by Kittelson, 1998 and Kittelson et al., 2002, 2006a. The *Union of Concerned Scientists* has stated that requiring the re-evaluation of tail-pipe standards and the improvement of particle measurement methods is "smart public policy" (Monahan and Friedman, 2004). A recent review on nanoparticles (Biswas and Wu, 2005) reported that a well-defined Diesel nanoparticle sampling protocol is necessary to allow for better inter-laboratory comparison studies and future assessments on the impact of nanoparticles in the environment.

While not required by current regulations, there are many advantages to measuring particle size, number concentration, and chemical composition (Maricq, 2007). The emission control systems used to reduce DPM, oxides of nitrogen (NOx), and hydrocarbons (HC) are extraordinarily complex chemical reactors. By measuring the chemical composition of the exhaust, these systems can be optimized for low emissions

and minimal secondary emissions while maintaining high engine performance. Detailed exhaust characterization allows us to evaluate how effectively DPM regulations improve air quality because both the physical (dimensions, mass, fraction or orientation of atoms on the surface) and chemical (composition, electronic energy levels, existence of free radicals) properties of particles are important in defining how particles interact physically, chemically, and biologically with their surroundings. For example, light scattering strongly increases with particle size but also depends on particle composition; sulfate particles that scatter light have a net atmospheric cooling effect while light absorbing soot particles contribute to localized warming (Jacobson, 2004, Hansen et al., 2003, Flanner et al., 2007). On the other hand, absorption of light is roughly independent of size (Hinds, 1999). Particle size and composition information will allow aerosol models to better estimate the impact of Diesel emissions on global climate change. When characteristics of Diesel emissions are identified, they can be used in source apportionment studies.

During some operating conditions, Diesel engines may emit millions of nanoparticles (particles <50 nm in diameter) per cubic centimeter of exhaust (Kittelson et al., 2006a, Swanson et al., 2009c). There is concern that nanoparticles may cause harm in humans (Donaldson et al., 1996, Peters et al., 1997, Penttinen et al., 2001, Gwinn and Vallyathan, 2006). To mitigate the potential risks of the inhalation of nanoparticles, future regulations may require reduced nanoparticle emissions from Diesel engines. While no formal partiality is currently in place, EPA and California Air Resources Board (CARB) may favor DPM and NOx emission control retrofit systems that minimize nanoparticle emissions.

Organization

The objective of this section is to describe the order of chapters in the body of this thesis. The body chapters contain material already published; each chapter is a separate paper.

Chapter 2 begins with a review the physical and chemical properties of DPM. These properties contribute to the fact that the gravimetric measurement is difficult at very low concentrations. As such the method is not useful for developing lower emitting engines, emission controls, fuels, and lubricants. A discussion of alternative metrics and methods that are potentially more accurate, sensitive, and specific follows. These alternative methods are used in experiments found throughout the rest of the thesis. Chapter 4 takes a detailed look at the dilution processes that influences particle size, concentration, and composition. After exhaust aerosols are diluted they typically pass through a preconditioning device before being measured. The thermal denuder and catalytic stripper are two preconditioning devices that are used to separate the solid and semi-volatile fractions that are discussed in chapter 5. The remaining three chapters are experiments used to illustrate how the particle size, concentration, and composition metrics already discussed are useful for characterizing the performance of fuels, emission control devices and for assisting in the evaluation of the engine state-of-maintenance.

Chapter 2: Alternatives to the Gravimetric Method for Quantification of Diesel Particulate Matter Near the Lower Level of Detection

Introduction

Requirements for DPM measurements vary widely. Health experts seek to elucidate metrics that are most health relevant while climatologists require detailed physical and chemical properties to predict how engine exhaust aerosols (including both particulate matter and particulate matter precursors) will influence transformations of particles and gases that occur in the atmosphere. Engine manufacturers make decisions that influence the quality and quantity of emissions. Fuel, lubricating oil, engine design, and emission control devices influence the fundamental nature of DPM. If DPM measurement technology does not keep pace with these changes, engine manufacturers will have a difficult time evaluating new engine technology to reduce emissions and improve air quality.

The objective of this chapter is to review alternatives to the gravimetric method used in engine certification that improve the sensitivity and specificity of the measurement. While this chapter specifically considers alternative measurement methods that are most likely to meet the need of engine manufacturers trying to develop technology to reduce DPM emissions now and in the future, the methods are applicable to other areas where the gravimetric method detection limit is approached and greater accuracy and sensitivity are required. The chapter is organized as follows. First, the unique physical and chemical characteristics of DPM are indentified because these properties influence its measurement. Next, the gravimetric method used for engine certification and its limitations are reviewed. Alternative particle volatility, number, size (and mass), and surface area metrics and methods to quantify them are discussed. Each discussion includes an introduction of the metric and its principle uses, possible calibration methods,

and common methods of application. Within each discussion, the most effective uses of these methods and unresolved issues when used to measure DPM are described. The review is limited to methods that meet the following characteristics or assumptions.

1. No *a priori* knowledge of particle composition is assumed or required. The goal is to have physical measurements that are as general as possible due to the ever-changing nature of DPM. This criterion eliminates carbon specific methods such as photoacoustic, laser-induced incandescence, and some optical absorption methods.
2. Measurements are performed in real or near real-time (minutes or less). Continuous emission monitoring is required to understand the time dependant performance of engines and emission control systems.
3. Particles in the nucleation and accumulation mode size ranges are measured. This requires particles that are semi-volatile (mainly the nucleation mode) and non-volatile (mainly the accumulation mode) to be considered because both types of particles are influenced by emission control, fuels, and engine design.
4. Measurements are made on suspended particles to minimize or avoid gas adsorption sampling artifacts.
5. Measurement sensitivity is 1 $\mu g/m^3$ or better. This resolution is needed to fully differentiate technologies like emission control systems, fuels, and engine design. Table 4 gives number, surface and volume concentrations as a function of particle size that correspond to this mass concentration.
6. Instrumentation and data reduction methods are robust enough to function in a Diesel engine test cell and able to be operated by trained technicians.

Table 4. Minimum detection limits required for number, surface area and volume measurements required for ~ 1 $\mu g/m^3$ sensitivity

Metric	Mobility diameter, nm			
	10	50	100	300
Number, part/cm^3	2.E+06	2.E+04	2.E+03	4.E+02
Surface area, $\mu m^2/cm^3$	669	134	94	94
Volume, $\mu m^3/cm^3$	1.1	1.1	0.5	0.5
Mass, $\mu g/m^3$	1.0	1.0	1.0	1.0

*In these calculations, 10 and 50 nm particles are assumed to have density of 0.9 g/cm^3, while 100 and 300 nm particles are assumed to consist of 13 and 72 primary particles each, where each primary particle is 32 nm in diameter and has a density of 2 g/cm^3; these assumptions follow from the calculations outlined by Lall and Friedlander (2006a). Calculations are based on monodisperse aerosols.

Detailed reviews of physical and chemical measurements of combustion aerosols that evaluate particulate matter properties and advanced measurements without such specific criteria are found elsewhere (Kittelson, 1998, Kittelson et al., 1999, Lighty et al., 2000, Burtscher, 2005, and Maricq, 2007).

Diesel Particulate Matter

Diesel exhaust contains a complex mixture of particles and gases. Gaseous emissions such as semi-volatile hydrocarbons, oxides of nitrogen, and carbon oxides are characterized by their concentration and composition. HCs form from incomplete combustion and range in volatilities. They are be found in the vapor (Siegl et al. 1999, Schauer at al., 1999, Schmitz et al., 2000, Zielinska et al., 2004) or in the particulate phase (Lowenthal et al., 1994, Schauer at al., 1999, Tobias et al., 2001, Sakurai et al., 2003, Ristimäki et al., 2007).

The physical and chemical characteristics of DPM are important considerations when measuring DPM. A typical DPM size distribution is shown in Figure 6 (Whitby and Cantrell, 1976; Kittelson, 1998). Figure 6 shows the relationships between the nucleation,

accumulation, and coarse modes for three weighted size distributions (number, surface area, and mass). The curves have a roughly lognormal, trimodal form and the concentration in any size range is proportional to the area under the corresponding curve in that range.

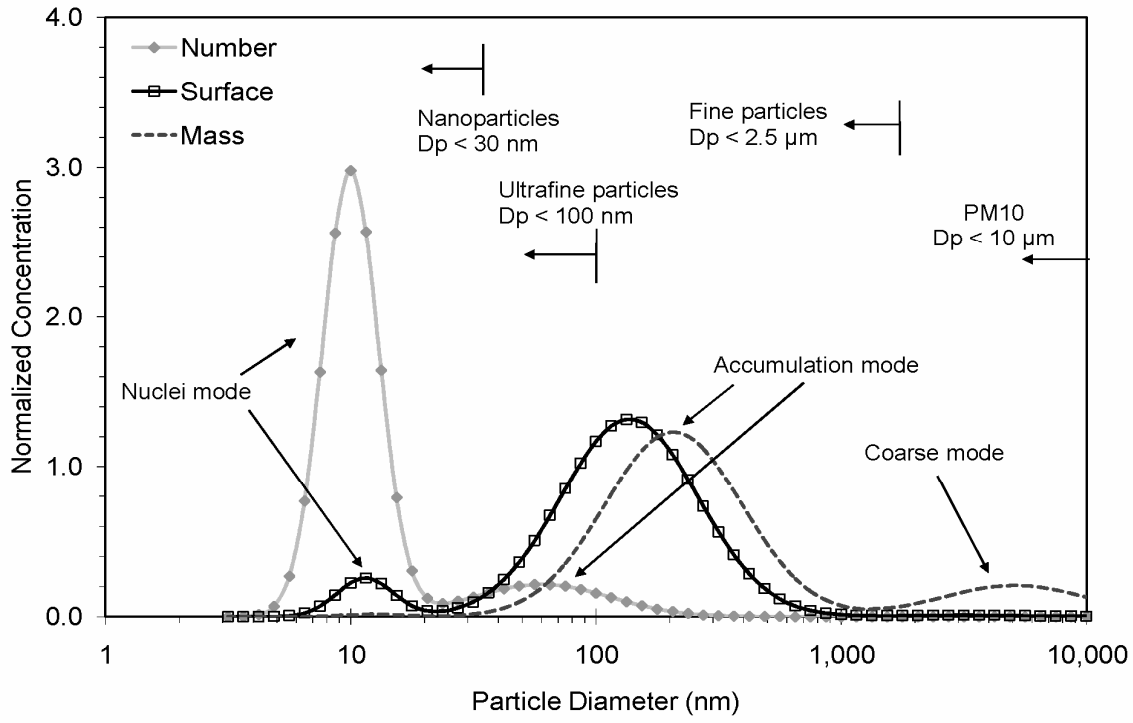

Figure 6. Typical Diesel number, surface area, and mass weighted size distributions (Whitby and Cantrell, 1976; Kittelson, 1998)

The coarse mode consists of particles larger than about 500 nm and contains 5-20% of the mass. Coarse mode particles are crankcase fumes or particles formed by re-entrainment of DPM that was deposited on cylinder and exhaust system surfaces. Most of the DPM mass is found in the accumulation mode (roughly 30-500 nm) that is composed of carbonaceous agglomerates with condensed or adsorbed hydrocarbon and sulfuric acid vapors (Kittelson, 1998).

The nucleation mode (3-30 nm) typically contains <10% of the particle mass but >90% of the particle number. Nucleation mode particles are usually composed of mostly all semi-volatile material (Kittelson et al., 2005, 2006a). Hydrocarbons and sulfuric acid are the main constituents of these particles for engines running under normal conditions with ultra-low sulfur (<15 ppm) fuels (Sakurai et al., 2003, Tobias et al., 2001). All three modes are better defined by their discrete nature than by rigid size boundaries.

The size and concentration of semi-volatile particles that form downstream Diesel engines is strongly dependent upon dilution and sampling conditions (Khalek et al., 1999, 2000, Kittelson, et al., 2002). Sulfur and hydrocarbon compounds are generally found in the vapor phase in the tailpipe but lower volatility components undergo gas-to-particle conversion during dilution and cooling. The gas-to-particle conversion processes: nucleation, condensation, and adsorption are highly nonlinear and extremely sensitive to prevailing conditions. This is especially true for nucleation mode particles. Conversely, accumulation mode particles are less influenced by the dilution conditions. The presence of a large carbonaceous accumulation mode will act to suppress the formation of the nucleation mode because the carbonaceous agglomerates scavenge volatile material reducing the likelihood of nucleation (McMurry and Friedlander, 1979, Bagley et al., 1996, Khalek et al., 2000). Exhaust filters remove the solid accumulation mode particles very effectively so that nucleation of semi-volatile materials that become supersaturated during dilution is more likely.

The precise composition of the nucleation mode is not fully known. Baumgard and Johnson (1996), Shi and Harrison (1999), Khalek et al. (2000) and Kim et al. (2002a,b) have suggested that the formation of nucleation mode particles is due to the nucleation of sulfuric acid and water, resulting in the formation of ~1 nm sized semi-volatile particles. Nucleated particles grow by condensation and sorption of hydrocarbon species. The relative fraction of each is influenced by fuel selection, engine condition, sampling

conditions and use of emission control. For example, Tobias et al. (2001) and Sakurai et al. (2003) measured the composition of nanoparticles emitted by engines without emission control and found the mass fraction of sulfur to be less than a few percent. Conversely, Schneider et al. (2005) and Grose et al. (2006) showed that nucleation mode particles measured downstream of Diesel particulate filters were composed primarily of sulfuric acid or sulfuric acid that was partially neutralized by ammonia.

The CRC E-43 project found evidence of a distinct, non-volatile nucleation mode at idle for different vintages of heavy-duty Diesel engines, including 1988, 1993, and 1998 Cummins or Caterpillar engines (Kittelson et al., 2002, 2006a). This result was confirmed in the University of Minnesota's laboratory with a 1998 Caterpillar C-12 engine that emitted a non-volatile nucleation mode only at very light loads and idle (Jones and Kittelson, 2002, Kittelson et al., 2005). Filippo and Maricq (2008) measured solid nucleation mode particles at idle using a thermal denuder (TD), transmission electron microscopy, and electrical charge measurements. Some evidence suggests that non-volatile particles many form when lube oil metals volatilize in the cylinder and later nucleate to form solid nucleation mode particles (Abdul-Khalek et al., 1998). The likelihood of metal nucleation at idle or very low load is enhanced because soot production is low, leaving little carbonaceous surface area available to condense volatilized metals.

The explanation is not as clear for other operating conditions. Recent experimental evidence supports the contention that solid nucleation mode particles between roughly 3 and 10 nm form at other engine and exhaust conditions not previously expected to produce solid particles, such as during high load, high exhaust temperature operation or downstream of emission control systems (Ronkkö et al., 2007, Johnson et al., 2009, Lahde et al., 2009). One hypothesis is that nucleation mode particles form with a solid core that serves as a site for condensation and sorption of organic material during exhaust

dilution (Ronkkö et al., 2007). This hypothesis is supported by physical models (Du and Yu, 2008). However, this mechanism would rule out the possibility of tiny solid particles downstream of highly efficient filtration devices but such particles have been reported (Johnson et al., 2009).

Compliance with the On-road 2007 DPM Standard for Heavy-Duty Diesel Engines

In 2000 the U.S. EPA adopted emissions standards taking effect for model year 2007 heavy-duty, on-highway trucks. The new standard reduced DPM emissions by a factor of ten to 0.01 g/hp-hr**.** As a result of this rule and the introduction of new engine and emission control technology and the adoption of the ultra-low sulfur (<15 ppm sulfur) Diesel fuel, DPM emissions were drastically reduced and the physical and chemical makeup of DPM was markedly changed. For example, prior to 2007 DPM was typically comprised of 20-90% elemental carbon but DPM emitted by post-2007 engines typically contains <20% elemental carbon (Spears, 2002, Burtscher, 2005, Khalek et al., 2009). The fractional reduction of solid carbonaceous aerosol is in part offset by a fractional increase in sulfate and organic carbon that is very difficult to sample accurately, especially at the low concentrations resulting from compliance with the 2007 standard. Evaluations of commercial heavy-duty Diesel engines with emission controls show DPM emissions are typically at $1/10^{th}$ of this standard (Khalek et al., 2009).

EPA significantly changed the methods used to determine compliance with the 2007 DPM gravimetric certification standard to improve the repeatability and accuracy of the measurement. Many aspects of the sampling process such as dilution air and dilute mixture temperatures, dilution air filtering, sample flows, and other parameters were more precisely defined. A particle pre-classifier was added to reduce the variability of the measurement because previous studies showed that very large particles were spontaneously re-entrained in the exhaust during transient test cycles and that re-

entrainment was influenced by pre-conditioning the exhaust system (Kittelson and Johnson, 1991, Abu-Qudais and Kittelson, 1997, Andrews et al., 2001, 2002).

In addition, greater stability of the environmental conditions in the filter weighing room and better balance precision/resolution were required. The procedure for weighing each filter was well defined with added requirements for charge neutralization, stabilization time, and repeat weighings of sample filters. New weighing requirements greatly improved the quantification of mass. This measure (mass) is very well defined and it remains one of few particle measurements that are traceable to National Institute of Standards and Technology (NIST) standards. Consequently, the gravimetric method is the standard for evaluation of alternative methods, including those that rely on integrated particle size distribution measurements, to estimate total mass.

These improvements did not improve the accuracy sufficiently to allow emissions to be quantified at $1/10^{th}$ the 2007 standard. For example, filter artifacts due to the adsorption of semi-volatile gas molecules on a sampling filter or on particulate matter already collected may lead to an overestimation of the true suspended particle mass (Park et al., 2003, Maricq, 2003, Chase at al., 2004, Khalek, 2005, 2006, Andersson et al., 2004a, Swanson and Kittelson, 2009a). In addition, the amount of DPM collected depends on the filter face velocity (Khalek, 2006, McDow and Huntzicker, 1990, Zhang and McMurry, 1987, 1991, 1992). The change in DPM collected is due to either a change in adsorbed artifact or a change in the sampling efficiency of semi-volatile particles or a combination of both. These artifacts constitute significant shortcomings in the gravimetric measurement when applied to low emitting engines.

Particulate Matter Definition

The gravimetric method relies on the operational definition of “particulate matter” as the “mass collected on a filter” at 47 ± 5°C and specifies the measurement and analysis

methods in detail. Physical properties like morphology or size and chemical properties like composition are not considered. Thus, it implicitly allows filter artifacts to contribute to DPM although they should not. A new definition of DPM is needed that distinguishes between suspended particulate matter and gas molecules that behave like particles and stick on filters. This definition is necessary to make filter artifacts to be a better substantiated quantity. While there is no consensus on how to make this distinction, Girshick (2010) and Preining (1998) have outlined criteria to provide guidance for defining a "particle" that depends on the context. For example, in fundamental studies of homogenous nucleation, a substance becomes a particle once it has reached the size of a "critically size cluster" of molecules where the cluster has a statistically greater likelihood to grow rather than shrink or dissociate in the system of interest. The following definition makes the distinction between molecules (or clusters of molecules) and particles so that the "suspended particle mass" for Diesel aerosols can be precisely identified.

A particle is a homo or heterogeneous cluster of molecules with a mobility diameter larger than 3 nm

This definition has merit because:

1. It excludes most single, large hydrocarbon molecules that are typically considered "artifact." For example, the estimated dimension of a curled up molecule of $C_{40}H_{82}$ is 1.5 nm.
2. It includes the tiniest particles that are formed by engines in high number concentrations whose formation are sensitive to fuels, emission controls, and engine developments. Condensation nuclei <3 nm exist in engine exhaust, but they are extraordinarily difficult to sample using realistic dilution schemes or measure without huge particle losses.

3. It is consistent with the lower limit of detection of instruments commercially available.

Particle Volatility

A common thread throughout the previous discussion is the difficulty in dealing with the semi-volatile nature of the hydrocarbon and sulfur-containing compounds found in Diesel exhaust that influence the method of measurement. Distinguishing between solid and semi-volatile particles adds specificity and assists in understanding some of the variability inherent in filter-based measurements. Volatility measurements also provide valuable information in terms of understanding engine and emission control system performance. In addition, the response of some instruments, such as the photoemission aerosol sensor (PAS), is strongly influenced by the physical and chemical nature of the Diesel aerosol (Burtscher, 1992, Siegmann and Siegmann, 2000, Bukowiecki et al., 2002, Jung and Kittelson, 2005, and Kittelson et al., 2005). Specifically, the PAS response is suppressed by the presence of a large, predominantly semi-volatile nucleation mode, and/or the presence of semi-volatile material on the surface of the solid carbonaceous agglomerates present in the accumulation mode.

Available methods that enhance specificity and enable the measurement of the solid, and by difference the semi-volatile fractions, include the thermal denuder, catalytic stripper, and volatile particle remover. Each device is shown schematically in Figure 7. These devices are used as pretreatment devices upstream of the real time instruments that are discussed in subsequent sections of this chapter.

1. Thermal denuders (TD) are used to remove semi-volatile material by adsorption (Burtscher et al., 2001). First, the aerosol is heated to 300°C in a length of stainless steel tubing. Evaporated semi-volatile material is adsorbed by activated

carbon in a subsequent section. The adsorption section is arranged as a diffusion dryer that is cooled with water circulating at roughly room temperature.

2. The catalytic stripper is an oxidation catalyst that is used to remove the organic carbon fraction by passing the dilute Diesel exhaust over a catalyst heated to 300°C. The flow rate depends on design but is typically between 1 and 10 L/min (Abdul-Khalek and Kittelson, 1995, Kittelson and Stenitzer, 2003, Stenitzer, 2003). It may be used with or without a second ceramic substrate that has a washcoat that acts as a trap for sulfur containing compounds.
3. The volatile particle remover (VPR) is a method specified by the European Union (EU) to determine compliance with the EU solid particle number standard. The VPR consists of three components: a hot dilution section, an evaporation tube to evaporate (wall temperature must be 300 – 400°C) semi-volatile material, and a cool dilution section to cool the aerosol and to reduce its concentration to <10,000 part/cm^3 (Sandbach, 2007). The minimum penetration required of 30, 50, and 100 nm solid particles is 60, 70, and 80%, respectively and the required removal efficiency of 30 nm hydrocarbon ($C_{40}H_{82}$) particles is 99%.

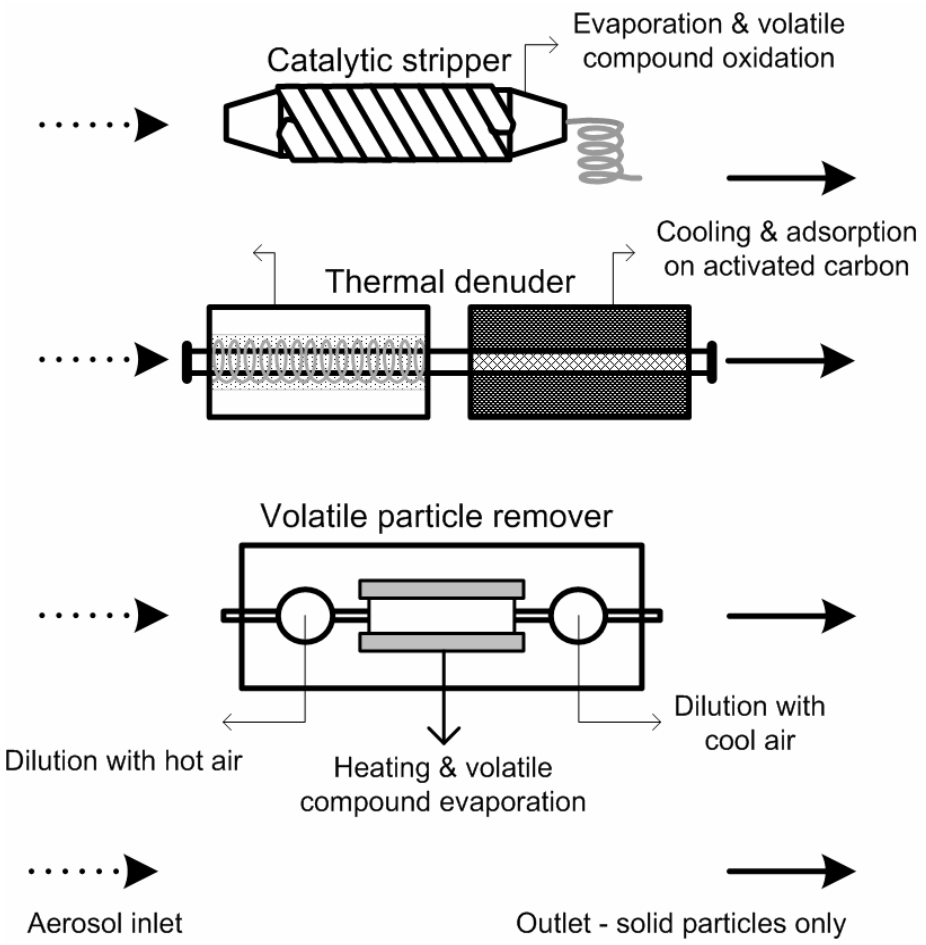

Figure 7. Schematic of the thermal denuder, catalytic stripper, and volatile particle remover

The TD, CS, and VPR as a whole are quite useful but issues remain and no standards exist for CS or TD performance. These devices must demonstrate that they fully remove semi-volatile material to prevent nucleation or re-condensation, while at the same time demonstrate high penetration of nanometer-sized suspended particles. The performance of these devices for removing simple compounds such as alkane vapors is easily established, but further work is needed to elucidate the roles of other compounds. This is critical for a number of reasons. Diesel exhaust is a complex mixture that includes DPM and vapors. The vapor phase material is chemically complex and dependent upon fuel,

operating conditions and other parameters. With the introduction and wider use of alternative fuels such as biodiesel produced from various feedstocks, the impact of these fuels on DPM is less well understood compared to petroleum-based ultra-low sulfur diesel fuel. A new concern is that particle heating may result in the formation of solid particles due to charring or pyrolysis (Swanson and Kittelson, 2009b).

Number Concentration

The primary instrument for particle number counting is the condensation particle counter (CPC). The principle of operation of a CPC is the condensation of liquid (typically butanol) on particles to grow them to an optically detectable size before they are counted by an optical particle counter (Agarwal and Sem, 1980). Calibration of a CPC is performed with a differential mobility classifier and an aerosol electrometer (Liu and Pui, 1974a, b, 1975, Liu et al., 2005). The apparatus for performing this calibration is shown in Figure 8. The number concentration from the mobility-classified aerosol is measured by the electrometer and CPC in parallel. The electrometer operates by measuring the current flow resulting from collection of the charged particles. Since the particles leaving the DMA are predominantly singly charged, the concentration can be calculated from the measured current and the flow rate through the electrometer. Knowing the measured current, (I, A) from the charged particles collected and the flowrate (Q, cm^3/sec), the aerosol concentration (N, part/cm^3) can be calculated as shown:

$$N = \frac{I}{Q \cdot e}$$

where e is the elementary unit of charge (e = 1.602E-19 C), and it is assumed that particles are carrying unit charge. For highest accuracy, an additional small correction for the interference effect due to the small number of multiply charged particles of the same mobility in the aerosol stream is needed. Components critical to the success of this

measurement include the flow meters, electrometer noise and measurement accuracy, and ensuring proper mixing of the makeup air with the aerosol stream.

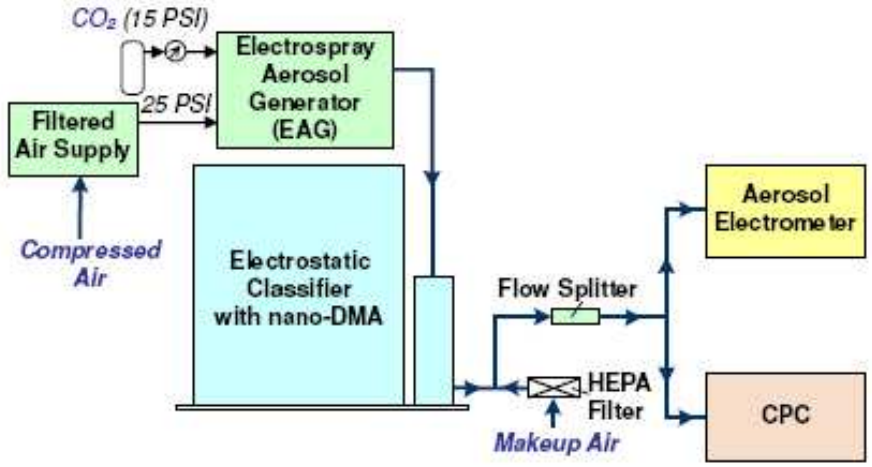

Figure 8. CPC calibration schematic (reprinted from Liu et al., 2005)

Recently, Fletcher et al. (2009) described how this procedure could be performed using fully NIST traceable methods. The methodology is identical in principle to that shown in Figure 8, with added corrections for coincidence, multiple charge, and the minimization of agglomerated particles. The authors estimated total uncertainties of 27% for 500 part/cm^3 to 6.5% for 3,000 part/cm^3 to 4.8% at 12,000 part/cm^3.

Additional work to develop calibration methods for number concentration measurements is ongoing. For example, the International Organization for Standardization (ISO) group is developing the standard ISO/WD 27891, with the working title: *Validation and calibration of aerosol particle number counters*. Japan's National Institute of Advance Industrial Science and Technology (AIST), which is equivalent to U.S. NIST, has published a calibration methodology for a number concentration measurements and it is described by Sakurai (2008). AIST predicts lower uncertainties than the NIST method described by Fletcher et al. (2009), roughly 10% for 500 part/cm^3 to 2% for 3,000

part/cm^3 to 0.6% at 12,000 part/cm^3. Similar tests by a commercial CPC manufacturer indicate that calibration uncertainties are on the order of 5% (Liu et al., 2005).

Application to Diesel Particulate Matter

Besides traditional causes of uncertainty like flow rate, CPC response is affected by particle size and composition. The 50% cutpoint of a CPC (D_{50}) is the diameter where particles are counted at 50% efficiency and this value ranges between 3 and 10 nm for commercial CPCs. This narrow range on a relative scale can lead to very different total number concentration readings. Kittelson et al. (2002) have explicitly used differences in the lower particle size detection limit of CPCs, such as the concentration difference between low (3 nm) and high (10 nm) D_{50} cutpoints to estimate or explain the presence of a nucleation mode. CPCs exhibit strong dependence on composition near their D_{50}. For example, Sakurai (2007) found that in a butanol-based CPC the D_{50} counting efficiency at 10 nm of emery oil, sucrose, sodium chloride, and ammonium sulfate aerosols varied from 0 to 65%, depending on the composition with butanol soluble compounds detected with higher efficiencies.

CPCs that use water as the condensing fluid provide an alternative to traditional butanol-based CPCs. Studies have shown that “pure” compounds such as dioctyl sebacate and emery oil are so hydrophobic that they are activated with much lower efficiencies in water CPCs, resulting in significantly higher D_{50} cutpoints (Hering et al., 2005, Liu et al., 2006). However, Franklin et al. (2010) reported that ultrafine butanol and water-based CPCs performed well when measuring the concentration of <10 nm sized nanoparticles. No significant change in D_{50} was detected because the semi-volatile lubricating oil and unburned biodiesel fuel droplets were hygroscopic (or contaminated) enough to support growth by water. Their result supports the use of water-based CPCs for measuring Diesel aerosols.

The European Particulate Measurement Programme addressed issues in particle concentration, composition, and size for the EU 5/6 solid particle number standard. For example, particle concentration must be reduced (by dilution) to <10,000 part/cm^3. The concentration limit was chosen based on the requirement that the CPC used can detect concentrations up to this number while still operating in single particle counting mode. In addition, particles are heated to remove semi-volatile material and therefore only "solid" particles, likely consisting of mainly carbonaceous aggregates, are measured by the CPC. This largely negates any affects of composition on counting efficiency. Finally, the D_{50} is set to 23 nm. This choice of D_{50} does not reflect indifference towards particles smaller than 23 nm, but rather the assumption that these particles will be very efficiently filtered by exhaust particle filters that are all but required to meet the exhaust particle number standard. It also eliminates the possibility that semi-volatile compounds that do not fully evaporate in the VPR are included in the standard. PMP studies have shown that when adopting these limits, particle number concentrations measurements are repeatable to generally around 20 - 30%, but can be as low as 5% when the engine – out emissions are very stable, such as when the engine is not equipped with a filtration device that undergoes periods of regeneration that produce fluctuating particle concentrations (Giechaskiel et al., 2008).

Particle number concentrations are very accurately measured with CPCs and their measurement is NIST traceable. However, issues remain and the suggestions below are given to ensure the validity of measurements made on Diesel exhaust aerosols.

1. For cases where number concentration is desired, CPC measurements are highly preferred over number concentrations determined by integrating particle size distributions, where the result is based on certain assumptions and inferences. Reporting the number concentration based solely upon CPC measurements should become a standard practice.

2. More detailed, size dependant CPC counting efficiencies for Diesel exhaust generated from a wider variety of engines with and without emission controls fueled by regular or alternative biofuels are needed.
3. CPC measurements often exhibit high levels of "variability" that are incorrectly interpreted negatively. Often this variability is not the result of a poorly performed measurement or instrument but a consequence of the variability of the source. Thus, the sensitivity of instruments like CPCs allows further elucidation of the complex and changing nature of engine emissions that were previously unresolvable.

Particle Size

The wide size range and trimodal nature of the DPM size distribution complicates the measurement. The DPM size distribution roughly covers the range from 3 to 1000 nm. That range includes particles in the free molecular, transition, and continuum regimes. The particle size regime is described by the Knudsen number (*Kn*), defined as 2 times the ratio of the gas mean free path (λ) to the particle diameter (d_m), as shown:

$$Kn = \frac{2 \cdot \lambda}{d_m}$$

For particles in dilute Diesel exhaust at room temperature, λ is ~66 nm. The free molecular regime is characterized by Kn > 10 or d_m < ~10 nm. The continuum regime (Kn < 0.1) corresponds to particles where d_m > 1000 nm. Thus, most DPM aerosol is within the transition regime where 10 < d_m < 1000 nm.

Particle morphology also affects charging, and many, if not most commercial instruments rely on particle charge/charging to directly or indirectly measure size or concentration. Typically during particle charging the mean free path of the charging ions is only 15 nm

(Liu and Pui, 1974b). In that case, charging a 300 nm particle occurs in the continuum regime. Most diffusion charging theories assume spherical particles to describe unipolar (ions of one polarity charge the particle) or bipolar (positive and negative ions bring particle to equilibrium state) diffusion charging processes (White, 1951, Gunn, 1954, Fuchs, 1963, Liu et al., 1967, Gentry 1972, Pui, 1976, Liu and Pui, 1977, Pui et al., 1988, Hinds, 1999). Later studies have shown that unipolar and bipolar diffusion charging processes are affected by particle morphology and to a much lesser extent, composition (Laframboise and Chang, 1977, Chang, 1981, Rogak and Flagan, 1992, Brown et al., 1995; Biskos et al., 2004, Biskos et al., 2005, Oh et al., 2004, Jung and Kittelson, 2005, Shin, 2009). In summary, these studies have shown that:

1. Geometric surface area and electrical capacitance are two important morphology-related parameters that determine charging properties of non-spherical particles.
2. Aggregated and spherical particles are not charged with the same efficiency in the bipolar charging process. For example, imagine a singly charged 100 nm sphere and 100 nm mobility diameter aggregate. Both particles have the same electrical mobility diameter. However, if both pass through a bipolar charger, the charging probability is different for each. Morphological properties of the aggregate dictate the distribution of charge states and it may acquire a greater or lesser number of charges than the sphere (difference is ~20% or less).
3. Aggregated particles acquire a higher mean charge than spherical particles with the same mobility diameter for unipolar charging, the increase being ~10 – 30%.
4. The dependence on composition of unipolar diffusion charging for particles ranging from 10 to 200 nm is very small (Shin et al., 2009).

Liu and Pui (1974a), Knutson and Whitby (1975), Liu and Pui (1975), Wang and Flagen (1990) described differential mobility classification as a means to determine particle size. The differential mobility analyzer (DMA) classifies particles according to electrical mobility diameter. For spherical particles, the electrical mobility equivalent diameter equals the geometric or Stokes diameter and is independent of particle density. DMA's are usually calibrated for spherical particles, and provide number, area, and volume distributions for spherical particles. Figure 9 is a schematic of the apparatus used to generate and size-classify particles. The system consists of an atomizer, a bipolar diffusion charger (neutralizer), a differential mobility analyzer, and an electrometer or CPC. In the apparatus, generated particles are introduced into the neutralizer to bring them to a state of charge equilibrium with the bipolar ions. A mobility size is selected by setting the voltage on the inner column to the appropriate value and particles of a single mobility exit the through the bottom outlet. NIST takes this general approach, using a TSI long column DMA to size 100 nm standard reference materials (Kinney et al., 1991). In addition, a new standard has been adopted by the International Standards Organization (ISO) for particle sizing using the DMA entitled "*ISO 15900:2009, Determination of particle size distribution – differential electrical mobility analysis for aerosol particles*."

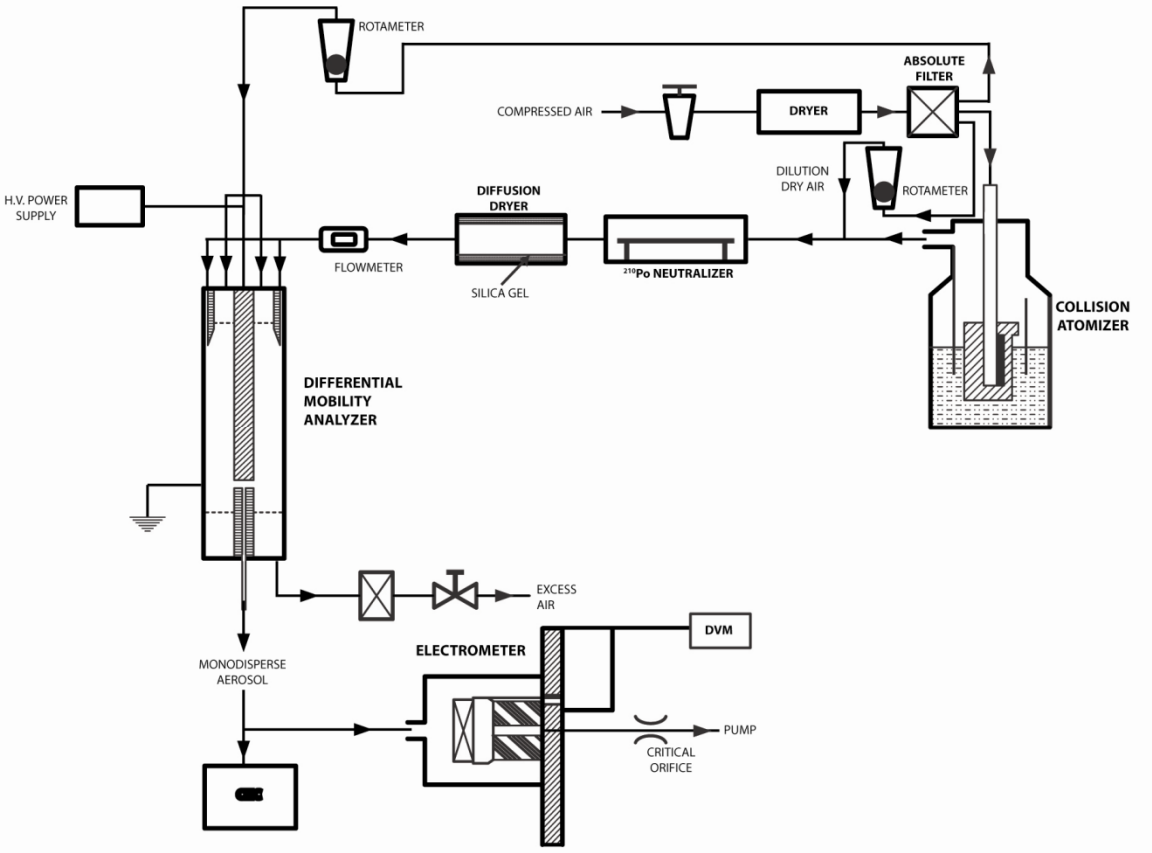

Figure 9. Differential mobility analyzer and particle generation apparatus (redrawn and reprinted from Liu and Pui, 1974a)

Application to Diesel Particulate Matter

The accumulation mode of DPM is approximately lognormal with mean mobility particle diameters ranging from 60 to 120 nm (Harris and Maricq, 2001). These particles are collections of aggregated primary particles whose fractal dimension ranges from 2.2 to 2.8 with primary particles that range in diameter from 13 to 40 nm (Maricq and Xu, 2004; Virtanen et al., 2002; Park et al., 2003; Park et al., 2004; Virtanen et al., 2004; Van Gulijk et al., 2004; Olfert et al., 2007; Rissler et al., 2009). One study showed primary particle size tends to decrease with air/fuel ratio and engine speed (Lapuerta et al., 2007). These and other variables, like sampling conditions may contribute to the variability because the measured fractal dimension may depend on the amount of vapors that have

condensed on the soot (Skillas, 1998, Olfert et al. 2007). Figure 10 is an electron micrograph showing a 200 nm mobility classified Diesel particle that is made up of 24 nm primary particles. The primary particles are lognormally distributed with a standard deviation of 7 nm.

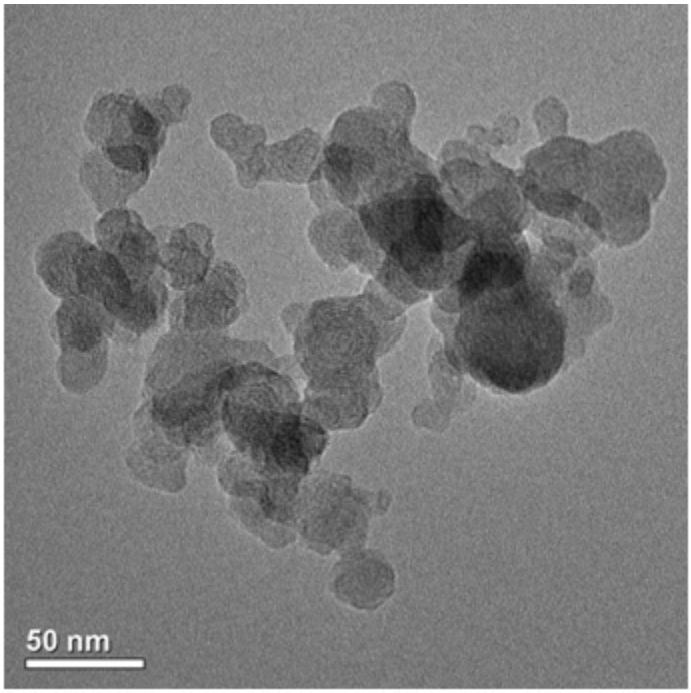

Figure 10. A 200 nm mobility classified Diesel aggregate sampled from a 2005 4.5 L John Deere Diesel engine at UMN's engines laboratory running at 1400 rpm, 75% load. Primary particle size was determined to be 23.9 ± 6.8 nm based on 212 particles analyzed (Particles sampled by Jacob Swanson; image analysis performed by Weon-Gyu Shin)

A motivating factor for pursuing size measurements of Diesel aerosols is that mass weighted, integrated particle size distribution measurements may be a more sensitive and robust measure of suspended particle mass than gravimetric measurements (Liu et al., 2009). However, the primary size standards discussed above relate to sizing spherical particles of known morphology and composition, as opposed to the complex chain aggregates common in Diesel aerosol. Effective density techniques are used to account

for the fact that mobility diameter is not a geometric measure for aggregate particles due to their fractal-like nature. Effective density (ρ_{eff}) is defined as:

$$\rho_{eff} = \frac{\text{mass of particle}}{\text{volume of mobility equivalent sphere}} = \frac{m}{\frac{\pi}{6} d_m^3} = \frac{p_p \cdot N_p \frac{\pi}{6} d_p^3}{\frac{\pi}{6} d_m^3}$$

where m is the mass of a particle, d_m is its mobility diameter, and the following refer to properties of the primary particles in each aggregate: intrinsic density (ρ_p), number (N_p) and diameter (d_p), assumed to be spherical. Schmid et al. (2007) reviewed effective density measurement techniques in more detail than is given here. Approaches to improve estimates based on integrated size distribution measurements include:

1. effective density determination via aerodynamic/mobility measurements using an electrical low pressure impactor (ELPI, Keskinen et al., 1992), and DMA or scanning mobility particle sizer (SMPS, Wang and Flagen, 1990),
2. effective density determination using series DMA and aerosol particle mass analyzer measurements (APM, Ehara et al., 1996),
3. ultrafine aggregate analysis, described by Lall and Friedlander (2006a), which uses mobility theory, charging properties of aggregates, and primary particle image analysis to obtain mass concentrations from mobility distributions, and
4. a method that combines Lall and Friedlander's (2006a) approach with particle charge measurements using an instrument called the universal nanoparticle analyzer (UNPA, Wang et al., 2009).

ELPI and SMPS: Effective density determinations from aerodynamic/mobility diameter comparisons have been described by Kelly and McMurry (1992). In this technique, aerodynamic and mobility diameters are measured and effective density is calculated using the relationship:

$$\rho_{\text{eff}} = \rho_o \frac{d_a^2 \cdot C(d_a)}{d_m^2 \cdot C(d_m)}$$

where d_a refers to aerodynamic dynamic and C() refers to the Cunningham slip correction that is a function of particle size (Kasper, 1982). Ristimäki et al. (2002), Virtanen et al. (2004), and Van Gulijk et al. (2004) describe how effective density can be determined using a DMA or SMPS and the ELPI and various data interpretation schemes. Virtanen et al. (2004) suggested a 15% uncertainty is associated with these measurements. Maricq and Xu (2004) used this technique to characterize the effective densities of particles emitted by light duty Diesel engines at different speeds. Their overall conclusion was that the effective densities from these vehicles were virtually indistinguishable between engines and speeds. Rostedt et al. (2009) described how the ELPI could be modified with a mobility analyzer inserted into the impaction plate's column that enables the effective density of a unimodal aerosol to be determined without the SMPS. This addition resulted in density values that matched reference values within 15%. An additional variation to this approach is seen in the Dekati Mass Monitor (DMM) where the effective density is determined by comparing aerodynamic and mobility diameters that are measured by the same instrument (Lehmann et al., 2004). This instrument has shown promise for measuring ultra-low emissions (Khalek, 2007) but only for unimodel size distributions.

DMA and APM: The APM classifies particles by balancing the electrostatic and centrifugal forces in two concentric rotating cylinders (rotating at same angular velocity) that have a voltage difference applied between them (Ehara et al., 1996). Based on this

force balance, particles of a given mass-to-charge ratio will pass through the APM. To determine mass per particle, particles are mobility size-selected using a DMA. Singly charged particles exiting the DMA pass though the APM, which selects particles of a single mass/charge ratio. The number concentration of particles exiting the APM is measured to determine mass concentration. Studies have estimated that there is a calibration uncertainty of 5 to 7 % in the mass of NIST traceable particles (Ehara et al., 1996; McMurry et al., 2002; Shin et al., 2009). Olfert and Collings (2005) described the Couette centrifugal particle mass analyzer (CPMA) that is conceptually similar to the APM but whose cylinders rotate at different velocities. This modification improves the transfer function for the device.

Particle mass analyzer techniques have been successfully used to measure the mass or alternatively, the effective density of aggregate particles (Kelly and McMurry, 1992; Hering and Stolzenberg, 1995; McMurry et al., 2002; Park et al., 2003; Lall et al., 2008; Kim et al., 2009; Shin et al., 2009). Park et al. (2003) showed that the effective density of Diesel exhaust aerosols varies from ~1.2 to ~0.3 g/cm^3 in the size range of 50 to 300 nm. Olfert et al. (2007) measured slightly higher values and attributed the difference to higher levels of sulfuric acid vapor present in the exhaust due to sulfate oxidation by the oxidation catalyst. Condensation of sulfuric acid on aggregates during dilution leads to higher intrinsic and measured effective densities.

Effective Density Comparisons. The following example is given to estimate the robustness of the effective density technique for mass concentration estimates. First, experimental data (Park et al., 2003, Maricq and Xu, 2004, Olfert et al., 2007) were fit to the scaling law given by Skillas et al. (1998). This relationship shows that the mass of a particle scales with its mobility diameter and fractal dimension as follows: $\rho_{eff} = \text{constant} \cdot d_m^{d_f - 3}$. Further discussion of the proportionality constant is given by Maricq and Xu (2004). Liu et al. (2009) suggested $\rho_{eff} = 1.237 \cdot \exp(-0.0048 \cdot d_m)$ best fit data

given by Maricq and Xu (2004). The exponential relationship used by Liu et al. (2009) smoothly accounts for transition in the particle size distribution from the nucleation mode where particles have a fractal dimension of 3 and a density near 1 g/cm^3 to accumulation mode aggregate particles that have a fractal dimension between 2 and 3 and a size dependant effective density. Furthermore, they experimentally compared this relationship with filter mass measurements taken from a heavy-duty Diesel engine without emission control devices and found agreement. The results from these fits are shown in Figure 11.

Effective density relationships shown in Figure 11 were applied to the accumulation mode data shown in Figure 6 and the calculated mass concentrations were normalized to the concentration without a density correction. The size distribution in Figure 6 has a mean particle size of 60 nm with a geometric standard deviation of 1.9 in the accumulation mode. These results are tabulated in Table 5. The correction shows that assuming spherical particles overestimates the mass, in this case by about a factor of 2. However, the corrected mass concentrations span a range of about 50%. Thus, it is clear that a single effective density correction cannot be applied to all situations. It is also not fully clear which expression is most applicable to Diesel aggregates emitted by modern engines, how effective density varies with speed and load, or what measurement technique yields the most accurate result. It is also not known how biofuels and new lubrication oil formulations will impact the results.

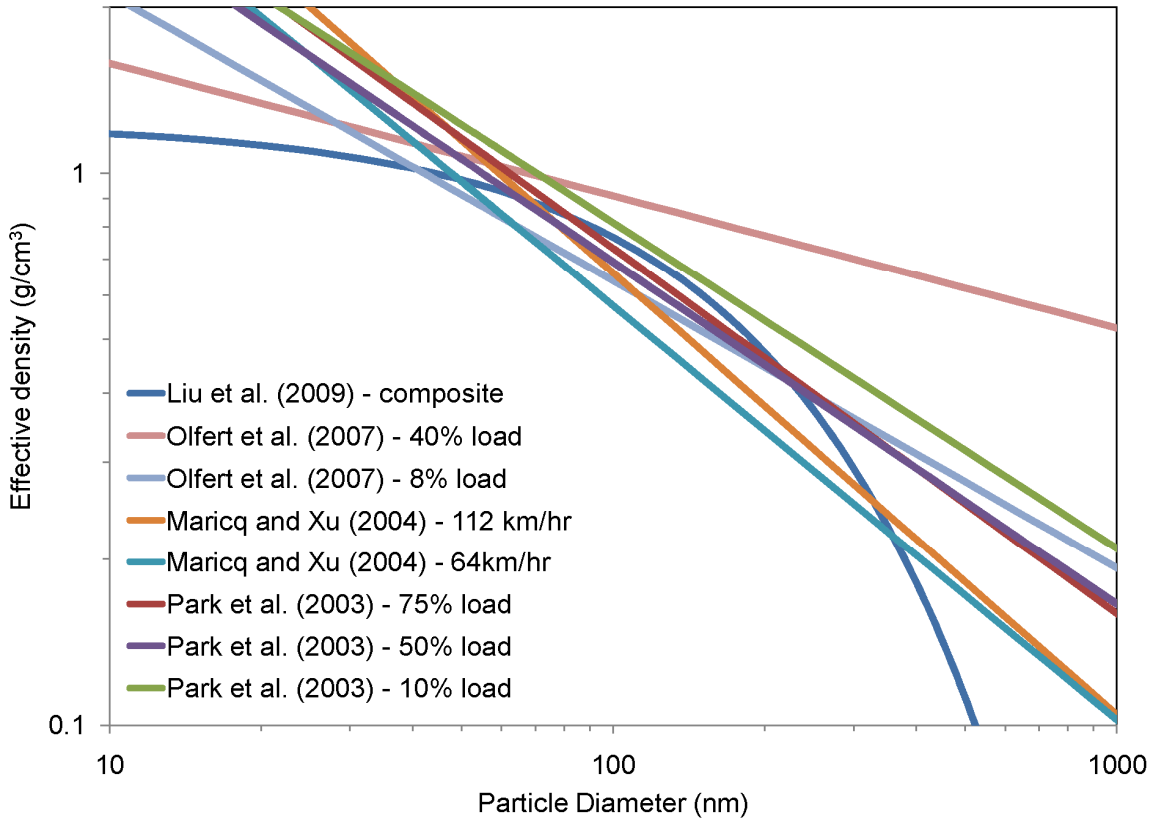

Figure 11. Comparison of effective densities determined from Liu et al. (2009), Olfert et al. (2007), Maricq and Xu (2004), and Park et al. (2003)

Table 5. Comparison of effective density calculations

Density function	constant	D_f	Mass concentration (normalized)
Standard – 1 g/cm^3, assume spheres	–	–	1
Liu et al. (2009) – composite	–	–	0.46
Olfert et al. (2007) – 8% load	7.0	2.5	0.46
Olfert et al. (2007) – 40% load	2.8	2.8	0.77
Park et al. (2003) – 10% load	12.3	2.4	0.57
Park et al. (2003) – 50% load	12.0	2.4	0.48
Park et al. (2003) – 75% load	15.4	2.3	0.50
Maricq and Xu (2004) – 64 km/hr	18.2	2.3	0.38
Maricq and Xu (2004) – 112 km/hr	26.3	2.2	0.42

Ultrafine Aggregate Analysis: Lall and Friedlander (2006) derived a relationship between primary particle diameter (d_p), number of primary particles and particle mobility diameter using work by Chan and Dahneke (1981) and bipolar charging expressions by Wen et al. (1984). Their model, combined with electrical mobility measurements, allows for size distribution, surface area distribution, and volume distribution of aggregates based on electrical mobility of improved accuracy.

Lall et al. (2006b) evaluated the method using DPM data from Park et al. (2003). Results, shown in Figure 12, illustrate both the gross error caused by assuming mobility diameter for the DPM mass concentration calculation and the improvement obtained using the aggregate analysis. Further experimental confirmation of this theory using artificially generated carbon particles is given by Lall et al. (2008).

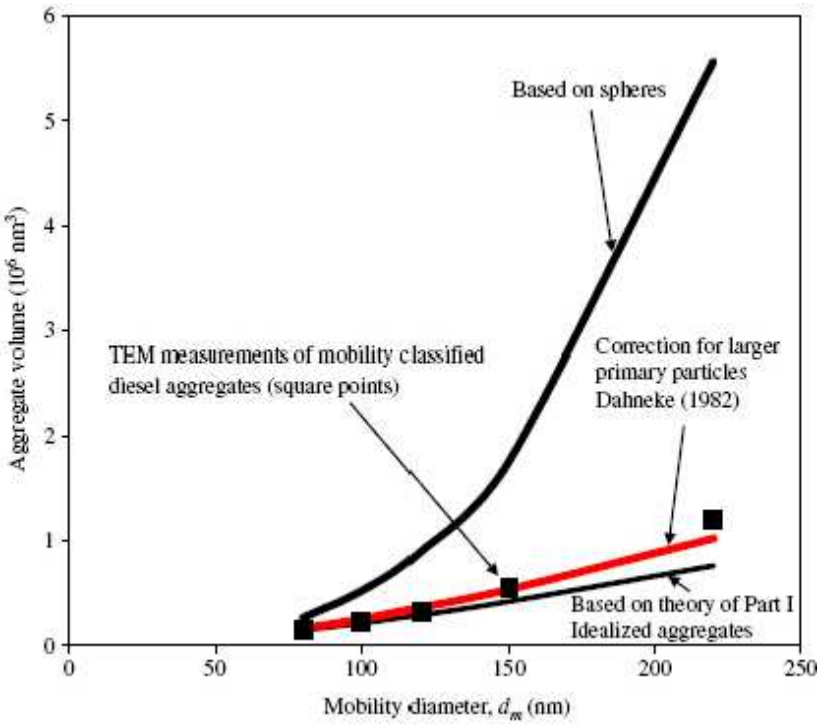

Figure 12. Comparison of mobility diameter and aggregate analysis calculations for determining the mass of Diesel exhaust particles (reprinted from Lall et al., 2006)

Universal Nanoparticle Analyzer. The UNPA utilizes a DMA, CPC, and Nanoparticle Surface Area Monitor (NSAM) that includes a unipolar charger combined with an electrometer, to characterize nanoparticle morphology and measure the number, surface area and volume distributions of loose nanoparticle aggregates (Wang et al., 2009), including DPM. The UNPA response to a size selected particle is given as a sensitivity (S) that is defined as the current measured by the NSAM divided by the number concentration measured by the CPC. Experimental data and theoretical modeling have shown that S depends on the particle morphology. S is larger for loose aggregates than for spheres at a fixed mobility diameter, and S for partly sintered aggregates is between S for loose aggregates and spheres. The measured value of S gives a direct indication of the particle morphology, described as follows. Loose aggregates are modeled as clusters of spherical primary particles. From UNPA sensitivities, the primary particle size is

determined using a fitting procedure. Using the model of Lall and Friedlander (2006a) for loose aggregates, the number of primary particles in aggregates is computed, from which the surface area and volume of aggregates are obtained. Multiplication by the density of the primary spheres (roughly 2 g/cm^3 in Diesel aerosol) yields mass distributions of loose aggregates. This measurement can be performed on particles in the range of 50 to ~300 nm in several minutes. Experiments to validate the response of this instrument to DPM are ongoing.

Surface Area

Previous discussions have highlighted the heterogeneous nature of Diesel exhaust particles – some are spherical while others are complicated aggregates; their volatility varies, as does their composition. In these contexts, it is not at all clear how to measure surface area, or even how surface area should be defined. Multiple approaches have been investigated: measurements of total surface area or BET surface area, measurement of Fuch's surface area (Fuchs, 1963) that is sometimes referred to as the active surface area, and measurement of the equivalent surface area. These measurements illustrate the difficulty in picking the metric that best suits the application.

BET surface is used widely in the health and carbon black communities to measure the total surface area (Brunauer et al., 1938), because it includes surface area due to particle porosity that can increase the amount of adsorbed or condensed material that may influence the health impact or other performance properties. In this method, the surface area is estimated from the equivalent surface area of a monolayer of N_2 molecules that adsorb to the surface of the material. Application of this method to accumulation mode DPM where chain agglomerates are common would result in greater sensitivity to particle porosity. However, it is not fully understood how porous primary spheres are, so BET may or may not measure the sphere equivalent surface area. BET measurements of carbon black particles show these particles are typically non-porous and BET and

geometric surface areas are similar (Lahaye and Prado, 1981). Diesel aggregates appear visually similar to carbon black, so this measurement may be a reasonable method for estimating geometric surface area. However, it is neither an online nor a fast technique and it requires a large sample mass. Surface area estimated from either of the other two techniques that rely on diffusion charging or mobility diameter measurement are more practical to an engine manufacturer interested in determining the effect of engine or emission control design because the surface area they respond to is more relevant.

Methods that use unipolar diffusion charging and subsequent measurement of the particle charge result in estimates of the active surface within a specified size regime (Rogak and Flagen., 1992, Jung and Kittelson, 2005). Equivalent surface is obtained from SMPS or similar measurements of mobility diameter. Because of its relatively widespread use and simplicity, further discussion is focused on different aspects of diffusion charging.

Diffusion Charging

A diffusion charger (DC) can be used to measure the total active surface area of particulate matter. The active surface is the effective surface area available for mass transfer in a kinetically limited situation. In this technique, positively charged ions are formed by a corona discharge in the DC. These ions charge the particles in the sampled aerosol stream and the charged aerosol particles collect on a filter. The current flowing from the filter to ground potential is measured and is proportional to the number of ions attached to the particles. For spherical particles in the free molecular range, the attachment is proportional to the surface area of the particles and is independent of composition (Adachi et al., 1985). In the continuum regime, the response is proportional to the mobility diameter.

Charging in the transition regime is more complex. Depending on instrument design, the proportionality as a function of particle size is different because of differences in the

charging process and particle losses. To quantify this process, the charging parameter, $N \cdot t$, where N is the number concentration of ions and t is the length of time over which charging occurs is used. The charged fraction depends on the $N \cdot t$ product, particle size, and the ion-particle combination coefficient (Pui et al., 1988). Different $N \cdot t$ products in different commercial chargers lead to different proportionalities, although this is just a calibration issue.

Jung and Kittelson (2005) found the responses of two diffusion chargers (LQ1-DC manufactured by Matter Engineering AG and the Electrical Aerosol Detector (EAD) manufactured by TSI) to spherical particles was proportional to $d_m^{1.36}$ and $d_m^{1.13}$, respectively. Ku and Maynard (2005) obtained similar results using the LQ1-DC and monodisperse silver aggregates. Fissan et al. (2007) found the EAD response function between 10 nm and 100 nm was proportional to $d_m^{1.133}$. The response of LQ1-DC agreed with the theoretically calculated active surface area, which was proportional to $d_m^{1.39}$ within 2.4% error. This result was consistent with Ntziachristos et al. (2001) who found $d_m^{1.37}$ proportionality for ASMO (a diffusion charger manufactured by Dekati). The sensitivity of these methods is roughly 10 $\mu m^2/cm^3$. Comparison with the rough calculations shown in Table 1 suggests that this technique should be sufficiently sensitive to changes in both the nucleation and accumulation modes in dilute Diesel exhaust.

The active surface technique is often combined with other measures to provide additional information. For example, the ratio of DC to CPC gives a measure of the average surface area per particle (Asbach et al., 2008). The DC to PAS ratio provides indication of chemical composition because DC measurement is independent of composition while the PAS has high sensitivity to the carbonaceous fraction (Kittelson et al., 2005). An instrument has recently been developed called the diffusion size classifier that includes a unipolar charger and electrometer, and a diffusion battery screen (Fierz et al., 2008). This

combination allows number concentration and “average diameter” to be measured, given a number of assumptions.

Application to Diesel Particulate Matter

Previous studies using particles of known size and composition have shown the DC response functions are predicable and consistent with theory. The application of diffusion charging instruments to DPM is not as straightforward. Issues include particle morphology, particle size regime, chemical composition, and pre-existing charge effects. Many of these issues were discussed earlier as they relate to particle size measurements. A specific new concern is the fact that the response function of diffusion chargers is typically based on a calibration with monodisperse particles within a specified range. Extending or narrowing this range will change the functional dependence. Thus, in cases where both the nucleation and accumulation modes contribute significantly to the surface area (or more generally, for polydisperse aerosols), the expected response is difficult to predict and more validation is needed.

Only a very small dependence on composition has been identified (Shin et al., 2009, Jung and Kittelson, 2005b), so this effect is not likely to play a significant role for DPM sampling because changes in concentration will dominate response. However, Jung and Kittelson (2005b) showed how humidity effects charging, and suggested sample dilution or drying may be needed. Work by Qi et al. (2009) showed that the unipolar charging process is sensitive to the amount of pre-existing charge on particles entering the charger. They quantified the bias on the surface area response of the NSAM (Shin et al. 2007; Fissan et al. 2007). Particles sized between 50 and 200 nm carrying 1 to 10 elementary charges increase the measured surface area by a factor of 1 to 1.3. For a given number of charges, smaller particles bias the measurement more than larger ones. A solution is to add a bipolar neutralizer upstream of the diffusion charger or add a series combination of a negative and positive unipolar charger.

Experimental measurements. The following example is given to illustrate how combining metrics and methods can lead to useful information. In this case, total active surface area was measured with an SMPS (with $d_m^{1.4}$ weighting) operated with and without a CS. The SMPS active surface measurement is used as a surrogate for active surface measured by a diffusion charger. Measurements were made at University of Minnesota's Center for Diesel Research using a 2004-emissions compliant Cummins heavy-duty Diesel engine that was equipped with a continuously regenerating trap (CRT®) and fueled 50% biodiesel. Data from 2 modes are shown in Figure 13: "low load" corresponding to 1800 RPM, 603 Nm and "high load" corresponding to 1800 RPM, 1388 Nm.

Figure 13 shows number distributions for cases with and without the CRT and with and without the CS upstream of the SMPS. Summary results in Table 6 show that for the low load condition, use of the CRT results in >99.9% reductions in total and solid particle surface area. However, for the high load case, there was only a 66% reduction in total surface area but >99.9% for solid particle surface area. The only modest reduction in surface area is attributed to high levels of particle-forming sulfate production by the CRT during high exhaust temperature operation that occurs during high but not low load operation. Use of the CS enables us to elucidate the nature of these emissions. For example, one can better estimate under what conditions sulfate production occurs and measure the surface area concentration of particles that form as a result. These simple yet but powerful results would be relevant to most DPM measurement stakeholders.

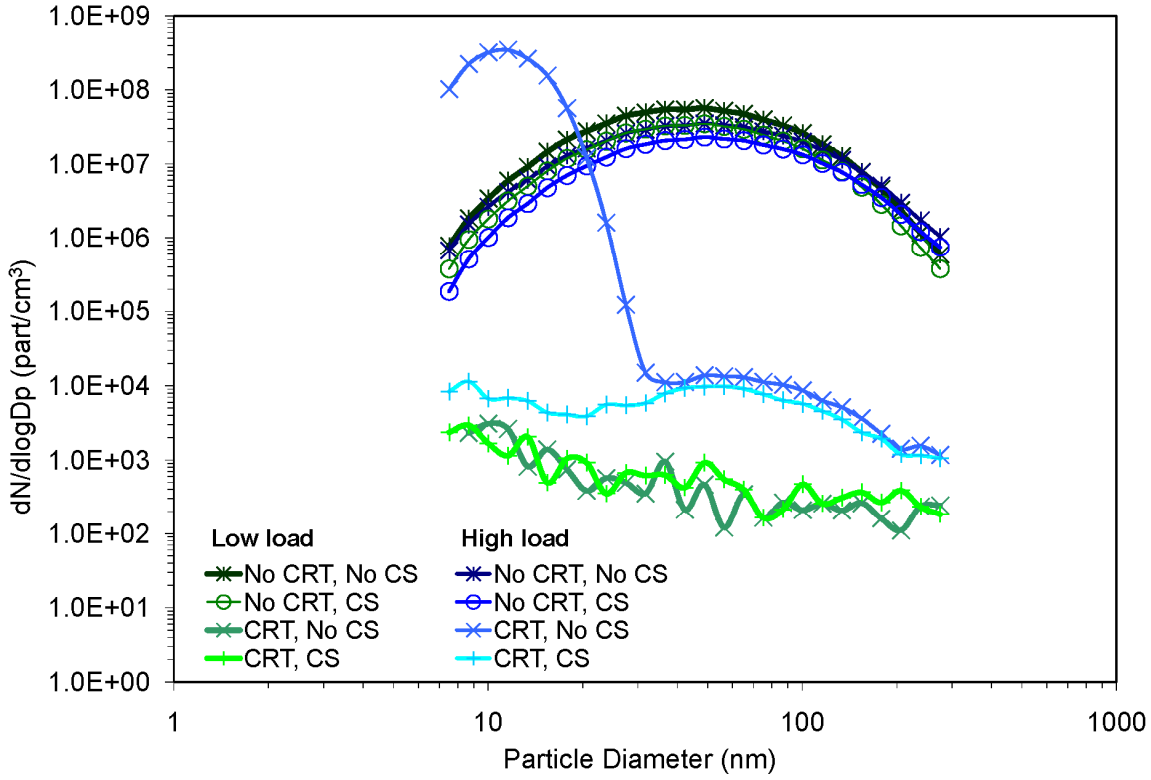

Figure 13. Number distributions measured in raw exhaust and downstream of a CRT from a 2004-emissions compliant Cummins Diesel engine fueled with 50% biodiesel fuel. Data is shown with and without the CRT and with and without a catalytic stripper used to remove semi-volatile content

Table 6. Active surface area reduction with use of a CRT

		Active surface area $\mu m^2/cm^3$	Solid active surface area $\mu m^2/cm^3$
Low load	Raw exhaust	36000	22000
	Raw exhaust + CRT	0.70	0.92
	Percent reduction	99.998	99.996
High load	Raw exhaust	27000	18000
	Raw exhaust + CRT	9100	9.7
	Percent reduction	66.296	99.946

Chapter 3: Diesel Engine Exhaust Aerosol Measurements Using Air-Ejector and Porous Wall Dilution Techniques

Introduction

Different sampling systems and methods are used to measure Diesel exhaust aerosol. The method is often optimized for a metric that is used to comply with a standard. This is the case with the mass and number standards used to evaluate Diesel exhaust. However, a method optimized for one metric like mass is not necessarily optimized for particle number. Further, it is not uncommon for metrics to poorly correlate with each other (Mayer et al., 1998, Hall et al., 2001). Vouitsis, et al. (2003) reviewed many sampling methods, including those intended for measuring regulated and non-regulated emissions for low-emitting Diesel engines. Burtscher (2005) and Mohr (2005) reviewed many instruments and measurement principles with a focus on non-mass based measurements. Despite the many sampling methods and instruments available for measuring Diesel exhaust aerosol, no combination is totally satisfactory in all instances. This is particularly true for low mass emitting engines where particle number emissions are a concern such as is the case in the European Union. The University of Minnesota's engines laboratory has promoted the development of alternative methods to the gravimetric method for the measurement of Diesel exhaust aerosol (Swanson et al., 2010), and in this chapter alternative designs for a porous tube dilutor and residence time chamber are presented.

In contrast to full-flow dilution tunnel measurements designed to determine compliance with a standard, laboratory measurements are often made in an attempt to mimic the particle size and concentration of Diesel aerosols found on-road under real-world dilution conditions using partial flow systems. The Coordinating Research Council's E-43 project made particle number and size measurements on-road and tried to duplicate those measurements in the laboratory (Kittelson et al., 2002, 2006a). This study and others

have shown that careful attention must be paid to dilution tunnel design and operation, dilutor geometry, dilution ratio, dilution rate, transfer line size and placement, residence chamber design, residence time, heat loss, and dilution air temperature because these parameters influence nanoparticle formation. For these measurements, only a small fraction of the total exhaust flow is diluted often two or more times so that the resulting concentrations are within the range of the aerosol instrumentation. After primary dilution, the exhaust flows through a residence time chamber where particles nucleate and grow before being diluted again to further reduce the number concentration and to quench the aerosol growth process. Numerous studies (Khalek et al. 1999, 2000, Kittelson et al., 2002) have described in detail how many of these parameters impact nanoparticle formation.

Their results show that nanoparticle formation and growth is favored by low dilution air and tunnel temperatures and high relative humidity. Particles appear larger as the residence time is increased due to growth via adsorption of gaseous compounds and coagulation. The dilution ratio and dilution rate are also important variables. The exact origin of the nucleation mode and the concentrations of precursor species are not often known so sensitivity analyses are needed to determine how strongly the dilution ratio and rate influence particle formation. Primary dilution ratios between 5 and 50:1 typically maximize particle formation. Typical secondary dilution ratios are also 5 and 50:1 but the exact value does not generally influence particle size or concentration. For a given engine condition, the dilution ratio that produces peak particle formation will depend on the sampling conditions and the concentration of gas phase species that contribute to nucleation and growth.

The literature reviewed above pertains to steady-state engine operation. Few researchers have attempted to evaluate particle size and number emissions during transient engine operation in the laboratory and those that do use typically must vary the dilution ratio

(Khalek et al., 2003, Ntziachristos et al., 2004, Liu et al., 2007). In summary, because the formation of semi-volatile particles strongly depends on the sampling conditions, the variability of these methods is high. Even so, sampling systems and methods designed to mimic real-world dilution paying particular attention to quantifying solid and semi-volatile nanoparticles have been proposed (Kasper, 2005).

The focus of this work is two evaluate two parameters impacting the dilution process: dilutor geometry and the residence time or aging chamber using two different dilution concepts: air-ejector and porous tube. Dilutor geometry determines how the exhaust sample is diluted, the rate at which it is diluted, and it can have a great impact on particle losses. The residence time chamber is important because flowrates, temperatures, and pressures in this chamber depend on the primary dilution and influence particle growth and the measured particle size distribution. Therefore, the residence time chamber is specific to the dilution geometry. Further design details are given in the experimental sections.

The air-ejector and porous tube dilutors are widely used. In the porous tube dilutor, dilution air is introduced under slight pressure into a cylindrical stainless steel chamber through the walls of a porous sintered metal tube. The air permeates the porous tube, creating a virtual “wall” of air. As a result, particle and particle precursor losses are held to a minimum. The porous tube concept has been used previously in the literature with varying degrees of success. Newton et al. (1980) proposed an early version of porous tube dilution. Mikkanen et al. (2001) extended the concept to Diesel engine exhaust dilution. A commercial version (Dekati FPS) of Mikkanen et al.’s design is described in Ntziachristos et al. (2004). The European Particulates project evaluated a similar device and found that during steady-state and transient operation exhaust pulsations pulled and pushed exhaust in and out of the dilutor, causing a significant variation in dilution ratio. This consequence is less of an issue for ejector dilutor because they operate at critical

flow conditions. Ntziachristos et al. (2008) evaluated a concept where the exhaust gas was sampled at atmospheric pressure through capillary tube that was intended to reduce pulsations. They found that the new concept leads to constant DR sampling, independent of exhaust gas pressure and pressure variations. However, the very low flow through the capillary tube would lead to large losses in nanoparticle precursors. Pyykönen et al. (2007) modeled and experimentally measured nucleation in a perforated tube dilutor (similar but not the same as a porous tube) and concluded that a chemical component's "nucleation tendency" would be accurately reproduced in this type of dilutor.

In contrast to the porous tube, the air-ejector uses a venturi to draw a sample of exhaust before it is very turbulently and quickly mixed with dilution air. Air-ejector pumps have been used by Khalek et al. (1998, 1999), Giechaskiel et al. (2005), Wong et al. (2003), and Kittelson et al. (2002, 2005, 2006a). However, no studies have compared the impact of dilutor geometry on nanoparticle formation under constant sampling conditions. Lyyränen et al. (2004) evaluated a porous tube dilutor, ejector dilutor, a AVL SPC 472 partial flow diluter, and various combinations of those listed. Results suggested particle size and concentration depended strongly on dilutor geometry depended strongly on dilutor geometry.

In this section, the design of an alternative porous tube dilutor is presented. For comparison, a TD260 air-ejector manufactured by Air-Vac-Engineering was evaluated. The design of a residence time chamber optimized to integrate with these dilution devices is presented and optimum design considerations are discussed. Exhaust aerosols were generated by a Deere 4045 Diesel engine running at low speed (1400 rpm) and low load (50 Nm). The primary dilution parameters varied included dilution air temperature and dilution ratio and particle measurements were made at various locations along the centerline to evaluate particle growth in the chamber.

Experimental section

Dilution system design and description

Transfer line

The transfer line is typically a short section of stainless tubing used to transport exhaust from the tailpipe to the dilutor. Wei et al. (2001a, b) showed that gas phase volatile and semi-volatile nanoparticle precursors can reversibly adsorb to the transfer line before primary dilution occurs, thus affecting the magnitude of the nucleation mode. To ensure a high transfer efficiency of particle precursors, exhaust must be transported using high flow rates and a relatively small value of the ratio of the transfer line surface area to the flowrate. Most dilution systems rely on a change in exhaust flow to change the dilution ratio, therefore a change in the penetration of precursors will inevitably lead to a change in number concentration or size of particles that cannot solely be attributed to a change in the physics resulting from a change in dilution ratio. The solution is a system designed such that the penetration is near 100% for all cases.

The efficiency of transporting gas phase compounds in a tube is shown below. For fully developed laminar flow, the penetration depends on the residence time (t), Sherwood number (Sh, 3.66), diffusion coefficient (D_i) and the diameter of the transfer line (D_t) as shown.

$$\text{Penetration} = \text{EXP}\left(-\frac{4 \cdot \text{Sh} \cdot D_i \cdot t}{D_t^2}\right)$$

This expression was used to calculate the penetration of tetracosane ($C_{24}H_{50}$) vapor for varying transfer line flowrates, lengths and temperatures where the transfer line inner diameter (ID) remained constant at 6.25 mm. It is assumed that molecules that diffuse to the wall stick to it. The results are shown in Figure 14. The penetration of tetracosane depends on the transfer line length, flowrate and to a less extent, temperature. In the case

shown, the penetration is >90% for typical exhaust temperatures and primary dilution ratios commonly used. The transfer line length is a variable that is impacted by the type of dilutor and as shown in Figure 14 increases in line length reduce penetration. At a DR of 14 that corresponds to a total dilute exhaust flow 180 standard liters per minute (slpm), a centimeter change in the transfer line length results in a very small change in penetration (penetration is ~98%). As a result, the exhaust sample should be representative of the exhaust flow, penetration should not change between dilutors if the transfer line length is held constant, and the magnitude of the nucleation mode should be less sensitive to dilution ratio because the loss of volatile and semi-volatile material will be minimized. This calculation is semi-quantitative because it was assumed that tetracosane is representative of the many HC species present in diesel exhaust, and that there is no interaction of these HCs with each other or PM during the dilution process.

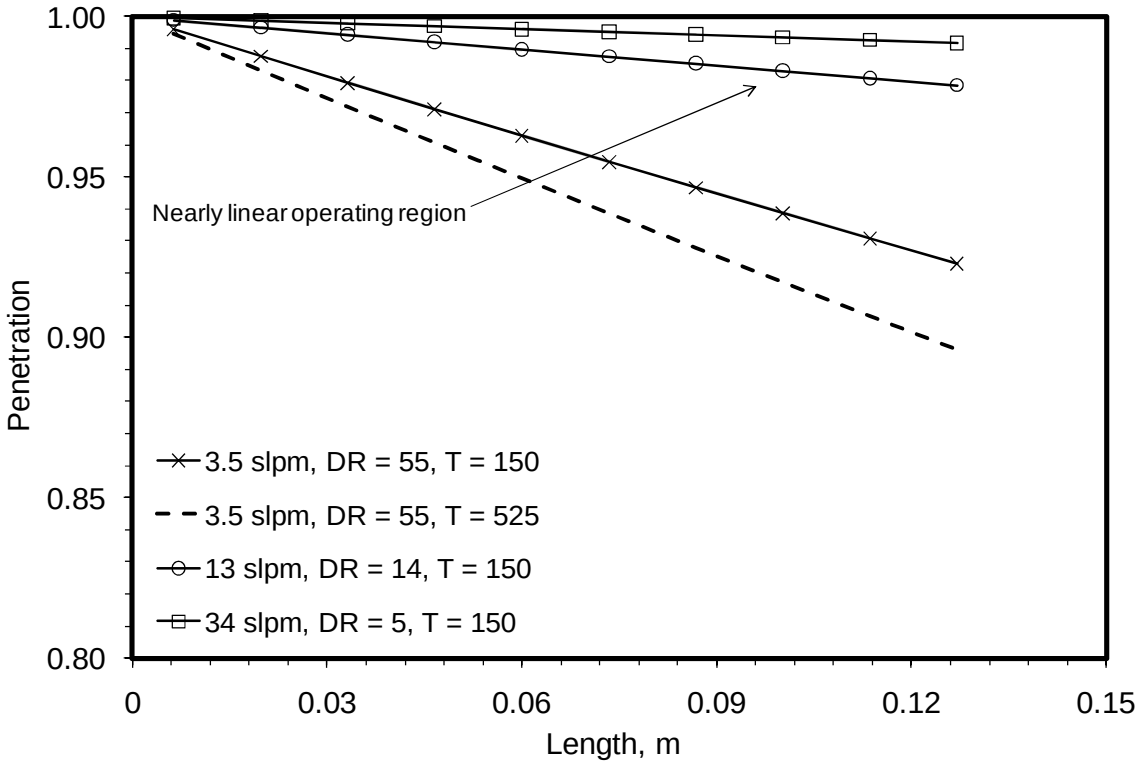

Figure 14. Penetration of gaseous nanoparticle precursors ($C_{24}H_{50}$) for varying transfer line flowrates, lengths and temperatures. The transfer line inner diameter is 6.25 mm and the total dilute exhaust flow is 180 slpm

Porous tube dilutor

The porous tube dilutor shown in Figure 15 consists of a porous stainless steel tube mounted concentrically within a stainless steel cylinder that is surrounded cooling jacket. During sampling, dilution air enters in a counter flow fashion and permeates the porous tube creating a virtual "wall" of air that may reduce particle loss. The design used a porous tube manufactured by Mott Corporation that was 152 mm long and had ID and ODs of 6.25 and 9.53 mm, respectively. The porous material has a gas permeability coefficient of 5 and the pressure drop across the porous wall is ~50 kPa at a flowrate of ~166 lpm. At this flowrate, the estimated residence time of the dilute exhaust mixture in the porous tube is ~2.7 ms.

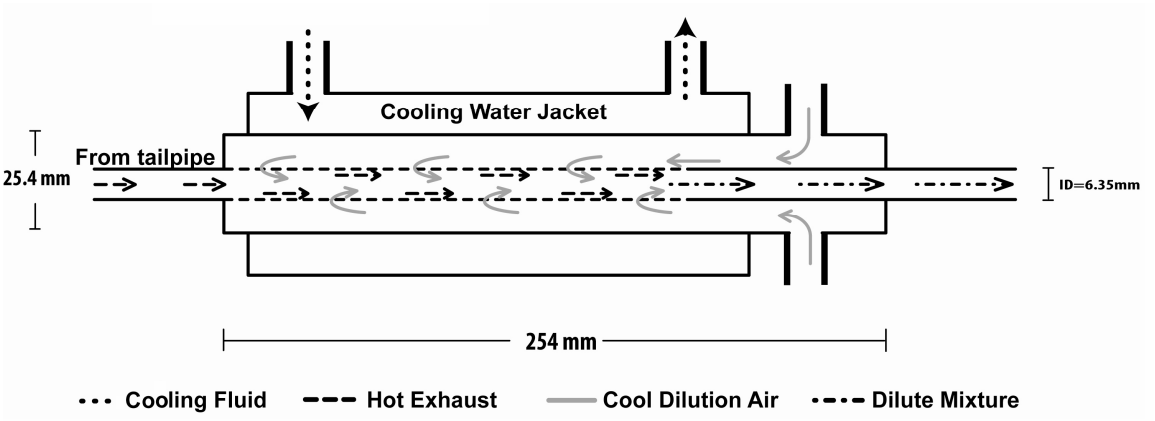

Figure 15. Schematic of a porous wall dilutor

Ejector dilutor

The ejector dilutor used in this study and shown in Figure 16 is a TD260 air-ejector manufactured by Air-Vac-Engineering with a critical flow orifice upstream of the dilution region. Typically, increasing the ejector pressure and increasing the ejector size increases the dilution ratio, while increasing the critical orifice size, decreasing the size of the ejector and reducing the ejector pressure decreases the dilution ratio. To vary the dilution ratio in this study, the orifice size and the dilution air pressure were changed such that the total flow was constant (180 slpm). At this flowrate, the estimated residence time of the dilute exhaust mixture in the ejector is ~0.3 ms. Orifice sizes that gave DRs of 55, 14, and 5 were 0.71 mm, 1.5 mm, and 2.4 mm, respectively. Similarly, dilution pressures resulting in total flows of 180 slpm were 30 - 40 psig. After dilution, the sample aerosol passes through a residence time chamber that is described next.

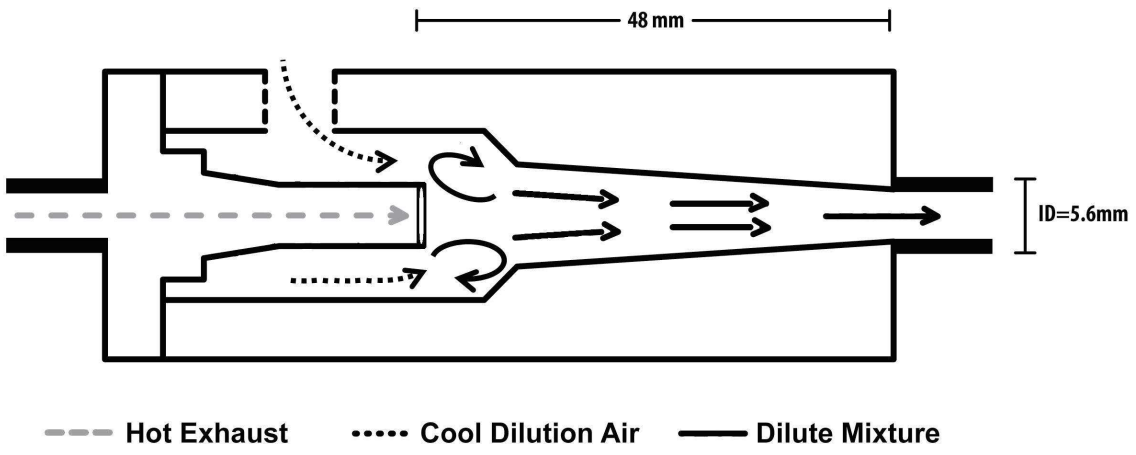

Figure 16. Schematic of an air-ejector dilutor

Residence time chamber

Figure 17 shows the residence time chamber used with both the ejector and porous tube dilutors that consists of a single piece of stainless steel tubing (100 cm long, 6 cm ID) with a cone shaped inlet (divergence angle is 8°) designed to smoothly transition the flow from a small to large diameter tube. The flow in the cylindrical region is turbulent (RE = 4000) to promote mixing and the total flowrate is constant, 180 slpm. When used with the ejector dilutor, the dilutor pressure and orifice size are changed to maintain this flow. For the porous tube dilutor, the flow is set by a mass flow controller pulling dilute exhaust through the tunnel outlet and another mass flow controller varies the dilution air flow. These different control schemes result in different pressures in the tunnel. For the ejector dilutor, the tunnel is above atmospheric pressure (~102 kPa at outlet) and a vent is required. For the porous tube, the tunnel pressure is below atmospheric pressure (~86 kPa) at the outlet. The reduced pressure is not characteristic of the technique itself but a result of the fittings and tube diameter in the porous wall dilutor that were not optimized for low-pressure drops. A water jacket around the tunnel maintains a constant tunnel wall temperature by circulating temperature controlled water. The water flowrate is high enough so that the circulating water does not change the temperature by > 1°C. The water

temperature is always set to the same temperature as the dilution air, leading to near isothermal conditions in the tunnel.

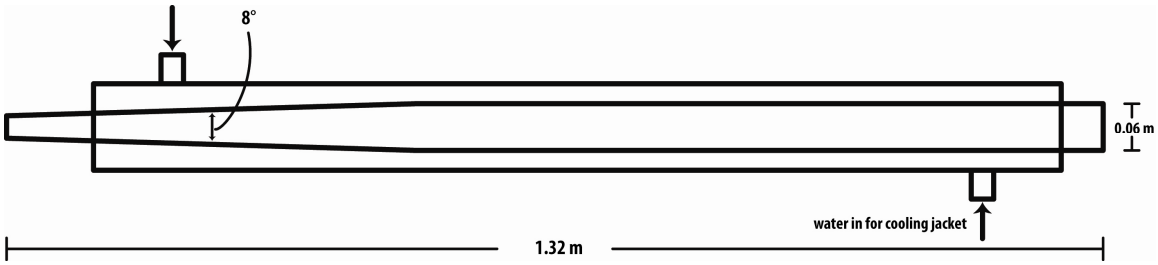

Figure 17. Residence time chamber schematic

To optimize the design of the residence time chamber velocity and temperature distributions in the inlet cone and cylindrical chamber were numerically modeled using ANSYS. Other residence time chambers previously built in the University of Minnesota's engines lab were also modeled. Model results show that for large entrance cone angles (~25º) typical in older designs large recirculation zones exist, with 20% of the flow recirculating in the residence time chamber. This results in a residence time that cannot be easily calculated. In the tunnel design shown in Figure 17, there is no recirculation. The mean fluid temperature is calculated as a function of tunnel length for a DR of 14, exhaust temperature of 152 ºC and two dilution air temperatures. Results in Figure 18 indicate that heat transfer occurs is minimal and the temperatures are almost constant throughout the length of the tunnel. This fact simplifies the particle growth calculations shown later. Mass transfer calculations show that gas phase particle precursors are not lost to the walls of the tunnel. For example, the calculated penetration of $C_{24}H_{50}$ vapor is 95%.

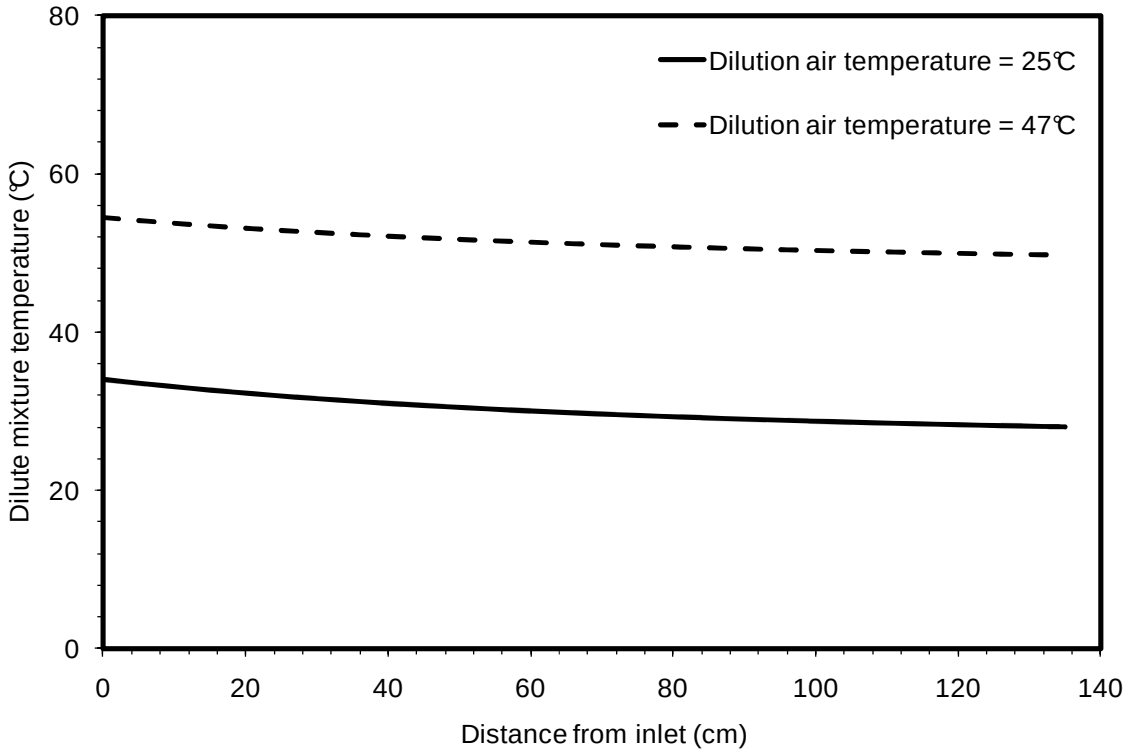

Figure 18. Mean fluid temperature in residence time chamber as a function of tunnel length for a DR of 14, exhaust temperature of 152 ºC and two dilution air temperatures. The tunnel wall temperature is set to the dilution air temperature for each case. Results obtained from ANSYS model

Test methods and procedures

Experimental apparatus

The test engine was a 2005 John Deere 4.5-liter, 4045H engine producing 129 kW @ 2400 rpm and 645 Nm @ 1400 rpm. This engine is turbocharged and intercooled with common rail fuel injection and has EPA tier 2 approval for off-highway applications. The engine was fueled with ultra low sulfur Diesel fuel containing <15 ppm sulfur. The engine was operated at 1400 rpm, 50 N-m and the emission characteristics for this condition are shown in

Table 7. Previous work (Kittelson et al., 2010) has shown that this engine condition generates a large nucleation mode.

Table 7. Engine exhaust parameters. Particle data (mass and number) refer to characteristics of the accumulation mode derived from lognormal fits to data averaged for both dilution systems for all tests conducted at 1400 rpm, 50 N-m, residence time of 0.3 s. Mass emissions are based on SMPS size distributions inverted to mass based on Park et al. (2003).

	Units	Avg	Stdev
Exhaust temperature	ºC	152	2
NO	ppm	187	1.3
NO_2	ppm	34	1.4
Mass	mg/m^3	7.2	0.7
Number concentration	$part/cm^3$	1.2E+07	3.9E+06
Geometric standard deviation	-	1.82	0.11
Number mean diameter	nm	52.9	11.2

Exhaust aerosol measurements were made as follows. Exhaust enters the stainless steel transfer line that was described earlier that was immersed in the exhaust flow and is passed through the transfer line to either the ejector or porous tube dilutor. The relevant dilution conditions that were evaluated are listed in Table 8. After dilution, the dilute exhaust mixture transverses residence time chamber where the residence time is varied by extracting the sample at various locations along the length of the chamber. For all measurements, the exhaust is diluted a second time with an ejector dilutor using a fixed dilution ratio of 16.5. Secondary dilution increases the total dilution ratio and is used to suppress aerosol growth and to reduce concentrations to measurable levels. Dilution ratios were determined as follows. Primary dilution ratios in the porous tube dilutor were determined from the mass flow controllers. Primary dilution ratios for the ejector dilutor were determined using the formula (raw NO)/(diluted NO) as determined by an AVL FTIR gas analyzer. Secondary dilution ratios for both types of dilutors were determined by measuring cold flows. A scanning mobility particle sizer was used to measure size

distributions of dilute engine exhaust. The SMPS was configured with a TSI 3081A electrostatic classifier and TSI 3010 CPC. It was configured to cover the size range of 13 to 500 nm over a period of 60 s with a 30 s interval between scans.

Table 8. Dilution conditions for porous tube and ejector dilution experiments. All experiments run at 1400 rpm, 50 Nm

	Dilution ratio			Dilution air temperature (°C)		Residence time (s)		
	5	14	55	25	47	0.3	0.75	1.0
Ejector dilutor	x	x	x	x	x	x	x	x
Porous tube		x		x	x	x	x	x

Results

Influence of dilution ratio

Figure 19 shows the impact of varying the dilution ratio from 5 to 55 on the particle number size distribution when the dilution air temperature and residence time are held constant at 25 °C and 1.0 s, respectively. In this case, the exhaust was diluted with the ejector dilutor. The results show a bimodal structure with a nucleation mode with a geometric number mean diameter between 10 and 30 nm range and an accumulation mode with a mean diameter near 50 nm. The accumulation mode appears minimally influenced by the dilution condition changes, consistent with the idea that the accumulation mode is composed primarily of carbonaceous aggregates that are not affected by the changes in the dilution conditions. On the other hand, the shape and magnitude of the nucleation mode is clearly altered by varying the dilution ratio. At a high dilution ratio (55), there is only a hint of bimodality with a nucleation mode that appears quenched by high dilution, which reduces the vapor pressure of the growth species. However, for lower dilution ratios, there is an order of magnitude increase in particle number concentration and the mean particle diameter increases by almost 20 nm. The total number concentration ranged from 4×10^8 to 4×10^{10} particles/cm^3 for dilution

ratios of 55 and 5:1, respectively. These results are consistent with Khalek et al. (1999) who also showed orders of magnitude changes in number concentration with dilution ratio. Since the focus of the study was to evaluate the nucleation tendency of diesel aerosol using different methods of dilution the 14:1 dilution ratio was chosen as the test condition for comparisons between the ejector and porous tube dilution systems.

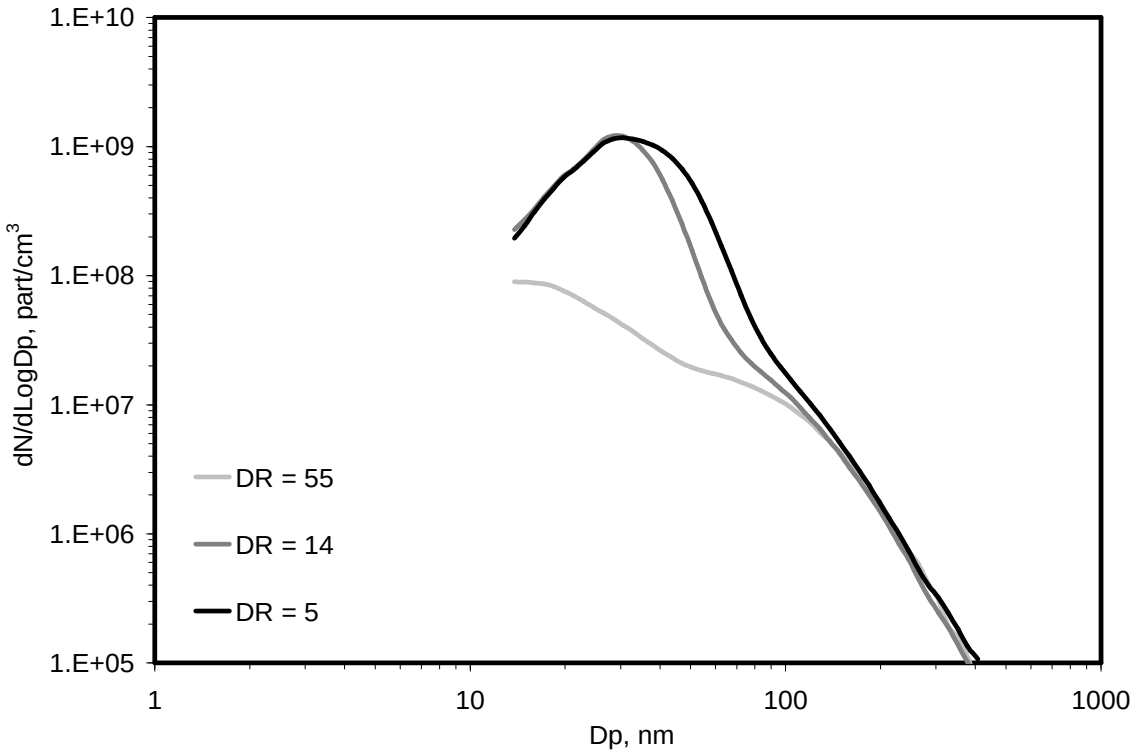

Figure 19. Influence of dilution ratio on the particle size distribution for a dilution air temperature of 25 °C and a residence time of 1.0 s. Exhaust was diluted with the ejector dilutor

Ejector and porous tube dilutor comparison

Figure 20, Figure 21, and Figure 22 show the influence of dilutor type and dilution air temperature on the particle size number distribution at a primary dilution ratio of 14 (total dilution ratio 230:1), and dilution temperatures of 25 and 47°C. The results show that size distributions downstream of the porous tube and ejector dilutor were qualitatively similar

in shape although porous tube dilutor concentrations were consistently higher with larger geometric mean diameters. These differences are quantified in Figure 23 and Figure 24 with summary statistics. The summary statistics shown in these tables were calculated from fits to the nucleation mode that was roughly lognormal with a geometric standard deviation that ranged from 1.35 to 1.25 with small standard deviations for longer residence times.

For both dilutors, the particle number concentration was roughly 50% lower at higher dilution air temperatures. This is because the higher temperature slows down the nucleation rate in the dilutor. Conversely, the geometric mean particle diameter was, on average, a few nanometers smaller at lower temperatures because of decreased growth due to lower molecular speeds of condensing molecules at lower temperature. The results also show the mode particle diameter to be larger for exhaust aerosol diluted with the porous tube dilutor than with the ejector dilutor. At a residence time of 0.3 s, porous tube dilutor particles are larger by about 5 nm at both dilution air temperatures. By 1.0 s, particles size is nearly the same, with porous tube particles 2 nm smaller at 25 °C but about 2 nm larger at 47 °C. Particle concentrations were always 50 to 100% higher downstream for the porous tube dilutor.

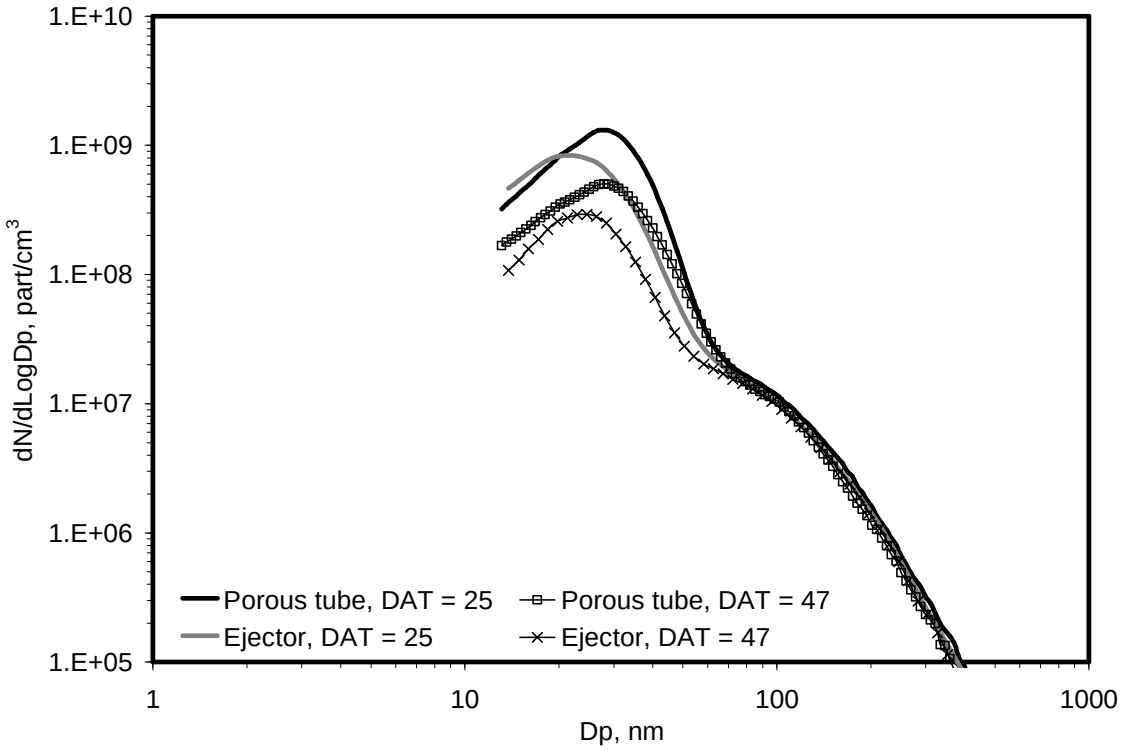

Figure 20. Influence of dilutor type and dilution air temperature (DAT) for a residence time of 0.3 s on particle size distributions

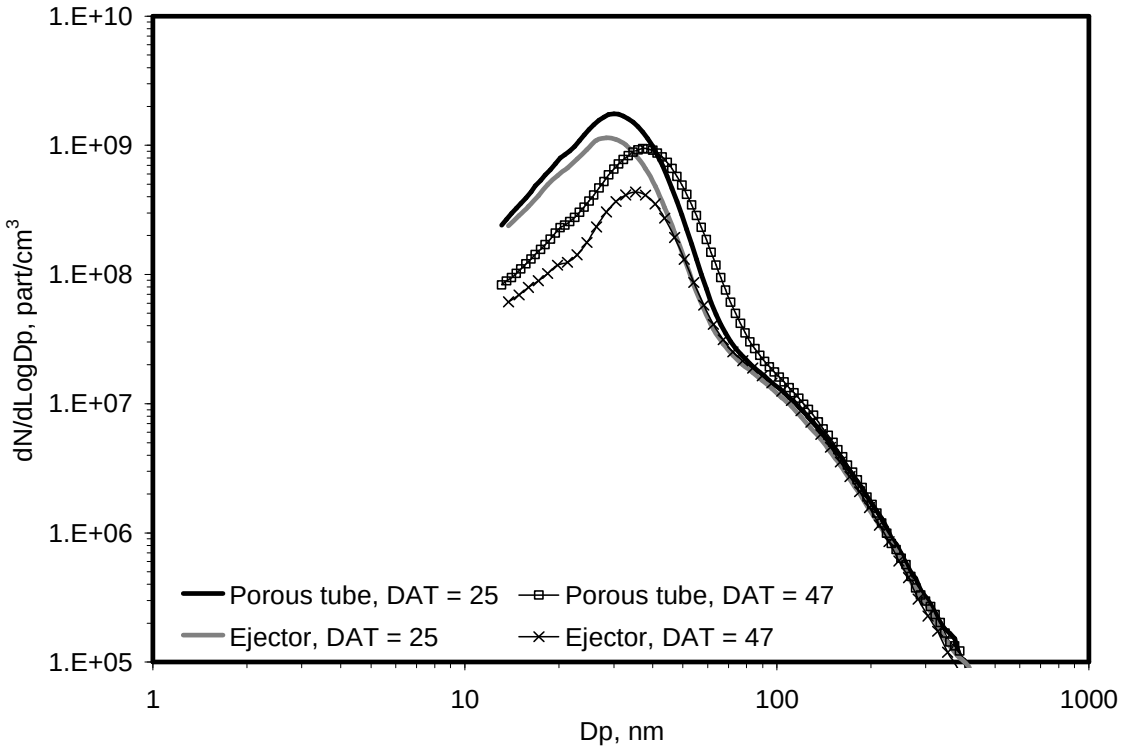

Figure 21. Influence of dilutor type and dilution air temperature (DAT) for a residence time of 0.75 s on particle size distributions

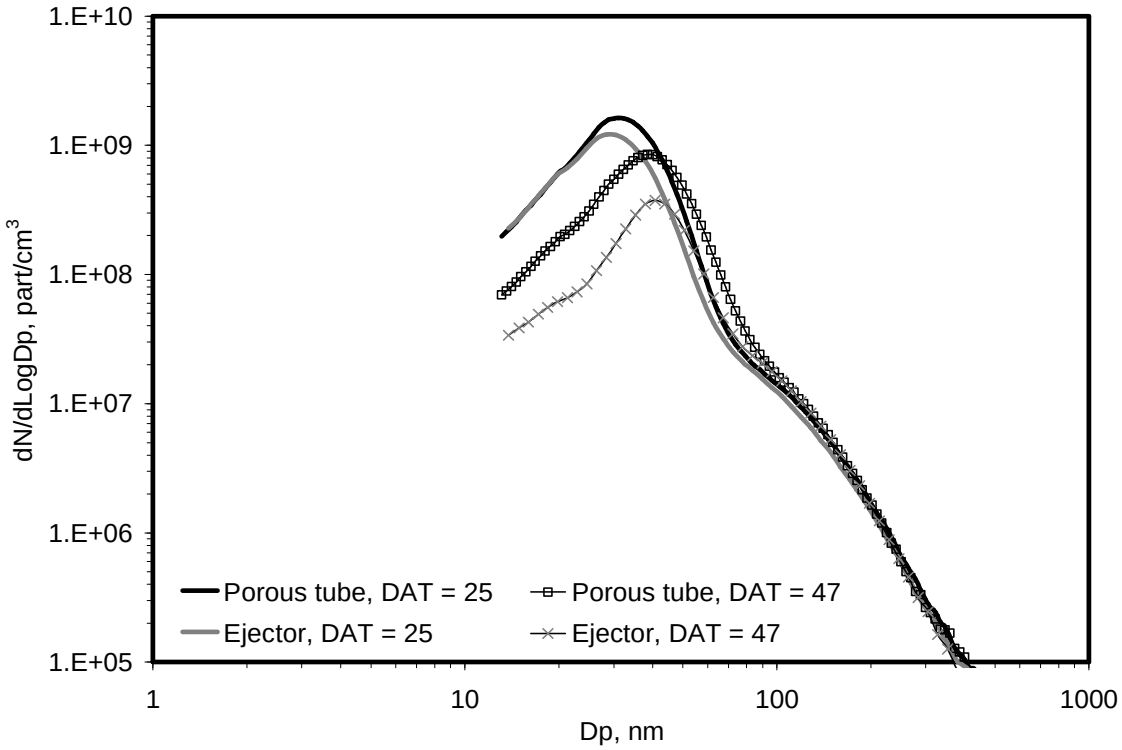

Figure 22. Influence of dilutor type and dilution air temperature (DAT) for a residence time of 1.0 s on particle size distributions

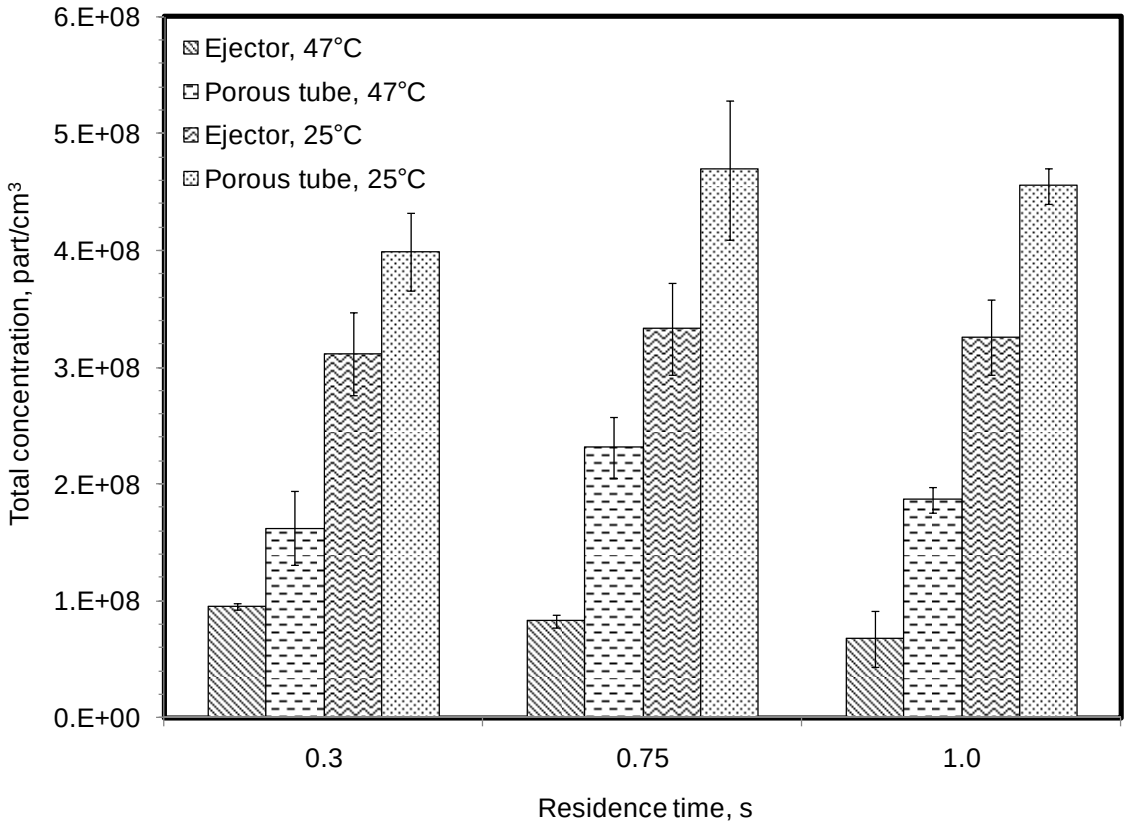

Figure 23. Total nucleation mode number concentration summary statistics as a function of dilutor type, residence time, and dilution air temperature calculated from lognormal fits to experimental data. Error bars are calculated as standard deviation of 5 SMPS scans

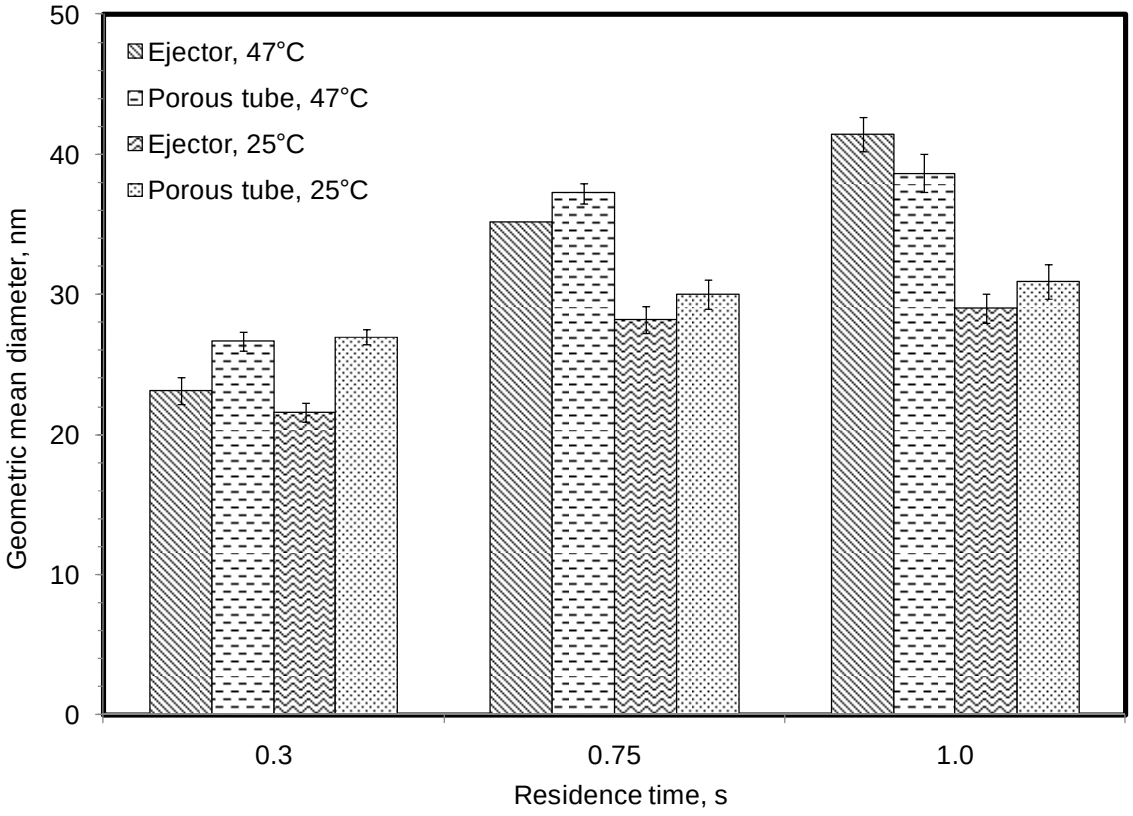

Figure 24. Average geometric mean diameter summary statistics as a function of dilutor type, residence time, and dilution air temperature calculated from lognormal fits to experimental data. Error bars are calculated as standard deviation of 5 SMPS scans

Growth of particles during dilution and residence time

Species that likely play a predominant role in nucleation in Diesel exhaust are sulfuric acid and possibly heavy hydrocarbons. Heteromolecular sulfuric acid-water nucleation leads to the formation of nucleation mode particles about 1 nm in diameter (Mirabel and Katz, 1974). Growth occurs via condensation of sulfuric acid and hydrocarbon vapors. Coagulation was not considered here because its influence is small. Tunnel concentrations were ~1E7 part/cm^3 and the characteristic time scale for coagulation at this concentration is on the order of minutes. In the absence of coagulation, the growth rate depends on the types and concentrations of growth species, the concentration of

carbonaceous aggregates in the exhaust and other exhaust/dilution parameters (Khalek et al., 2000). In this case, fuel sulfur content was very low (<15 ppm) and no diesel oxidation catalyst was used. Therefore, only heavy hydrocarbons, rather than sulfuric acid are considered as the condensing species. The following model was developed to qualitatively explain the differences in dilutor type, residence time and temperature on the particle size distribution. The approach is similar to that used by Lemmetty et al. (2006).

The dilution ratio is assumed to vary as an exponential function of time in each of the dilutors with an adjustable time constant and then remain constant as described by the following functions. The system is assumed to be isothermal. Thus, the partial pressure of the condensing species, the solid particle concentration, and mean dilute exhaust temperature all vary subject to these expressions.

$$DR = 14^{t/t_d} \text{ for } t < t_d$$

$$DR = 14 \text{ for } t > t_d$$

Next, a free molecular growth model (Hinds, 1999) was applied to nuclei in the exhaust to model their growth as a function of time. The size of initial nuclei was set to 0.5 nm at t = 0 s and condensing hydrocarbon species is tetracosane ($C_{24}H_{50}$). Tetracosane is representative of the heavy hydrocarbons that typically comprise nucleation mode particles (Sakurai et al., 2003, Tobias et al., 2001). The model accounts to both hydrocarbon vapor depletion by adsorption onto carbonaceous solid particles and absorption into the growing particles themselves. Additional inputs to the model include the initial exhaust temperature (152°C) and dilution air temperature (47°C).

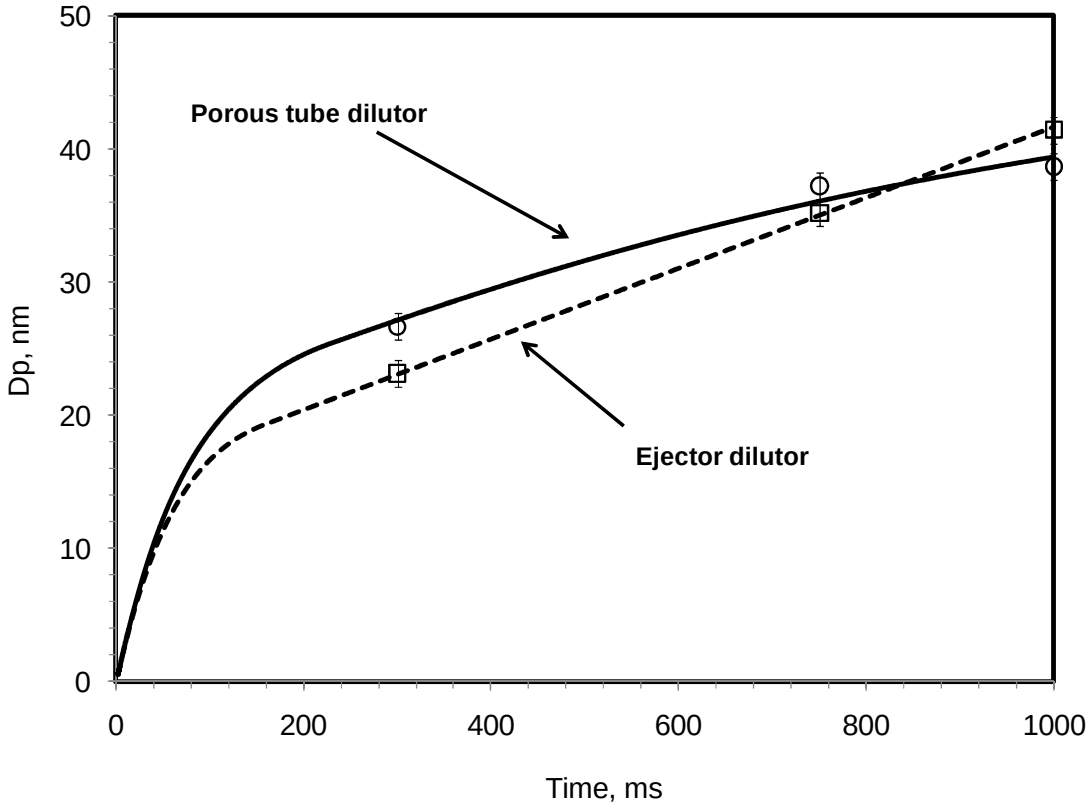

Figure 25. Model and experimental data for particle growth in the free molecular regime

Results from the model are shown in Figure 25 and Table 9 lists the fitted parameters: time constant, partial pressure of $C_{24}H_{50}$, and surface area of carbonaceous solid particles that deplete the condensing vapor. The partial pressure of $C_{24}H_{50}$ and surface area parameters were forced to be equal for both dilutors because that is physically realistic. The partial pressure of tetracosane (0.07 Pa) was the result of fitting because there was no independent measure of hydrocarbon concentration. However, the fitted value corresponds to 0.3 g/kW-hr, a value that is reasonable for a Tier 2 engine at this condition. For both the ejector and porous tube, the dilution rate expression and free molecular growth model appear to fit the data reasonable well. For ejector dilutor, the calculated particle growth rate is 26 nm/s, a value larger than the growth rate of 17 nm/s for the porous tube system although these rates are similar to rates than observed by

others at comparable conditions. For example, Khalek et al. (2000) measured a growth rate of 24 nm/s using a primary dilution temperature of 48 °C and dilution ratio of 12. The higher time constant for the porous tube suggests dilution occurs slower and as a result, particles appear larger. Larger particles subsequently deplete vapor faster, which leads to a slower overall growth rate. The time constant is nearly an order of magnitude higher than the residence time in each dilutor, but the trends are the same. Longer time constants suggest the exhaust is not fully mixed upon exiting the dilutor and there is additional dilution and mixing before the exhaust is sampled at 0.3 s.

Table 9. Fitted parameters include the time constant, partial pressure of $C_{24}H_{50}$, and surface area of carbonaceous solid particles that deplete the condensing vapor

	Time constant (τ_d)	$C_{24}H_{50}$ partial pressure	Surface area concentration
	ms	Pa	m^2/m^3
Ejector	160	0.07	0.3
Porous tube	228	0.07	0.3

Chapter 4: Evaluation of Thermal Denuder and Catalytic Stripper Methods for Solid Particle Measurements

Introduction

Diesel exhaust contains a complex mixture of particles and gases. Semi-volatile compounds like hydrocarbons and sulfur containing compounds are found as gases or vapors. HCs form from incomplete combustion and range in volatilities. They may be found in the vapor (Siegl et al., 1999; Schauer et al., 1999; Schmitz et al., 2000; Zielinska et al., 2004) or in the particulate phase (Lowenthal, et al., 1994; Schauer et al., 1999, Sakurai et al., 2003; Ristimäki et al., 2007). Sulfur dioxide gas can react to form sulfuric acid droplets or sulfates (Laresgoiti and Springer, 1977; Truex et al., 1980; Schneider et al., 2005). HCs and sulfur containing compounds that form nucleation mode particles are the focus of this study.

Nucleation mode particles emitted during most operating conditions are usually composed of nearly all semi-volatile material (Sakurai et al. 2003; Tobias et al. 2001; Kittelson et al., 2005; Kittelson, et al., 2006a). Operationally, “semi-volatile” means the particles will fully evaporate at 300°C within about a second or less. Modest concentrations of solid carbon or ash nanoparticles are present during idle or low load conditions. However, the precise chemical composition of the nucleation mode is not fully understood. Baumgard and Johnson (1996), Shi and Harrison (1999), Khalek et al. (2000), Kim et al. (2002a,b), and Vouitsis et al. (2005) have suggested that the formation of these particles is due to the nucleation of sulfuric acid and water, resulting in the formation of ~1 nm sized volatile particles. Nucleated particles grow by condensation and sorption of organic species. The relative fraction of each is influenced by fuel selection, engine condition, sampling conditions, and use of emission control. Tobias et al. (2001) and Sakurai et al. (2003) measured the composition of nanoparticles emitted by

engines without emission control and found the mass fraction of sulfur to be less than a few percent. These experiments are consistent with theory, for example, modeling by Vouitsis et al. (2005) and Vouitsis et al. (2008) suggests that engine out nucleation mode particles contain roughly 4% sulfate, the rest being organic carbon. Maricq et al. (2002) found that a Diesel oxidation catalyst (DOC) increased semi-volatile nucleation mode particle emissions when low sulfur (350 ppm) fuel was used and attributed the increase to an increase in fuel sulfur conversion to sulfate. Schneider et al. (2005) and Grose et al. (2006) directly measured the composition of nucleation mode particles downstream of DOC + Diesel particulate filter emission control systems and found particles were composed primarily of sulfuric acid or sulfuric acid that was partially neutralized by ammonia. The modeling results by Vouitsis et al. (2005, 2008) also show an increase in the fraction of sulfate in particles downstream an oxidizing catalyst, although they still predict a higher fraction of organic carbon than sulfate. This discrepancy could be explained by the fact that DOC + DPF systems are prone to sulfate storage and release effects (Swanson et al., 2009b) that significantly influence the composition of particles, making it quite difficult to define “average compositions.”

On the other hand, not all nanoparticles are semi-volatile. The CRC E-43 project found evidence of a distinct, non-volatile nucleation mode at idle for different vintages of heavy-duty Diesel engines, including 1988, 1993, and 1998 Cummins or Caterpillar engines (Kittelson et al., 2002; Kittelson et al., 2006a). This result was observed again in the University of Minnesota’s engines laboratory with a 1998 Caterpillar C-12 engine that emitted a non-volatile nucleation mode at light loads and idle (Jones and Kittelson, 2002; Kittelson et al., 2005) and has been observed by others (Filippo and Maricq, 2008). Evidence suggests that solid particles form when lube oil metals volatilize in the cylinder and later nucleate to form solid nuclei mode particles (Abdul-Khalek et al., 1998). The likelihood of metal nucleation at idle or very low load is enhanced because soot

production is low, leaving little carbonaceous surface area available to condense volatilized metals.

Evidence for the presence or absence of solid nanoparticles at other operating conditions is less clear. Recent experimental evidence supports the contention that solid nucleation mode particles between 3 and 10 nm are present in the exhaust during high load, high exhaust temperature operation (Rönkkö et al., 2007; Lahde et al., 2009; Lahde et al., 2010). Solid nanoparticles have been measured downstream of emission control systems (Johnson et al., 2009). One hypothesis is that nucleation mode particles form with a solid core and serve as sites for condensation and sorption of organic material during exhaust dilution (Rönkkö et al., 2007). This hypothesis is supported by physical models (Du and Yu, 2008). However, this mechanism would rule out the possibility of tiny solid particles downstream of highly efficient exhaust filtration devices but such particles have been observed (Johnson et al., 2009). Another explanation is that solid particles may be caused by an artifact of the measurement. For example, the thermal denuder (TD) used to determine volatility might not be efficiently removing very low volatility particles that form from combinations of sulfuric acid and unburned organic carbon vapors. In the current study, this explanation is investigated.

The semi-volatile particle removal efficiencies of the catalytic stripper (CS) and TD were evaluated to test the hypothesis that solid artifacts are formed. The TD and CS were challenged with atmospheric and laboratory generated aerosols that included organic carbon particles (tetracosane) and organic carbon particles (tetracosane and dioctyl sebacate) containing sulfuric acid. Tetracosane / sulfuric acid particles were chosen because they roughly simulate the composition of semi-volatile particles found in Diesel exhaust.

These experiments were not specifically designed to mimic or evaluate the performance of the volatile particle remover (VPR) used to determine compliance with the European Union's EURO 5/6 solid particle number standard (ECE/TRANS/WP.29/2008/62). However, the results are relevant in the context of the Particulate Measurement Programme's methodology because the "heating" component of these methods mirrors the VPR approach specified by the PMP method. The PMP methodology is used to measure the solid particle number concentration above a particle size of 23 nm at 50% counting efficiency using a VPR and a condensation particle counter. Understanding the performance of these methods is relevant because the TD and CS methods are often favored in practice over the exact PMP (e.g. VPR) method (Abdul-Khalek and Kittelson, 1995; Mohr et al., 2003; Ntziachristos et al., 2004; Ntziachristos et al., 2005a; Giechaskiel, et al., 2008). In addition, the California Air Resources Board (CARB) has and is evaluating this method (Robertson et al., 2007; Jung and Durbin, 2008; Johnson et al., 2009).

Instrumentation

Removal of semi-volatile material by the CS and TD was evaluated by placing them upstream of a scanning mobility particle sizer (SMPS). The SMPS consisted of a TSI nanoDMA and TSI 3025A condensation particle counter. The SMPS was operated with sheath and sample flows of 15 and 1.5 L/min, respectively, giving a size range of 3 to 60 nm. Size distributions include error bars that are calculated as the standard deviation of multiple measurements. The size and volume distributions of the challenge aerosols was measured with the engine exhaust particle sizer or EEPS (Johnson et al., 2004). Total volume concentrations are calculated by integrating the EEPS size distribution and converting to volume. For some experiments, particles are mixed and contain unknown mass fractions, so density is not known. Thus, volume concentrations of spherical particles are reported because they are directly measured and note that 1 $\mu m^3/cm^3$ = 1 $\mu g/m^3$ for particles of density 1 g/cm^3 to aid in the readers' estimation of mass.

Catalytic stripper – The CS removes the volatile and semi-volatile organic carbon organic fraction by passing dilute Diesel exhaust over an oxidation catalyst heated to 300°C. The flowrate depends on the catalyst size, but it is typically between 1 and 10 L/min. The CS used in this research is operated at 10 L/min and is similar in design to others described elsewhere (Abdul-Khalek and Kittelson, 1995; Kittelson and Stenitzer, 2003; Stenitzer, 2003). The CS had a washcoated ceramic substrate located upstream of the oxidation catalyst that trapped sulfur containing compounds that is referred to as the S-trap. Stenitzer (2003) estimated that particle penetration at 3 and 100 nm was 5% and 75%, respectively. Both the S-trap and oxidation catalyst were provided by Johnson Matthey.

Thermal denuder – The TD is used to remove volatile material by adsorption (Burtscher et al., 2001). First, the aerosol is heated to 300°C in a 20 cm stainless steel tube. Evaporated volatile material is adsorbed by activated carbon in an adsorption section is arranged as a diffusion dryer that is cooled with water circulating at 25°C. The design of TD used in these experiments is given by Burtscher et al. (2001). It was operated with a flowrate of 2.5 L/min, giving a total residence time in the heating and cooling sections of ~4.5 s. At this flowrate, calculated particle penetration at 3 and 100 nm was 35% and 70%, respectively. For the calculated penetration, the main loss mechanisms were diffusion and thermophoresis as described by Hinds (1999). The temperature measured in the center along the lengthwise axis is shown in Figure 26.

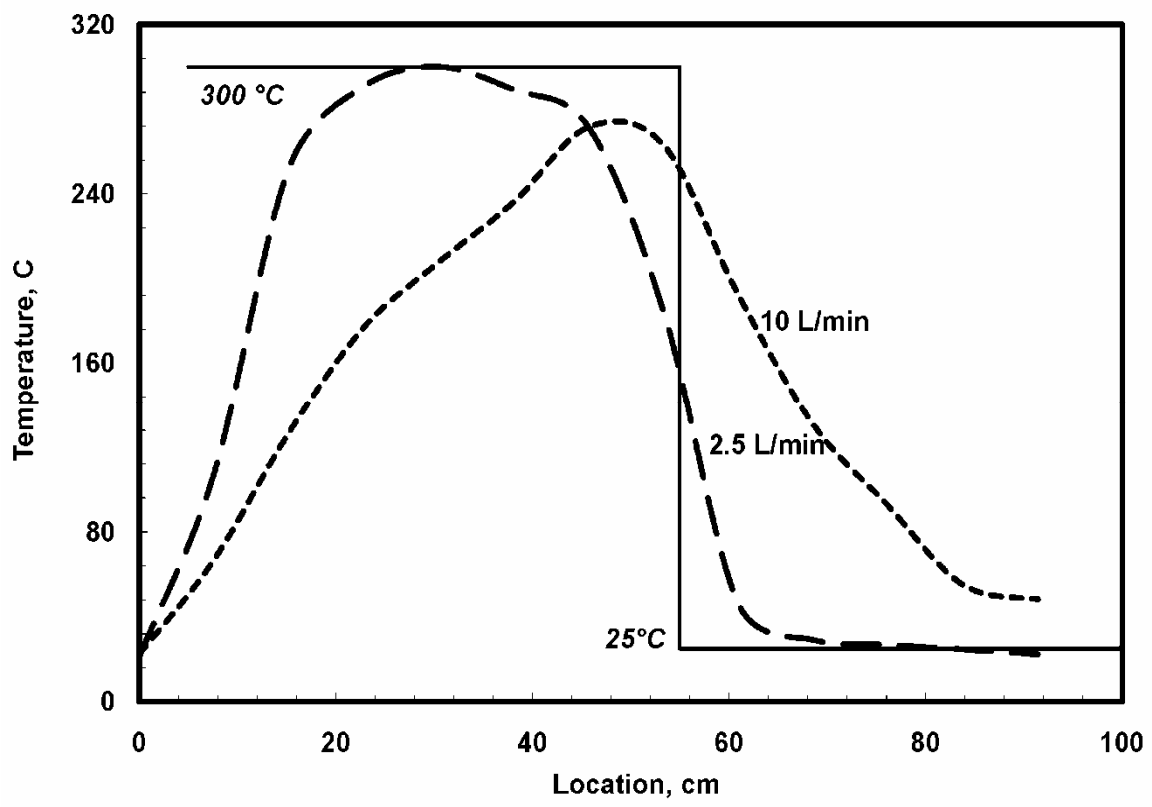

Figure 26. Measured temperature profile in TD for flowrates of 2.5 and 10 L/min. The solid line shows the outer wall "setpoint" temperature for each section. The actual temperature differs from the wall temperature due to heat transfer effects

Volatile particle remover – While a VPR was not used in this study, its specifications are listed for comparison. The VPR is specified by PMP to determine compliance with the European Union's particle number standard. The VPR consists of three components, a hot dilution section, an evaporation tube to evaporate semi-volatile material (equivalent to the heating section in the TD), and a cool dilution section to cool the aerosol and to reduce its concentration to <10,000 particles/cm^3 (Sandbach, 2007). The minimum penetration required of 30, 50, and 100 nm solid particles is 60, 70, and 80%, respectively. The required removal efficiency of 30 nm hydrocarbon (C_{40}) particles is 99%. The VPR wall temperature must be 300 – 400°C. Unlike the TD or CS, the VPR

relies on dilution of volatile components, rather than removal by adsorption or oxidation to prevent the nucleation of particles downstream of the device.

Laboratory Apparatus And Test Procedures

Atmospheric aerosols

Atmospheric city aerosol from an area near a heavily traveled road was drawn into the laboratory by a transfer line that distributed the sample to the SMPS before or after passage through a TD or CS as shown in Figure 27. The challenge aerosol contained roughly 5 x 10^4 particles/cm^3, corresponding to a calculated mass concentration of ~2 µg/m^3. Based on CS results, 20% or 0.4 µg/m^3 of this aerosol consisted of solid particles.

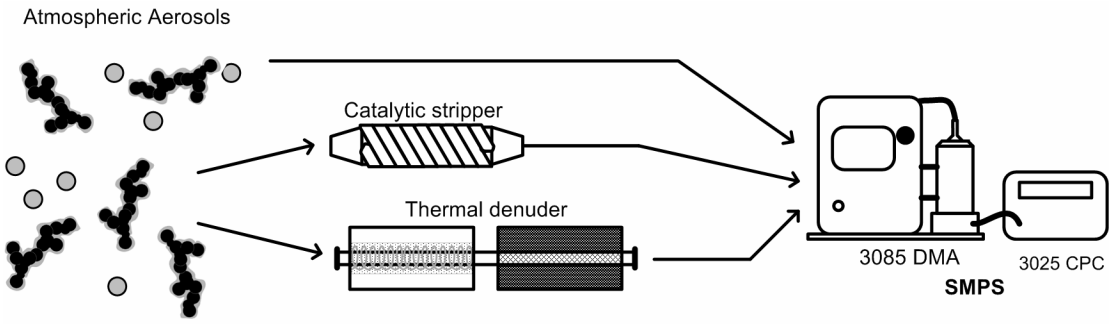

Figure 27. Test apparatus for evaluation of the TD and CS using atmospheric aerosols

Organic carbon and sulfuric acid aerosols

Additional experiments were performed to evaluate the volatile particle removal efficiency of the TD and CS and to explore the possibility that artifacts play a role in the measurement. The baseline performance of the CS and TD was established by using tetracosane ($C_{24}H_{50}$) particles with the instruments configured as shown in Figure 28. Next, a tetracosane and sulfuric acid aerosol was used to evaluate their performance to simulated Diesel aerosol. Finally, dioctyl sebacate, an oxygenated hydrocarbon, ($C_{26}H_{50}O_4$) and sulfuric acid particles were used as the challenge aerosol. In all

experiments, a CS was placed downstream of the TD to evaluate the volatility of the particles that exit the TD. The following describes the test aerosol generation technique.

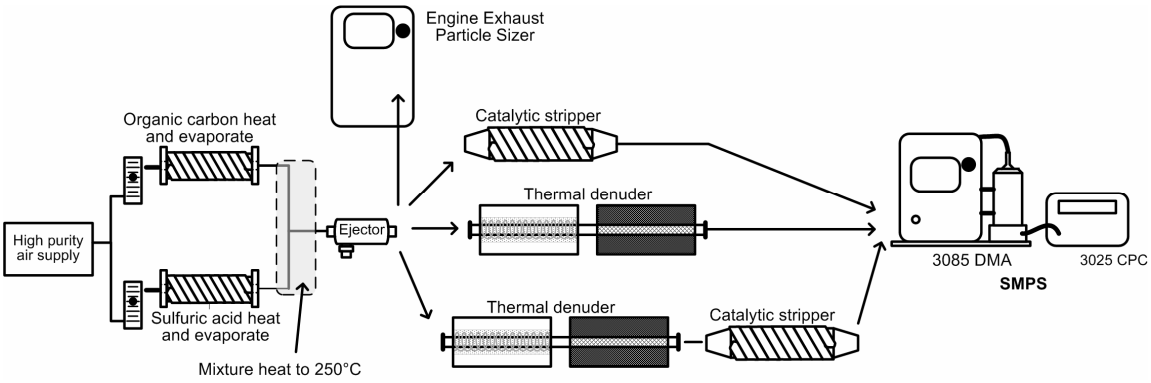

Figure 28. Test apparatus for evaluation of the TD and CS using organic carbon compounds and sulfuric acid. Experimental measurements were not made simultaneously

An evaporation and condensation technique (Veranth et al., 2003) was used to generate nanometer sized challenge aerosol particles. The test compounds, sulfuric acid (reagent grade 99.9% pure, 18 M, Sigma-Aldrich), solid tetracosane flakes (reagent grade 99.9% pure, Sigma-Aldrich) or dioctyl sebacate liquid (technical grade 90% pure, Sigma-Aldrich) were heated in an alumina combustion boat located in a heating tube as shown in Figure 28 to various temperatures ranging from 120°C to 250°C. Temperatures were chosen such that the saturation vapor pressure above each compound was roughly the same, so that the evaporation rates would be similar and they would be similar mole fractions of each in the carrier gas stream at the time they were mixed. The vapor entrainment flowrate was ~1 L/min. The vapor(s) were entrained with hot dry air, mixed homogeneously (except in cases where challenge aerosol was pure, unmixed substance) and heated to 250°C, and then cooled by dilution using an ejector dilutor with a dilution ratio of ~20:1. The cooling causes the vapors to nucleate, forming a high concentration of nanoparticles composed of the evaporated compounds. For these experiments, the mass ratio of sulfuric acid to tetracosane or dioctyl sebacate in the particle phase was unknown.

Results

Atmospheric aerosols

Aerosol number size distributions are shown in Figure 29. Results are not corrected for particle loss in the CS and TD because these corrections have not been rigorously quantified, and the corrections would not affect the conclusions drawn from the data. The baseline atmospheric aerosol distribution shows the average of ~10 measurements without CS or TD treatment. The black line with cross markers shows the atmospheric aerosol after it has passed through the CS. The shape of the size distribution is lognormal with a mean particle size of 30 nm and standard deviation of 1.8, consistent with the idea that atmospheric aerosols are primarily composed of aged small solid carbon particles with a large amount of adsorbed organic material that is effectively removed by the CS. The same experiment yielded a different result when the TD replaced the CS. A large nucleation mode was measured downstream of the TD containing two distinct peaks appear in the nucleation mode range, one at ~3 nm and the other at ~9 nm suggesting that the evaporated organic material that was not fully removed by the activated carbon nucleated in the cooling section. However, the explanation for the two distinct peaks is not obvious. In any case, the assumption that only solid particles are found downstream the TD appears erroneous.

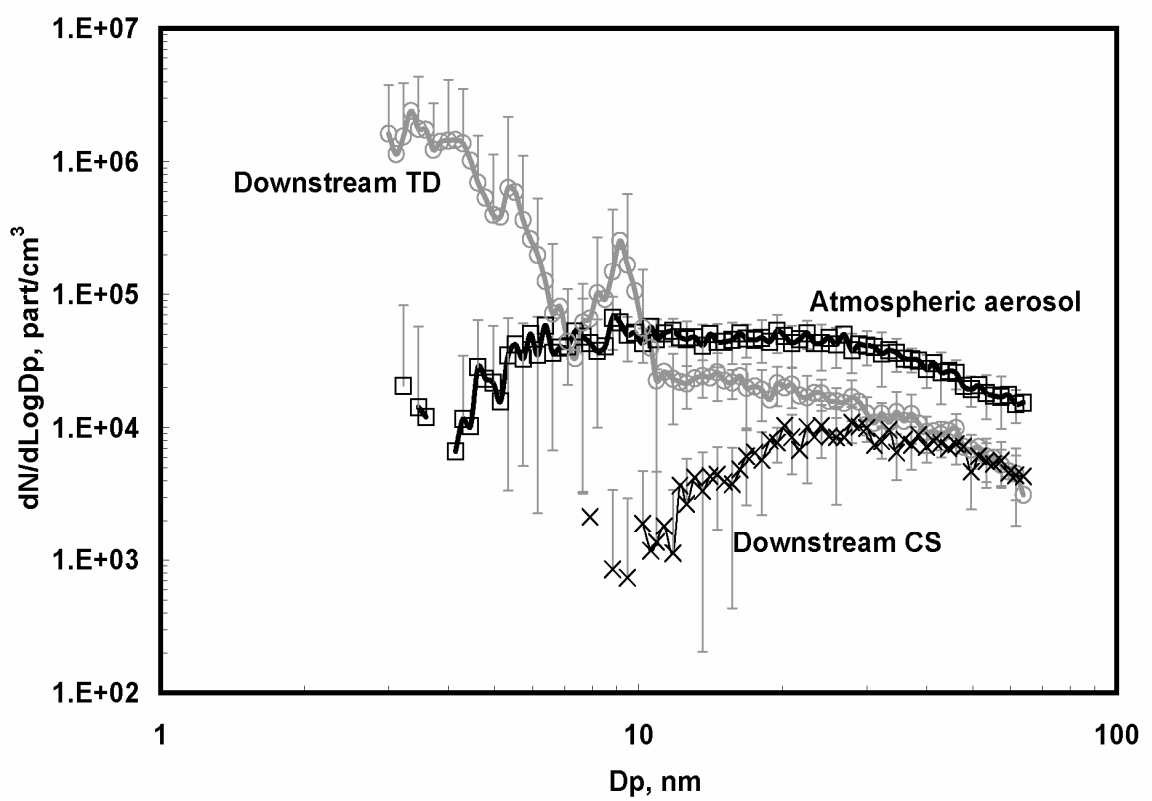

Figure 29. Evaluation of CS and TD method using atmospheric aerosol. Data shows the challenge atmospheric aerosol (squares) that is treated by the CS (crosses) and TD (circles)

This experiment was repeated with water diffusion dryers upstream of both the TD and CS, with no effect on the results, suggesting that residual water does not play a prominent role in the results. In addition, multiple types of activated carbon (all freshly regenerated) were evaluated to ensure neither the type nor saturation level of the activated carbon affects the performance of the TD. These variables did not impact the results.

Organic carbon and sulfuric acid aerosols

Figure 30 shows upstream and downstream particle size distributions for the CS, TD, and TD + CS evaluations with tetracosane particles. The estimated challenge aerosol estimated volume concentrations ranged from 14 to 380 $\mu m^3/cm^3$. The non-physical

distortions in the challenge aerosol size distributions around 50 nm measured by the EEPS have been discussed elsewhere (Swanson et al., 2009) and are due to low electrometer current reading being clipped to zero by the TSI EEPS software. For all concentrations, nucleation mode sized particles were observed downstream of the TD. The fact that particles were not found downstream of the CS or TD + CS configurations demonstrates they were originally composed of completely semi-volatile material. Nucleation in the TD was observed at even the lowest challenge particle concentration, and no particles were observed downstream of the CS or TD + CS configurations even at the highest challenge concentration. The downstream TD measurements show that increasing the challenge aerosol concentration results in an increase in the particle size and total concentration of nucleated particles. These experiments were repeated using particles that more closely simulate the composition of nucleation mode particles in Diesel exhaust.

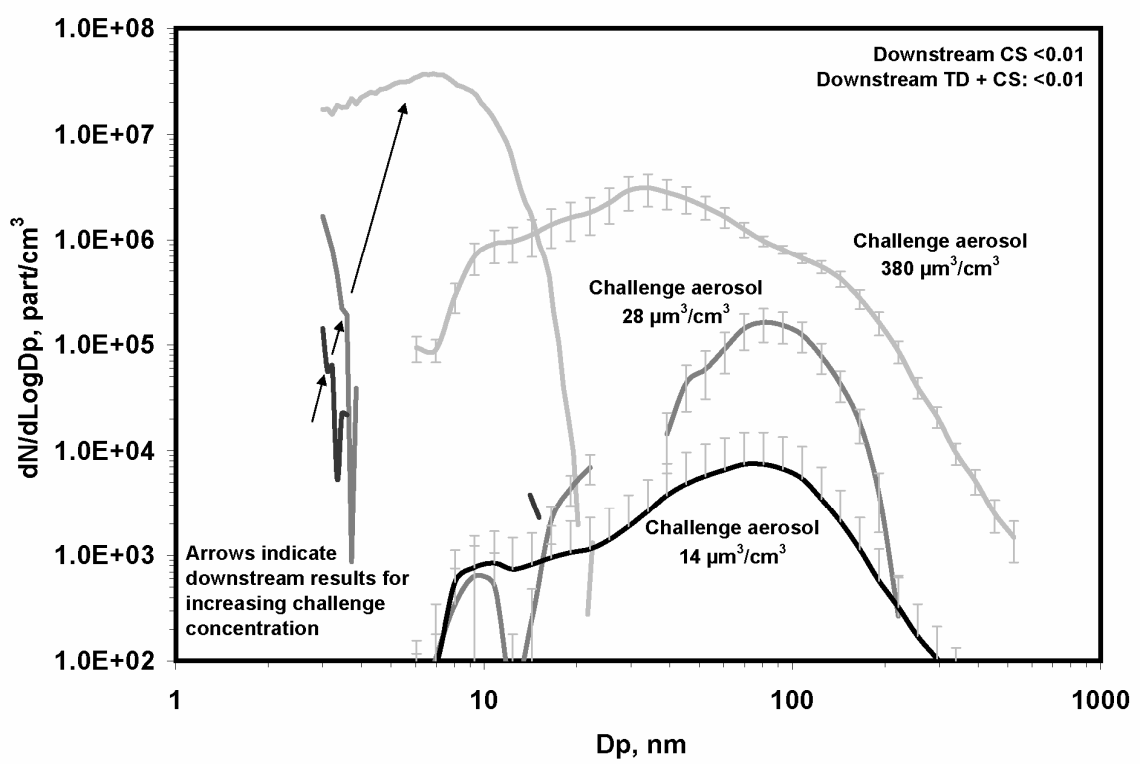

Figure 30. Upstream and downstream particle size distributions for the CS and TD evaluations with tetracosane particles. The downstream measurements (left hand side of graph) show increasing particle size and total concentration with increasing challenge aerosol concentration that is denoted with decreasing grayscale and arrows. Error bars are omitted from downstream results for clarity

Figure 31 shows particle size distributions measured downstream of the TD, CS and TD + CS configurations for a calculated challenge tetracosane / sulfuric acid aerosol concentration of 33 $\mu m^3/cm^3$ and results from the evaluation with pure tetracosane particles. Again, a nucleation mode was observed downstream of the TD, but not downstream of the TD or CS + TD, demonstrating that both the challenge aerosol and the particles downstream of the TD are semi-volatile. Further calculation shows that number of tetracosane/sulfuric acid particles formed by re-nucleation in the TD, as compared to the number of pure tetracosane particles, is higher by a factor of 50 ± 23. This results is for challenge volume concentrations of both compounds that were nominally equal.

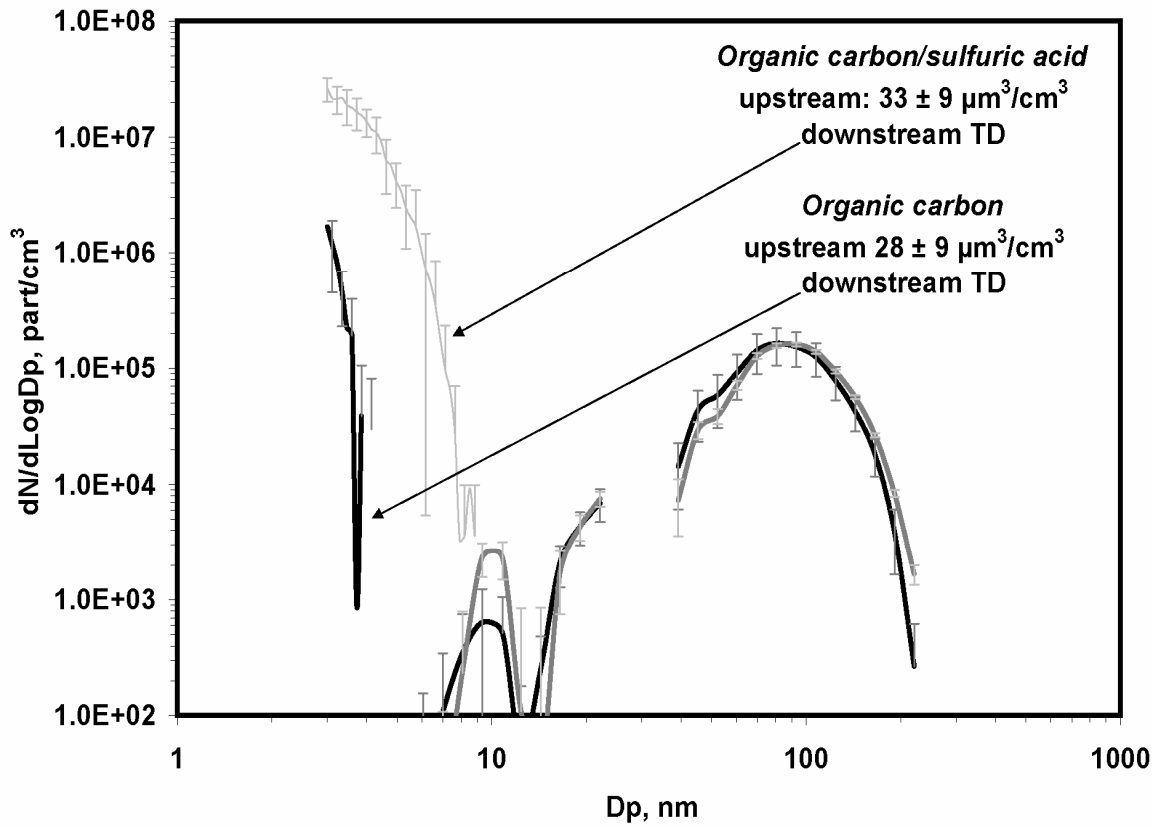

Figure 31. Tetracosane / sulfuric acid challenge aerosol (dark line) and particle size distribution measured downstream of the CS, TD (light line) and the TD + CS. In this case, the CS and TD + CS configurations removed all challenge aerosol; therefore, the curves are not visible

Additional experiments were performed to evaluate the performance of the TD and CS when challenged with low concentrations of potentially more reactive hydrocarbons. Figure 32 shows the evaluation of TD and CS with a dioctyl sebacate challenge concentration of 10 $\mu m^3/cm^3$. High concentrations of nucleation mode particles were again measured downstream of the TD, but no particles were observed downstream of the CS or TD + CS. Further calculation shows that the number of tetracosane/dioctyl sebacate particles formed by re-nucleation in the TD, as compared to the number of pure tetracosane particles, is higher by a factor of 40 ± 30. This result is for challenge volume

concentrations of tetracosane twice that of the tetracosane / dioctyl sebacate challenge concentration.

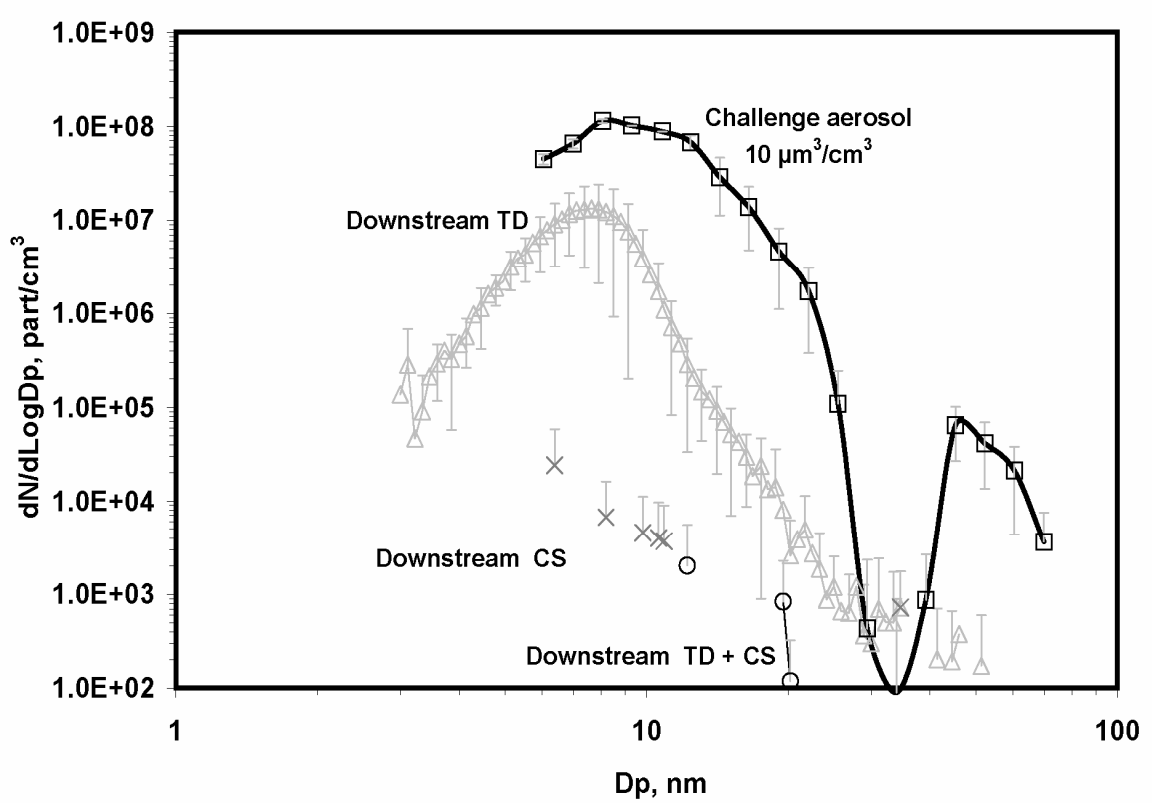

Figure 32. Dioctyl sebacate / sulfuric acid challenge aerosol and particle size distributions measured downstream of the CS (crosses), TD (triangles) and the TD + CS (circles). The few scattered CS and TD + CS points are considered measurement noise due to residual particles in the system

In summary of the results from the tetracosane, tetracosane / sulfuric acid, and tetracosane / dioctyl sebacate evaluations for low (<500 $\mu m^3/cm^3$) challenge aerosol concentrations, the data shows that: (1) regardless of the initial size, concentration, or composition of the semi-volatile challenge aerosol, particles were not observed downstream of the CS, (2) for varying particle size, concentration, and composition, nucleation mode particles were routinely observed downstream of the TD, (3) particles

composed of acid and organic carbon showed a higher propensity to re-nucleate than particles containing either substance alone.

In addition to these results, instances of solid particle formation (not just the appearance of solid particles) were observed for higher challenge aerosol concentrations that are of particular concern. One example is shown in Figure 33. As described earlier, a sulfuric acid/organic carbon aerosol was used to challenge the CS, TD, and TD + CS. The challenge aerosol was entirely removed by the CS. When the challenge aerosol is used to challenge the TD, a small percentage by mass (4%) of evaporated vapor re-nucleated, resulting in very high concentrations of particles downstream. The TD treated aerosol is then passed though the CS and a smaller nucleation mode is measured downstream. Because the CS is able to completely remove the acid and organic carbon, this smaller mode is a solid particle nucleation mode that evidently formed in the TD.

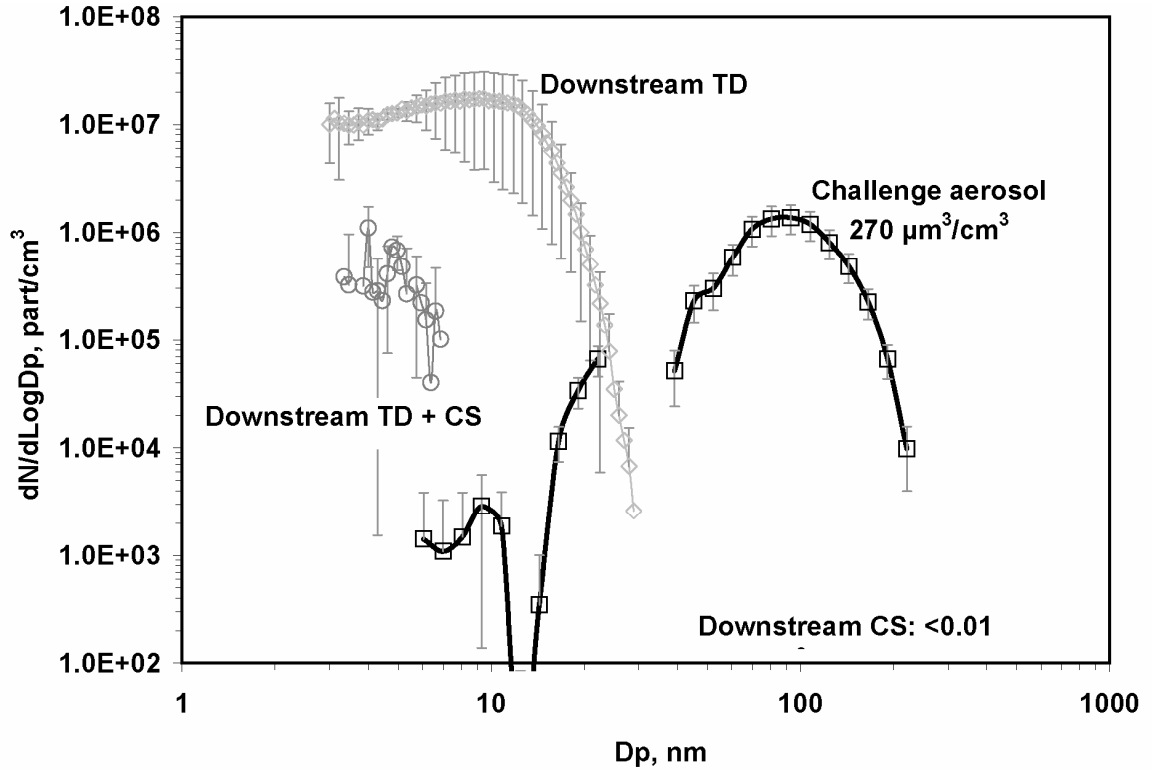

Figure 33. Tetracosane / sulfuric acid challenge aerosol (squares) and particle size distributions measured downstream of the CS, TD (triangles) and the TD + CS (circles). Solid particles were generated in the TD while all particles were removed by the CS

Figure 34 shows the results when the TD, CS, and TD + CS are challenged with a much higher concentration of sulfuric acid / tetracosane particles, 3800 $\mu m^3/cm^3$. This concentration was chosen as a worst-case scenario and it represents the highest volume concentration measured in the exhaust (diluted 15:1) of a heavy-duty Diesel engine equipped with a particulate filter (Swanson et al., 2009b). In those experiments, high concentrations were the result of storage and release of sulfate compounds that formed nanoparticles that may be similar in composition to the generated particles in these experiments. The results show the solid particle nucleation mode downstream of the TD much clearer than the one shown in Figure 33. The total concentration of solid particles was 1 x 10^6 part/cm^3. Even when challenged with 3800 $\mu m^3/cm^3$ of semi-volatile particles, the CS is able to completely oxidize and remove all material.

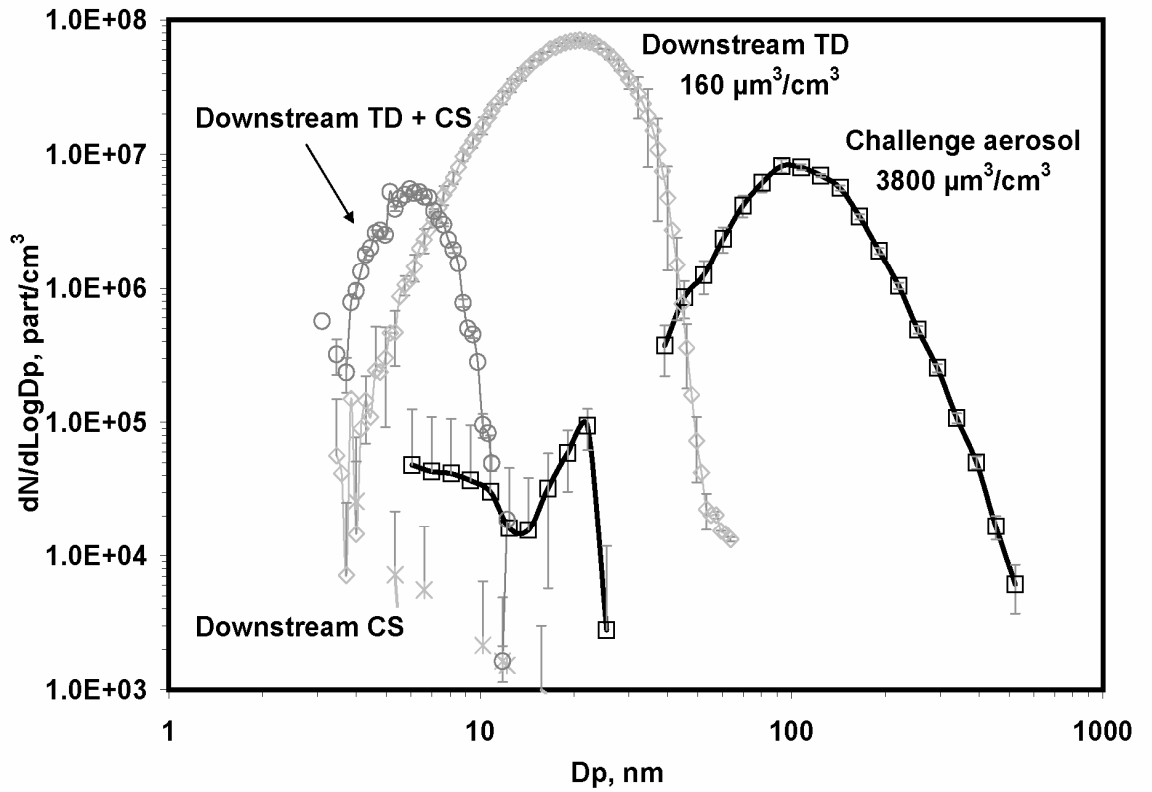

Figure 34. Tetracosane / sulfuric acid challenge aerosol (blue) and particle size distributions measured downstream of the CS (crosses), TD (triangles) and the TD + CS (circles). Solid particles were generated in the TD while all particles were removed by the CS

Discussion

The first experiment showed that semi-volatile material nucleated downstream of the TD suggesting that solid particles were present when in fact they were not. In this experiment, the concentration of solid carbon particles (~0.4 µg/m^3) was very low, which increases the potential for nucleation in the TD. This situation is analogous to the situation downstream of exhaust particulate filters – high concentrations of nanoparticles are often found with low concentrations of carbonaceous agglomerates. Conversely, high concentrations of carbonaceous agglomerates will act to suppress the formation of a nucleation mode because they scavenge volatile material, reducing the likelihood of

nucleation (McMurry and Friendlander, 1979; Bagely et al., 1996; Khalek et al., 2000). Thus, the presence of carbonaceous aerosols masks the potential for particle re-nucleation that would occur in these devices in the absence of solid particles. Improved and optimized heating and cooling sections in new TD designs (Wehner et al., 2002; Fierz et al., 2007) may help prevent the nucleation in the cooling section observed here.

However, in the second experiment it was demonstrated that the TD method applied to a semi-volatile aerosol could lead to the formation of solid particles. The formation mechanism may be pyrolysis of the hydrocarbon that is catalyzed by the acid, although the temperature was low for pyrolysis. The pyrolysis or charring of organic carbon that occurs during elemental carbon/organic carbon (EC/OC) analysis depends on many factors, especially temperature, but also composition and amount (Yu et al., 2002). Alternatively, dehydration may be occurring where the sulfuric acid is removing hydrogen's from the organic carbon, leaving just solid carbon that is measured in the particle phase. In this case, an analogous reaction is the well-known reaction of sucrose with strong sulfuric acid (Shakhashiri, 1983). It is not fully clear if the formation of solid particles depends on the size or concentration of semi-volatile particles or if solid particles formed at very low challenge aerosol concentrations but they were undetectable due to high losses in the system and instrument sensitivity at 3 nm. The estimated penetration of 3 nm particles through this system is only ~0.5%.

Formation of solid particles was only observed in the TD and not the CS. One explanation for this is that S-trap in the CS may remove the sulfuric acid precursors that are required for the solid particles to form. Additionally the details of the heating magnitude and duration may influence the result in ways not yet understood. Some TDs may be more susceptible to this effect than others. For example, Filippo and Maricq (2008) measured solid nucleation mode particles at idle using a TD. However, in their case, "artifact" is an unlikely explanation because the solid-like nature of the particles

was confirmed via their visibility in a transmission electron microscope, and with electrical charge measurements that suggested the particles were solid in the combustion chamber when the temperatures are high and semi-volatile compounds are not in the particle phase.

Chapter 5: Particle and Gaseous Emission Characteristics of a Formula SAE Race Car Engine

Introduction

Formula SAE® is an annual student design competition organized by SAE International. The goal of this competition is to design, build, and race a small formula-style vehicle. The engine used by the University of Minnesota Formula SAE team is a 599 cc motorcycle engine. The intake, exhaust, fuel delivery, and engine control modules are customized by the team. The engine is tuned for maximum performance with no regard for emission control. The two fuels that were examined were TrackTek® 100 octane gasoline and E85 purchased at the pump.

In 2006 EPA adopted their first change to the highway motorcycle emissions regulations in over 25 years. Under the previous standards, motorcycles produced more hydrocarbon and oxides of nitrogen emissions per mile than cars or large sport utility vehicles (EPA, 2003). EPA does not currently regulate particulate matter (PM) emissions on highway motorcycles.

Historically PM emissions have been a concern for Diesel engines, but advancements in electronic engine control, fuel delivery, and exhaust aftertreatment have substantially reduced PM emissions. As emission standards become tighter for heavy and light duty trucks, as well as passenger vehicles, motorcycles will contribute a larger fraction of on-road PM emissions.

In addition, reliance on mass concentration as the only estimate of exposure may not accurately reflect exposure to combustion aerosols (McCawley, 1990), because of the aerosol size distribution and predicted lung deposition (ICRP, 1994). The correlation of exposure to adverse health effects from PM may improve using the total particle surface

area or total particle number concentration as the exposure metric (Kittelson et al., 2002). Small particles in the nucleation mode (typically <50 nm in diameter) can penetrate deep into the alveolar portion of the lung but do not typically contribute to the total mass.

The objective of this study was to characterize gaseous and particle number emissions and aerosol size distributions from a Formula SAE engine fueled with 100 octane or E85 gasoline to determine the impact of fuel type on emissions. Engine tests were conducted in the laboratory under typical engine race conditions.

Laboratory Test Apparatus

Engine

The engine used by the 2005 University of Minnesota Formula SAE team was a 599 cc motorcycle engine from a 1999 Yamaha YZF-R6. The customized intake consists of a set of four runners bolted to the intake ports which are attached to an aluminum plenum. The intake plenum is fed by a piece of aluminum tube with a restrictor, butterfly valve, bell mouth, and filter on the other end. The rules of the competition state that the restrictor must be downstream of the butterfly valve. The rules also specify a 20 mm restrictor when using 100 octane fuel and a 19 mm restrictor when using E85. However, a 20 mm Venturi-style restrictor was used in both cases to allow a comparison of fuels on this engine. Therefore, any increase in power seen with E85 does not necessarily translate to an increase in power on the racetrack.

The 1999 Yamaha YZF-R6 in its stock configuration is carbureted, however, the team equipped this engine with fully sequential port fuel injection. A MoTeC M4 programmable engine control module (ECM) drives the fuel injection and “coil on plug” spark ignition system. The ECM determines “load” using a rotary throttle position sensor. This throttle position was kept constant for both fuels. The engine was tuned for

performance using an Eddy current dynamometer at a variety of engine speeds and loads. The ECM also has closed-loop feedback from a Bosch LSM-11 wideband oxygen sensor. This allows the ECM to maintain a target equivalence ratio at a given condition. In addition to the base fuel and spark maps, the ECM also has a target equivalence ratio map. This value varies with speed and load and allows the engine to compensate for changes in intake and exhaust pressure and temperature.

Fuels

Fuel consumption and target equivalence ratios for the ECM are shown in Table 10 below. Table 11 shows properties of gasoline and ethanol. Ethanol is an oxygenated fuel that has a stoichiometric fuel-air ratio higher than regular gasoline. Accordingly, the engine consumes almost 40% more E85 than gasoline. The closed-loop feedback from the wide-band oxygen sensor enables the engine to run property even when the fueling rate changes significantly.

Table 10. Fuel flow and equivalence ratio

Condition	Fuel	Speed	Throttle	Fuel flow (cc/min)	Equivalence ratio
1	TT100	6000	75%	166	1.10
2	E85	6000	75%	227	1.10
3	TT100	8000	50%	214	1.14
4	E85	8000	50%	292	1.14
5	TT100	8000	100%	284	1.14
6	E85	8000	100%	395	1.14

Table 11. Fuel properties (Heywood, 1988)

Property	Gasoline	Ethanol
Chemical formula*	C_8H_{14}	C_2H_5OH
Heat of vaporization (kJ/kg)	305	840
Lower heating value (MJ/kg)	44.0	26.9
Stoichiometric fuel/air ratio	0.068	0.111
Oxygen mass content (%)	0	32

*Gasoline chemical formula is based on average composition data for TrackTek® 100 Octane fuel (Tracktek, 2004).

When switching to E85 the base fuel map was trimmed 40% rich and the wideband oxygen sensor was allowed to modify the main table by 15% either way to ensure the engine was running at the same equivalence ratio for both fuels. This process is similar in design to other flex fuel vehicles using closed-loop feedback control (Filho et al, 2007; Gibson et al., 2001; Rakovec et al., 2008). Studies have also shown material compatibility to be an important issue when switching to a fuel containing a large fraction of alcohol (Black, 1991). The aluminum components of the intake and fueling system were anodized to protect against corrosion. Fuel lines and seals were switched to alcohol tolerant components.

Dilution System

Figure 35 shows a schematic of the sampling system. The raw exhaust sample was taken just upstream of the muffler. There was no catalyzed aftertreatment device in the customized exhaust. Dilution was achieved using a two-stage mini-dilution system (Khalek et al., 1999). The system includes: primary and secondary air ejector pumps, mass flow controllers to measure dilution air flow, pressure transducers at the inlet, supply and outlet of the air ejectors, and temperature monitoring. High purity dilution air was supplied by a Donaldson pressure swing adsorber (Swanson et al., 2007). A URG 852 cyclone with a 2.5μm cutpoint at 92 lpm was placed after primary dilution. Flow to the ejectors was 100 lpm and was set by the flow controllers, which allowed the pressure

transducers to be used to monitor the condition of the ejector pumps and orifices. At this flow rate, the aerosol spent 1 s in the residence chamber before continuing to secondary dilution. The total dilution ratio was determined with measured raw and dilute NO concentrations and was ~500 for all conditions. All data presented is corrected for dilution ratio.

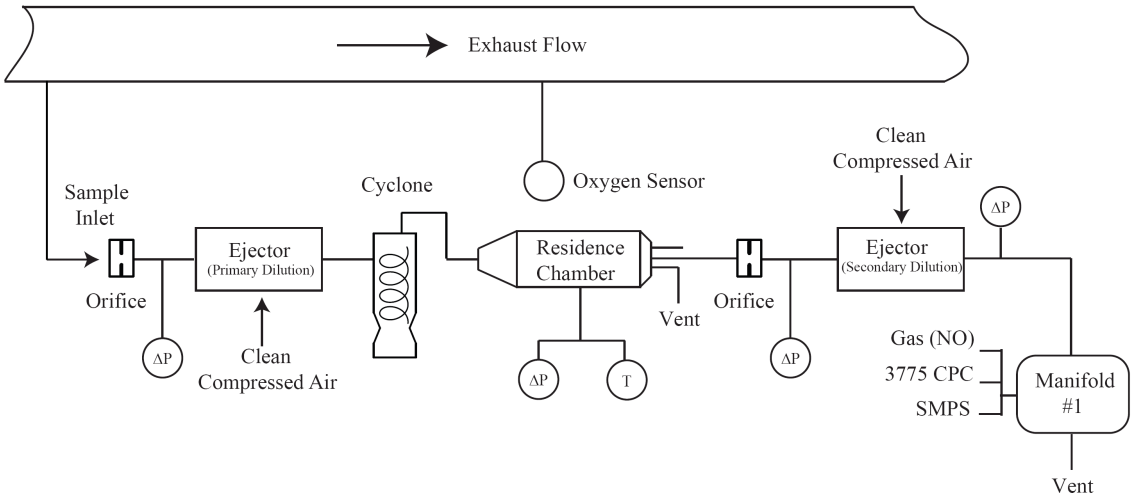

Figure 35. Schematic of the sampling system. Reprinted with permission from SAE paper number 2009-01-1400, © SAE International.

Instrumentation

Condensation particle counter (CPC)

A TSI 3775 CPC was used to measure total particle number concentrations. The 3775 measures particles from 4 to 3000 nm in diameter with a maximum concentration of 10^7 particles/cm^3; it has a response time of about 4 s. The 3775 CPC works by condensing n-butyl alcohol on the particles to grow them to an optically detectable size (Agarwal and Sem, 1980). This instrument was operated in high-flow mode taking 1.5 LPM with only 0.3 LPM going to the optics and bypassing the extra flow.

Scanning mobility particle sizer

The scanning mobility particle sizer (SMPS) consisted of a TSI 3071A electrostatic classifier and a TSI 3010 CPC. The SMPS was used to classify particles by electrical mobility equivalent diameter. The SMPS was configured to cover the range of 8–283 nm (10 L/min sheath air flow and 1 L/min aerosol flow). Data were collected using 60 s up-scan and 30 s down-scan times. Data were analyzed using version 8.0 of the TSI SMPS software with multiple charge correction and diffusion loss correction both enabled. SMPS data presented here include the number weighted size distributions and total number and volume concentrations.

Gas Analyzers

The gas bench used in this experiment to measure raw emissions consisted of a HORIBA PIR-2000 CO and CO_2 analyzer, and a Thermo Environmental Instruments Inc. Model 10 NO_x analyzer. Raw gas measurements passed through a drier to remove water vapor before entering the analyzer. The values reported (Tables 5-7) are the corrected wet mol fraction. Dilute NO measurements were made using a Monitor Labs Inc. Model 8840 analyzer. All gas analyzers were zeroed and spanned daily during testing.

Fuel Consumption

Fuel consumption was measured using a Micro-Oval flow meter. The fuel rail is maintained at a constant fuel pressure with a return loop passing through a fuel cooler. The cooled return fuel mixes with the new fuel entering the loop from the Micro-Oval and proceeds to the low pressure side of the fuel pump. The flow loop was flushed when the fuel was changed.

Test procedure

After a sufficient warm up period, the engine was brought to condition and allowed to stabilize for approximately 15 min. Once the engine was stabilized a minimum of 3 scans were taken using the SMPS software. The 3775 CPC concentration and other dilution tunnel sensors were logged using a National Instruments SCXI-1000 data acquisition system at 1 Hz. Reported total concentrations are the average over the entire sample period. The test conditions shown in Table 12 are representative of typical engine speeds during the autocross event with varying amounts of throttle.

Table 12. Engine operating conditions

Condition	Fuel	Speed, rpm	Throttle	Exhaust, °C	Tunnel, °C
1	TT100	6000	75%	740	29 ± 0.5
2	E85	6000	75%	710	24 ± 0.8
3	TT100	8000	50%	740	30 ± 1.0
4	E85	8000	50%	710	30 ± 0.7
5	TT100	8000	100%	720	25 ± 1.0
6	E85	8000	100%	680	30 ± 0.3

The tunnel temperature is defined as the temperature of the dilute exhaust measured in the center of the dilution tunnel.

Results and discussion

Engine performance

While the objective of this work was to measure the emissions characteristics of the formula SAE car engine, a number of performance trends are valuable to note. For all three conditions and for a given throttle position, the engine torque increased (~5%) with E85 also resulting in proportional increase in power. The increase is due to the significantly higher heat of vaporization of E85. A 5-11% increase in thermal efficiency with E85 depending on condition was observed. This increase was achieved without changing the compression ratio, spark advance, or using EGR (Brusstar and Gray, 2007; Brusstar and Bakenhsu, 2002). It is hypothesized the increase is partially due to the

charge cooling effect caused by E85's higher heat of vaporization. The pumping work is reduced and the cycle efficiency increases, but further study is needed.

Table 13. Engine performance

Condition	Torque, Nm	Power, hp	Thermal efficiency
1	40.0	33.6	28.0%
2	41.7	35.1	30.4%
3	35.5	39.8	25.7%
4	38.0	42.6	28.7%
5	47.0	52.8	25.6%
6	48.3	54.3	27.0%

Gaseous Emissions

Table 14, Table 15, and Table 16 show the gaseous emissions in fractional and brake specific forms for the first four conditions. Gaseous emissions data was not available for the last two conditions. To compute brake specific values, the exhaust flowrate is calculated using the fuel consumption and the equivalence ratio obtained from the oxygen sensor.

A decrease in CO but an increase in NO when switching to E85 was observed. This is in general agreement with Li et al. (2003). An increase in CO_2 was also observed with E85 that can partially be attributed to the decrease in CO. Similar results were reported by Jaroonjitsathian et al. (2007) who attributed a decrease in CO and increase in CO_2 to increased combustion efficiency when using an oxygenated fuel. The decrease in CO and CO_2 between E85 and 100 octane was greater on a brake specific basis due to the increase in power produced at a given condition. The implication is that total carbon emissions decreased when E85 is used, consistent with an increase in thermal efficiency. For NO, there was an increase on a concentration basis but a decrease when converted to brake specific.

Table 14. CO emissions

Condition	CO	
	%	(g/bhp-hr)
1	3.1	102
2	2.5	78
% increase	-24%	-31%
3	4	144
4	3.6	120
% increase	-11%	-20%

Table 15. CO_2 emissions

Condition	CO_2	
	%	(g/bhp-hr)
1	10	522
2	10.5	521
% increase	5%	0
3	9.4	535
4	10	524
% increase	6%	-2%

Table 16. NO emissions

Condition	NO	
	ppm	(g/bhp-hr)
1	1061	3.8
2	1141	3.9
% increase	7%	3%
3	972	3.8
4	1058	3.8
% increase	8%	0

Particle Emissions

Figure 36, Figure 37, Figure 38, Figure 39, and Figure 40 are the number and/or volume aerosol size distributions as a function of the fuel composition and operating condition. Figure 36 shows that the size of the nucleation mode increases with increasing engine

power output, while the accumulation mode decreases with power for the 100 octane fuel. Figure 37 also shows that the size of the nucleation mode increased with engine power for the E85 fuel. However, the E85 fuel showed less sensitivity in the accumulation mode to changing engine loads.

Figure 38, Figure 39, and Figure 40 directly compare the number and volume size distributions obtained from both fuels for all test conditions. At 6000 RPM (Figure 38), there was a lower number concentration across most of the range with E85 fuel. However, both of the 8000 RPM cases (Figure 39 and Figure 40) there was no change in the nucleation mode. A decrease in the accumulation mode with E85 that was independent of test condition was observed. This reduction translates to a significant decrease in total PM emissions. Similar PM reductions have been seen in other studies comparing gasoline to E85 (Price et al., 2007; Ericsson et al., 2008; Ragazzi and Nelson, 1999; Mulawa et al., 1997).

Reductions in the accumulation mode attributed to reducing soot formation have also been observed with other oxygenated fuels (Litzinger et al, 1999). Although the process is not fully understood it is believed that oxygenated fuels reduce the mass of soot by reducing the concentration of key intermediate species required for the formation of soot precursors (Price et al., 2007; Litzinger et al, 1999; Ni et al., 1994). Typically, when the concentration of carbonaceous particles is reduced, the volatile organic fraction (VOF) will increase (Bagley et al., 1996). Volatile material that would have condensed on the surface of the soot is now available to form nucleation mode particles (Bagley et al., 1996). Since the conditions tested are 10 – 14% fuel rich of stoichiometric, the nucleation mode is likely comprised of semi-volatile material from incompletely burned fuel.

Previous work by Graskow et al. (1998) and Johnson and Kittelson (1996) has shown an engine operating at a fuel rich condition, can result in excess particulate emissions. At

high speed and high load conditions when the engine is running rich, a catalyst will have very poor removal efficiency (Kittelson et al., 2006). Therefore, even if a catalytic converter were used it would be expected to be unable to remove much semi-volatile material and thus, have negligible impact on the size distributions and mass emissions.

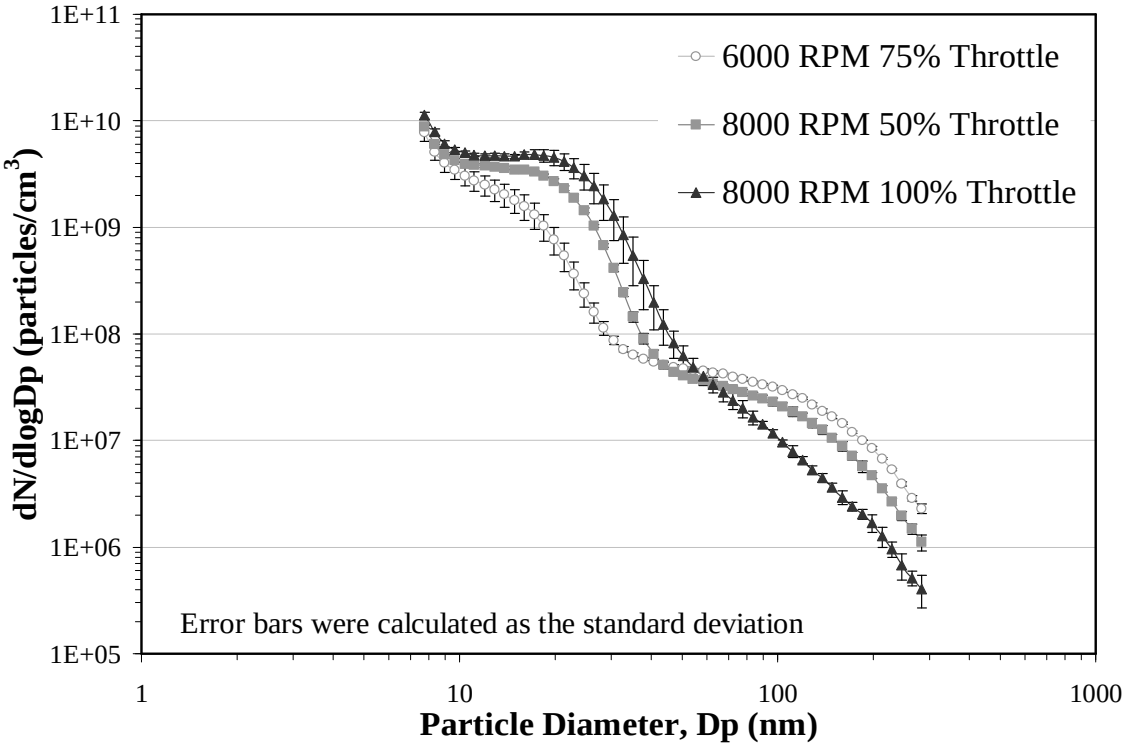

Figure 36. Number distributions for TT100 gasoline. Reprinted with permission from SAE paper number 2009-01-1400, © SAE International.

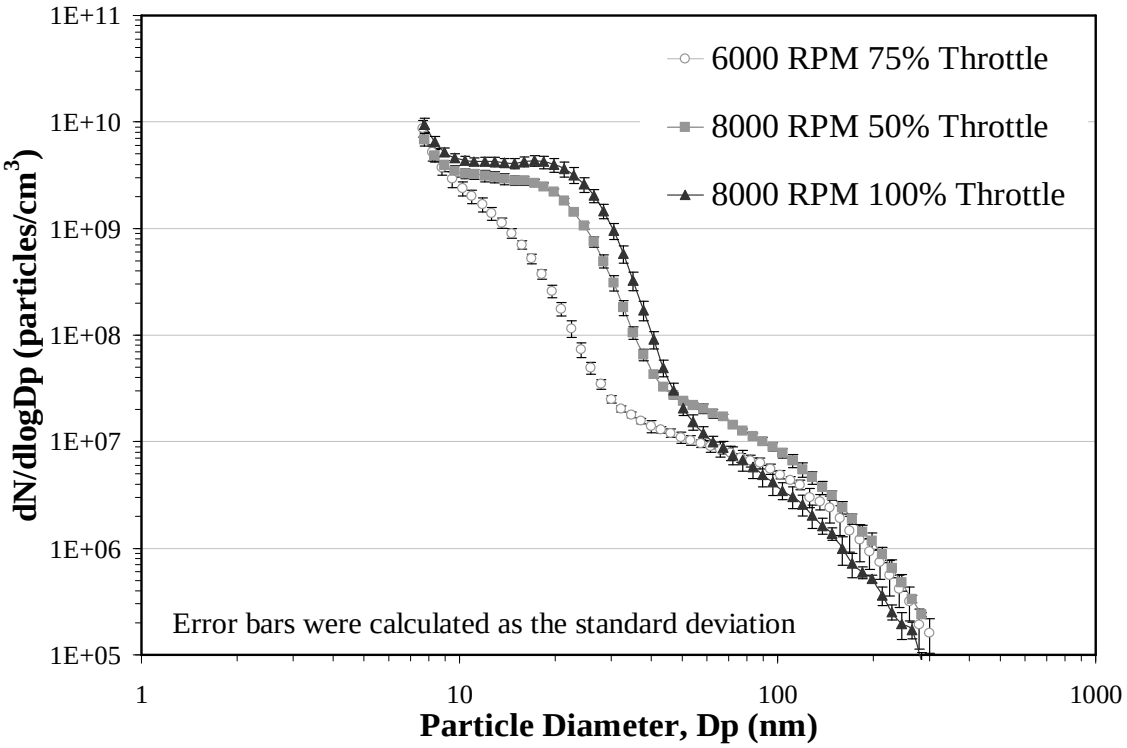

Figure 37. Number distributions for E85. Reprinted with permission from SAE paper number 2009-01-1400, © SAE International.

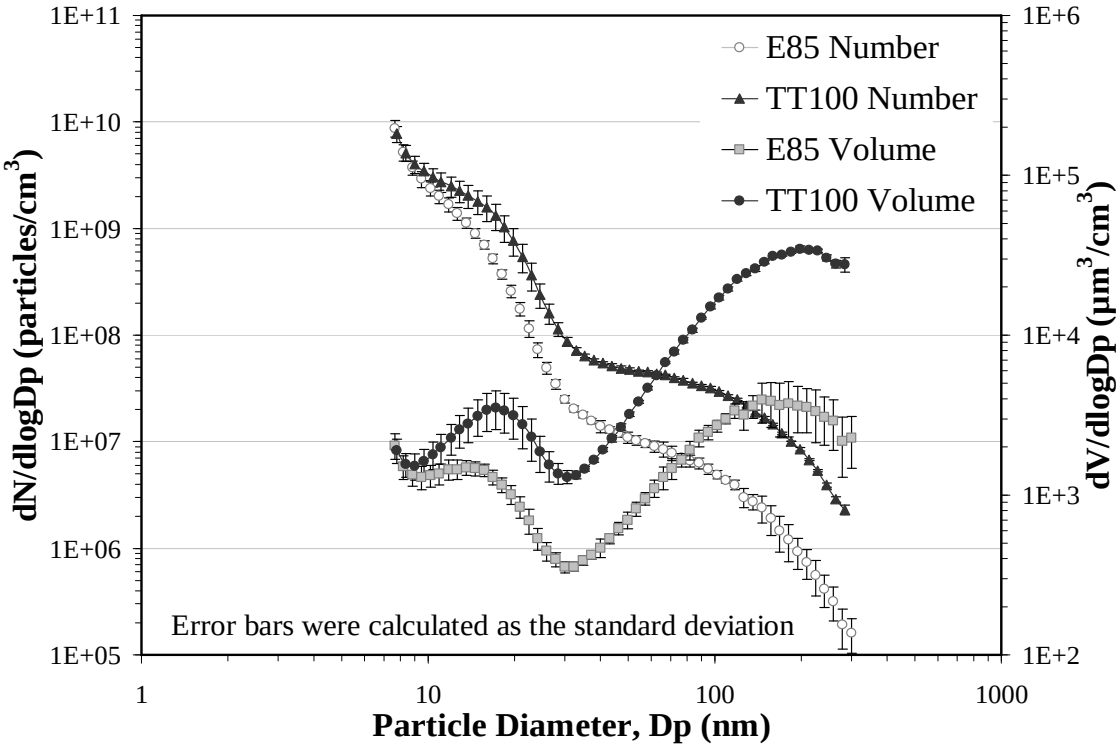

Figure 38. Number and volume size distributions for 6000 RPM 75% throttle. Reprinted with permission from SAE paper number 2009-01-1400, © SAE International.

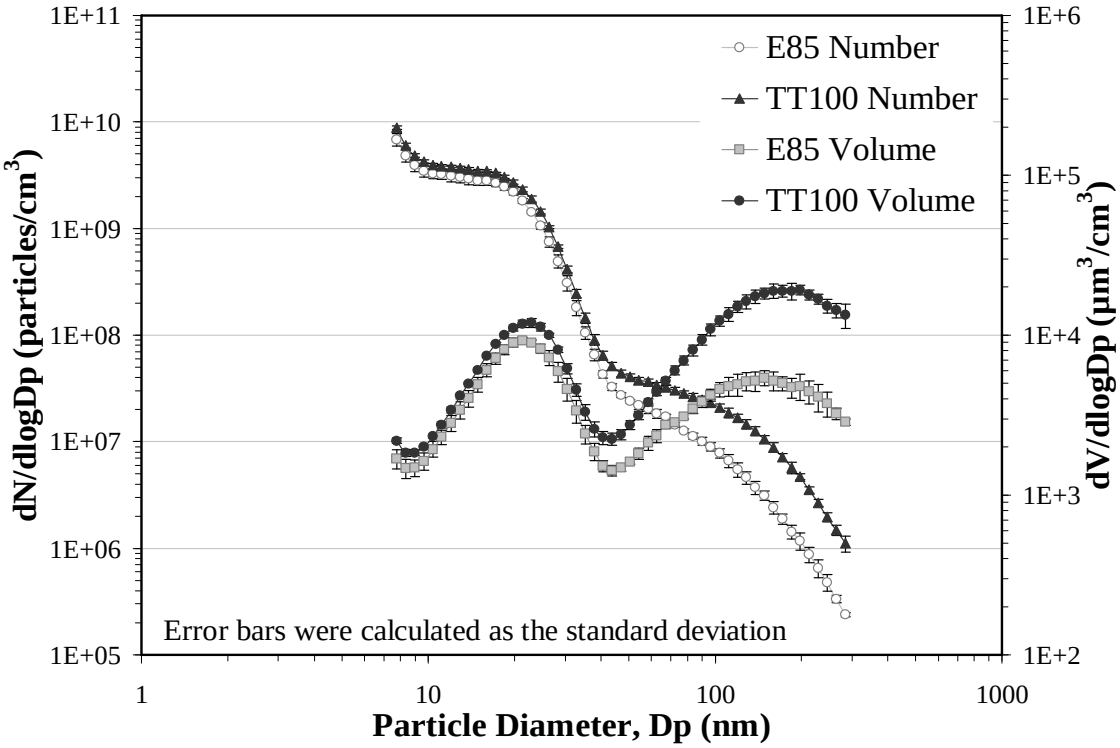

Figure 39. Number and volume size distributions for 8000 RPM 50% throttle. Reprinted with permission from SAE paper number 2009-01-1400, © SAE International.

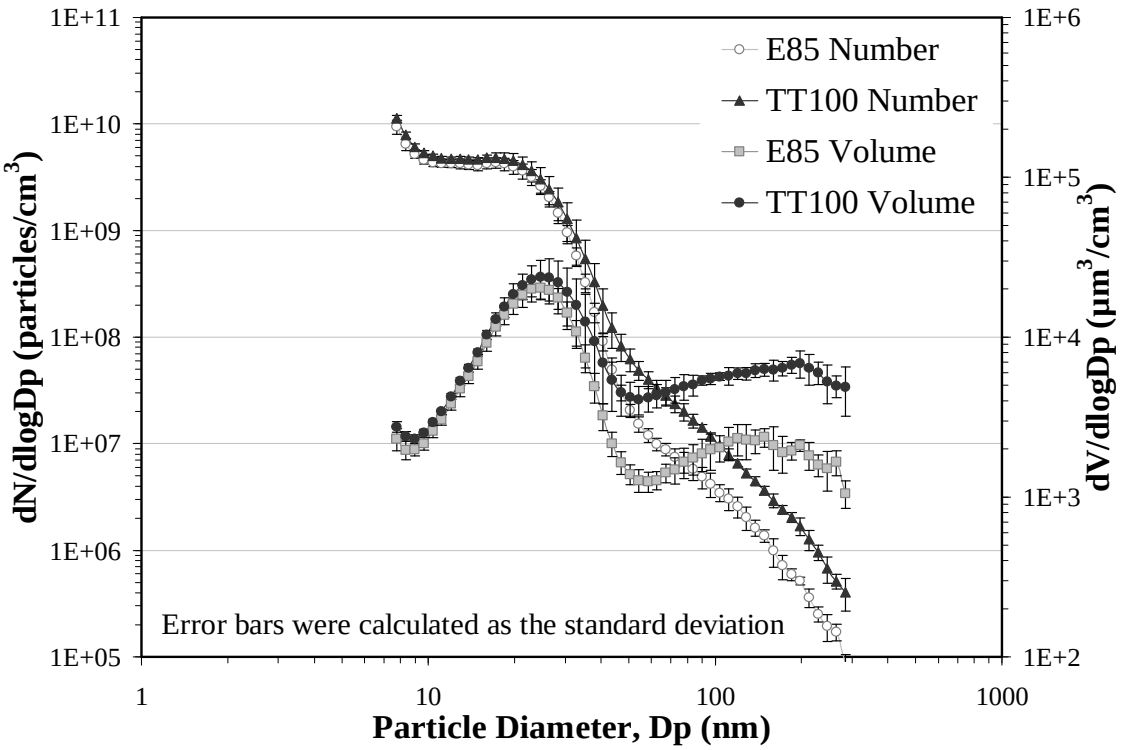

Figure 40. Number and volume size distributions for 8000 RPM 100% throttle. Reprinted with permission from SAE paper number 2009-01-1400, © SAE International.

Figure 36, Figure 37, Figure 38, Figure 39, and Figure 40 showed bimodal size distributions with one mode <30 nm and the other >30 nm. To quantify the relative importance of these modes, the N30/N and V30/V statistics are shown. Table 17 shows N30/N or the total number of particles < 30 nm divided by the total SMPS integrated number concentration. For all conditions, the N30/N ratio shows that over 95% of the particles are 30 nm or smaller in diameter. The V30/V ratios, defined as the total volume concentration of particles < 30 nm in diameter divided by the total integrated volume from the SMPS are also shown in Figure 42. The results show that the particles < 30 nm make up a significant volume fraction of the aerosol. N/V is the total number divided by the total volume, both integrated from the SMPS. Kittelson et al. (2005) reported N/V

ratios for a number of Diesel engine operating modes. The values of N/V seen here are 10 to 100 higher than those typically associated with untreated Diesel exhaust.

Table 17. Volume and number fractions

Condition	V30/V	N30/N	N/V, part/μm^3
1	0.08	0.98	7.5E+4
2	0.24	0.99	3.3E+5
3	0.27	0.98	1.5E+5
4	0.46	0.98	2.6E+5
5	0.50	0.96	2.3E+5
6	0.67	0.97	3.1E+5

Figure 42 quantifies the total volume concentration reductions that occurred when E85 fuel was used. The total volume decreased with engine power for 100 octane race fuel, but increased with engine power for E85. The volume increase with E85 is due an increase in the nucleation mode than more than offsets a small decrease in the accumulation mode. The 100 octane racing fuel showed a reduction in the accumulation mode with increased engine power causing the total concentration to decrease with power. Overall, these volume concentrations are roughly 100 times higher than have been observed from a fuel injected 1990's spark ignition engine (Kittelson et al., 1998).

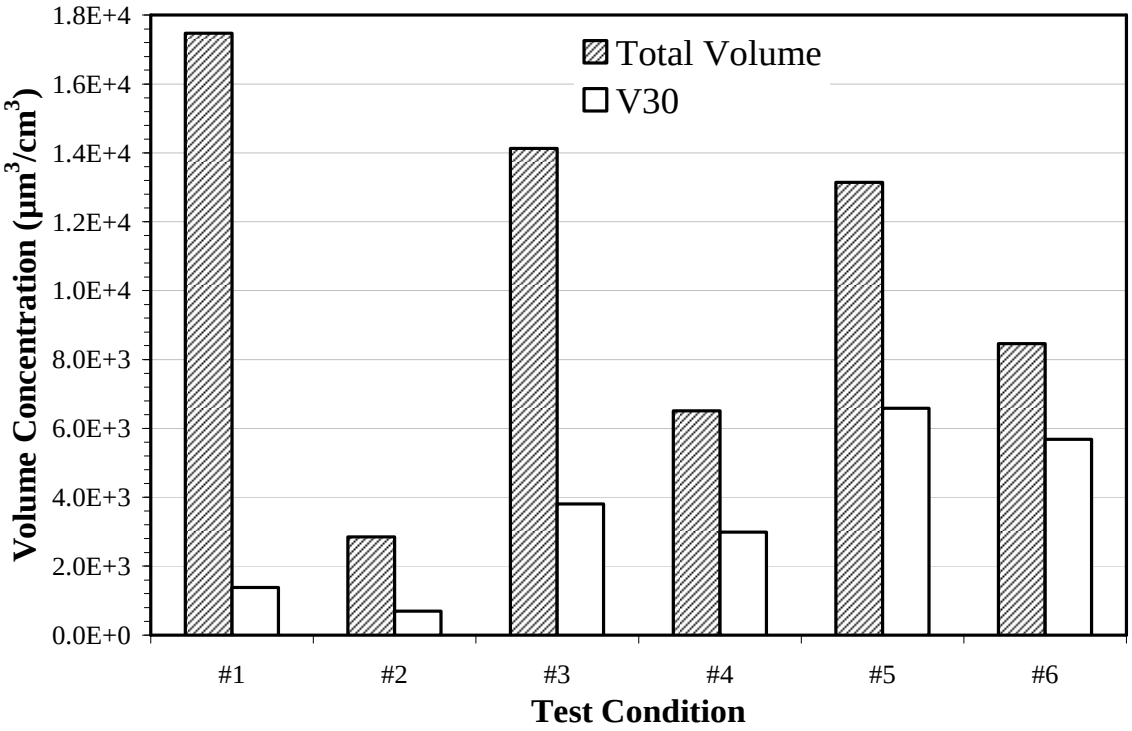

Figure 41. Total volume concentration for all conditions. Reprinted with permission from SAE paper number 2009-01-1400, © SAE International.

Figure 42 shows a comparison of the CPC and total integrated number concentration for the SMPS. Generally, there is no significant difference between the CPC and SMPS, showing consistency between instruments. In addition, the comparison suggests that the instrument is not missing, at least in number, many particles sized between 0.3 and 3 µm.

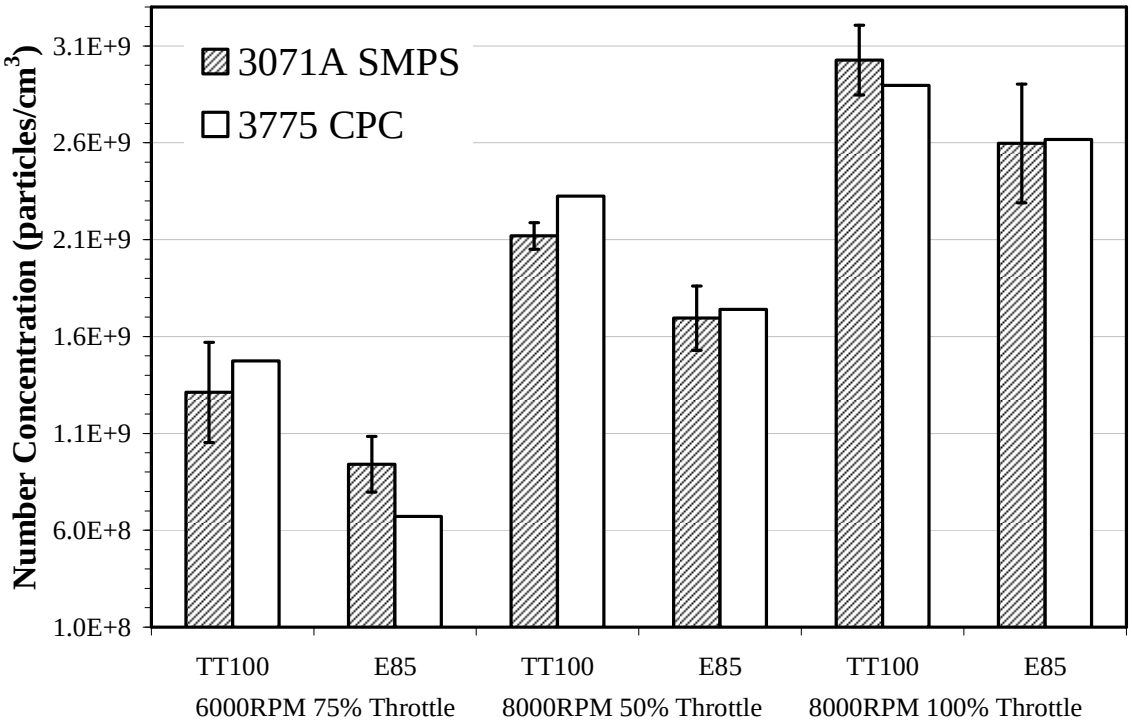

Figure 42. Total number concentrations. Reprinted with permission from SAE paper number 2009-01-1400, © SAE International.

A typical on-road Diesel aerosol size distribution (Kittelson et al., 2006) is shown in Figure 41 alongside of one E85 and one gasoline distribution obtained in this study. Diesel, rather than spark ignition, engines are traditionally known for high particulate emissions (Kittelson et al., 1998). In this case, the spark ignition race car engine running on gasoline is producing significantly more soot and nucleation mode particle emissions per unit volume exhaust than is typically observed in Diesel exhaust.

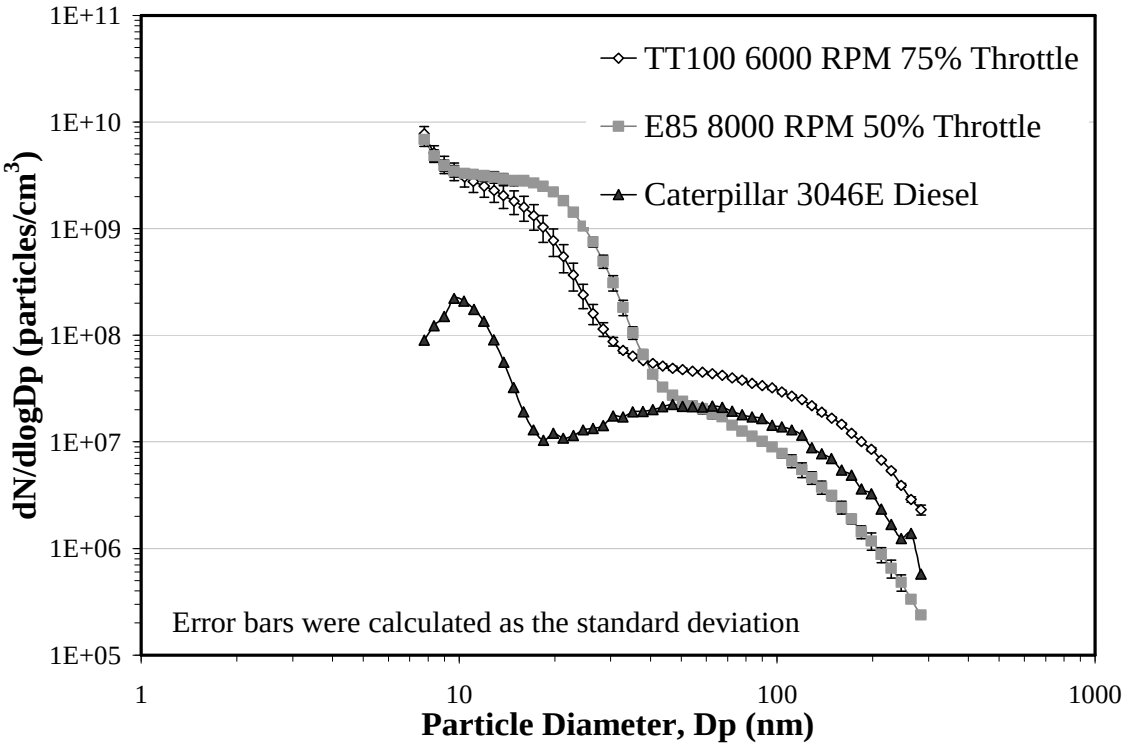

Figure 43. E85 and gasoline particle size distributions compared with an average on-road Diesel size distribution (Kittelson et al., 2006). Reprinted with permission from SAE paper number 2009-01-1400, © SAE International.Table 18 shows the mass concentration emissions that were calculated by multiplying the total volume concentration by 1 g/cm^3 and then converted to brake specific values. The numbers are not corrected for particle loss in the air ejector pumps. Therefore, the BSPM calculation may underestimate the PM emissions that would be observed during a certification test. Even so, the data shows that the PM emissions were higher than those of a MY2007 Diesel engine (0.01 g/bhp-hr) by at least factors of 3 to 20.

Table 18. Brake specific emissions

Condition	1	2	3	4	5	6
BSPM, g/bhp-hr	0.18	0.03	0.16	0.07	0.14	0.09

Chapter 6: Nanoparticle Measurements used to Detect an Engine Oil Control Ring Fracture

Introduction

Diesel engines are a source of particles that can be characterized by their size, concentration, and composition. Most of the particle number concentration is in the nucleation mode range, diameter (D_p) <50 nm, while most of the mass is in the accumulation mode, 50 nm<D_p<1000 nm range. Nanoparticles (D_p<30 nm) are typically composed of hydrocarbons or sulfate and form by nucleation during dilution and cooling of the exhaust, while accumulation mode particles are mainly carbonaceous soot agglomerates formed directly by combustion (Kittelson et al. 1998). Emissions depend on operating conditions, sampling parameters, and other factors but emissions from improperly or inadequately maintained engines can be much higher than from well-maintained engines (Bransstetter,et al., 1983; Chan et al., 1992; Ullman and Hare, 1984; Ullman and Human, 1991; Human and Ullman, 1992; Zeller, 1992).

Emissions assisted screening procedures and maintenance programs have been developed to detect and diagnose high emitting engines due to engine faults or neglected maintenance (Chan et al., 1992, Human and Ullman, 1992; Carlson et al., 1982; Spears, 1997; Chernick, 2003; McGinn, 2000; Anyon, 2008). Relationships between emissions and faults are complex. For example, higher particulate matter (PM) or carbon monoxide (CO) levels may indicate an obstructed air intake, clogged fuel injectors, or retarded timing (Ullman and Hare, 1984; Ullman and Human, 1991**)**. For routine applications, screening procedures must be inexpensive, precise, accurate, and relatively quick and easy to conduct (Spears, 1997). This chapter describes a series of experiments performed in a controlled laboratory setting that show how real-time nanoparticle measurements were used to detect an engine fault in a 4-cylinder Diesel engine by measuring fluctuations in semi-volatile particle number concentration.

Test Apparatus

Engine

The test engine was a 2005 John Deere 4.5-liter, 4045H engine producing 129 kW @ 2400 rpm and 645 Nm @ 1400 rpm. This engine is turbocharged and intercooled with common rail fuel injection and has EPA tier 2 approval for off-highway applications. At the time of this work, the engine was new, having run 20 – 30 hrs. The engine was fueled with ultra low sulfur Diesel fuel containing <15 ppm sulfur.

Particle measurement

Detailed results from the condensation particle counter (CPC), scanning mobility particle sizer (SMPS), photoemission aerosol sensor (PAS), and electrical low pressure impactor (ELPI) are presented here.

The principle of operation of the TSI 3775 CPC is the condensation of liquid butanol on particles to grow them to an optically detectable size before they are counted by an optical particle counter. The 3775 has a maximum concentration of 1E7 part/cm^3, a response time of roughly 1 s, and an effective counting range of 4 to ~1000 nm.
The SMPS was configured with a TSI 3071A electrostatic classifier and TSI 3010 CPC. It was configured to cover the size range of 8 to 300 nm over a period of 90 s with a 30 s interval between scans. From the number distribution, the integrated mass concentrations are calculated assuming spherical particles with a density of 0.9 g/cm^3, although the conclusions of the chapter do not depend on this choice of density.

The PAS responds to photo-emitting substances on the surface of aerosol particles. Ultraviolet irradiation of the sampled aerosol leads to the emission of photoelectrons from surface material that readily undergoes photoemission (Burtscher, 1992). The remaining positively charged aerosol particles are collected on a filter connected to an

electrometer. Previous work by Min et al. (1998), Jung et al. (2005), and Kittelson et al. (2005) has shown that the response of the PAS is strongly influenced by the physical and chemical nature of Diesel aerosol. In particular, its response is suppressed by the presence of a large, predominantly volatile nucleation mode, and/or the presence of volatile material on the surface of the solid carbonaceous agglomerates present in the accumulation mode.

The ELPI operates by aerodynamically sizing charged particles in a cascade impactor. Concentration is determined in real-time (1 Hz) by measuring current due to impacted particles. The size range is approximately 7 to 10,000 nm. The ELPI covers a much wider size range than the SMPS but with much less size resolution.

Sampling system

Particle measurements were made using a two stage ejector dilutor system similar to one described previously (Abdul-Khalek et al., 1999). As shown in Figure 44, exhaust enters the system through a stainless steel sampling probe immersed in the exhaust flow. An air ejector pump with a flow orifice mixes the exhaust with dilution air, providing the first stage of dilution. After dilution, the exhaust mixture passes through a cyclone with 50% cutpoint at 1 µm, transverses a residence chamber for 1 s and is diluted a second time. The system was designed to give a primary dilution ratio of roughly 15:1 and a secondary dilution ratio of 20:1 with dilution air flows of 100 L/min (each).

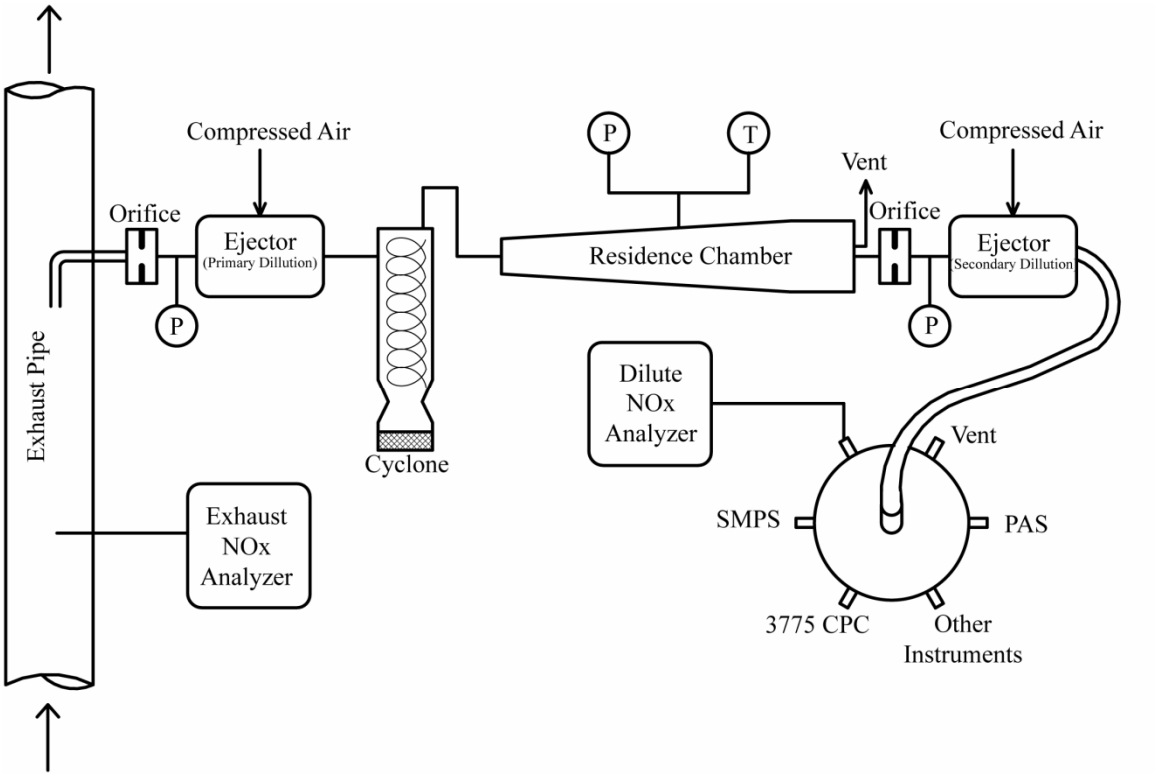

Figure 44. Particle and gas sampling system

Experiment and Diagnosis

Data from representative measurements are shown in Figure 45 (1400 rpm, no load) and Figure 46 (1400 rpm, 100 Nm). During stable engine operation, there was a cyclic variation in total particle number concentration measured by the CPC while at the same time the exhaust temperature and raw exhaust NOx emissions remained unchanged. These pulses occurred regardless of speed and load although the magnitude and frequency varied. For all cases, the PAS response decreased when the number of particles measured by the CPC increased. The diminished PAS responses are consistent with the idea that the PAS is adversely impacted by the presence of volatile nucleation mode particles Kittelson et al. (2005). To further support this contention, Figure 47 shows representative size distributions taken from areas of high and low concentration at a 1200 rpm, 75 Nm. Both the real-time (ELPI) and semi real-time (SMPS) instruments show the

increase in total particle concentration is due to an increase in nucleation mode particles. The increase in dilute aerosol mass concentration is ~ 1µg/m^3.

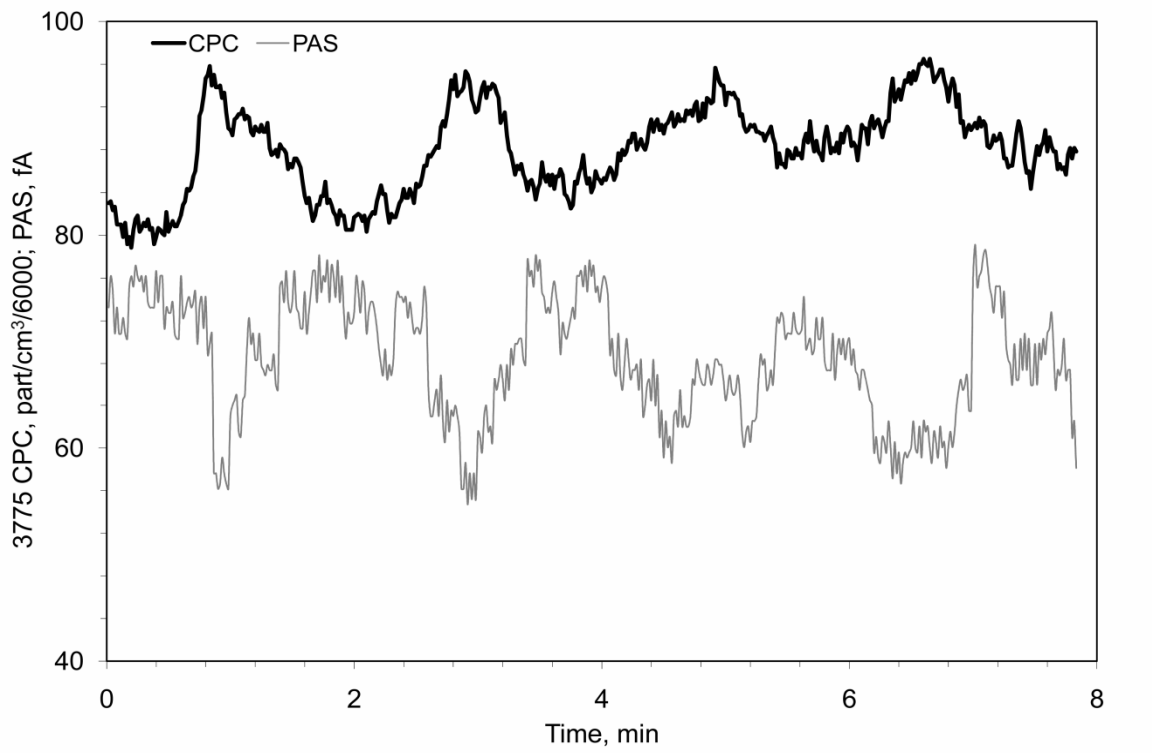

Figure 45. Time series graph showing particle measurements at 1400 rpm and no load, not corrected for dilution. Concentration is scaled arbitrary to show effect

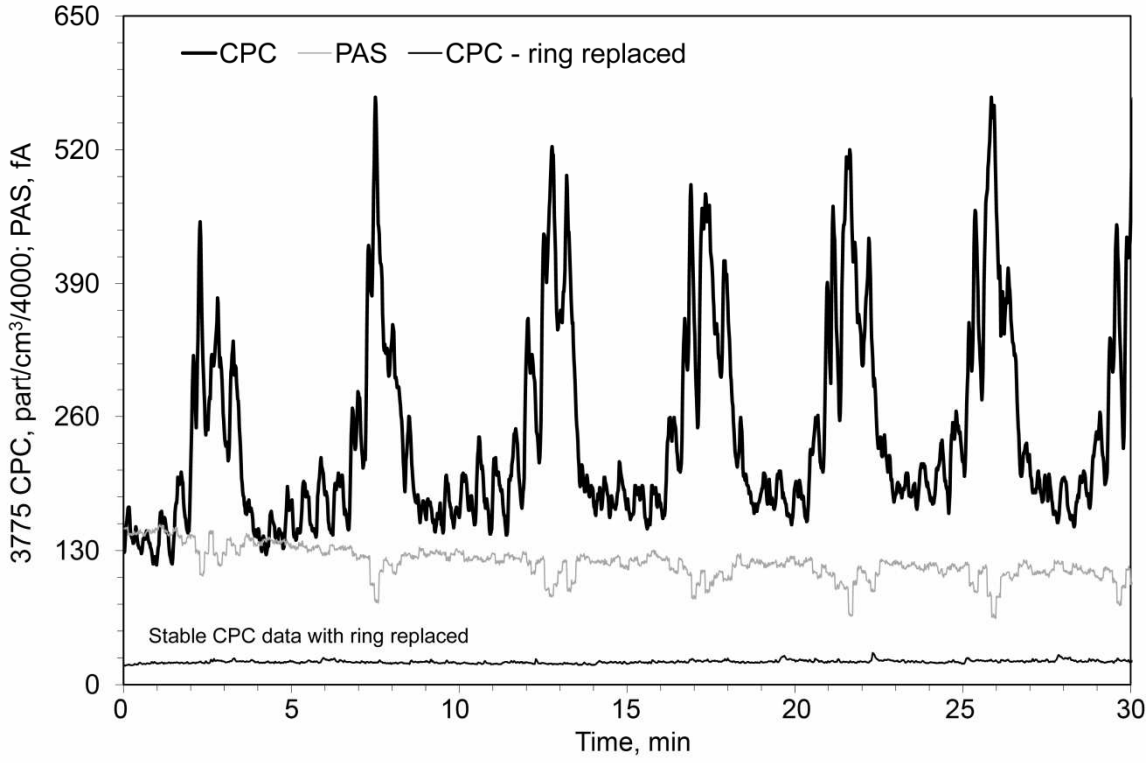

Figure 46. Time series graph showing particle measurements at 1400 rpm and 100 Nm, not corrected for dilution. Concentration is scaled arbitrary to show effect. Data shown are before ring replacement except as indicated

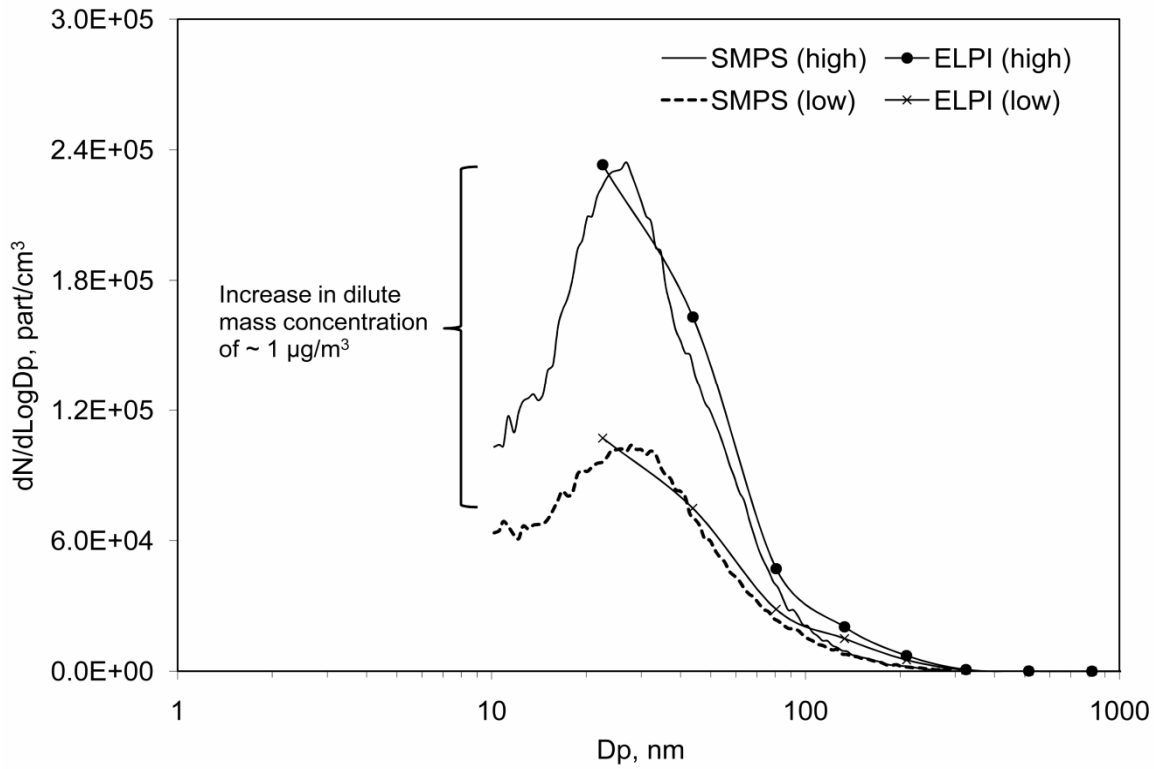

Figure 47. Representative ELPI and SMPS size distributions showing the increase in particle concentration is due to an increase in nucleation mode particles. High and low refer to concentration

Many operating parameters were scrutinized to determine the cause of this irregularity. These included dilution air flowrates, temperatures, and pressures as well as engine operating parameters like speed, torque, intake airflow, cylinder head/ coolant/ intercooler/ exhaust/ oil temperatures, and turbo boost and exhaust pressures. None were identified as unsteady or unusual. A small fluctuation in crankcase pressure associated with a change in blow-by flow suggested there might be an in-cylinder problem. The engine's electronic control module (ECM) was used to sequentially cut fuel to each of the four cylinders. The particle number fluctuation disappeared when cylinder 2 was shutdown. Visual analysis of the components in this cylinder was needed to further diagnose the problem.

The engine was disassembled, and the problem was traced to a fractured oil control ring on piston 2. Lubricating oil - derived particle emissions are primarily semi-volatile organic carbon particles containing trace metals (Miller et al., 2007; Sakurai et al., 2003). Thus, the evidence suggests that oil was migrating through the fracture and was periodically released into the exhaust forming high concentrations of semi-volatile nanoparticles during exhaust cooling and dilution. The cyclic nature of these emissions was due to the natural rotation of the piston rings that is necessary to reduce wear and oil consumption. Studies have evaluated ring rotation and have estimated rotation rates at ¼ to 2 rotations/min, depending on conditions, with higher rotation rates at lower loads and higher speeds (Min et al., 1998, Schneider et al, 1993; Schneider et al, 1990). These rates are consistent with observation of particle pulses every few minutes and the trends are the same. The ring was replaced and the particle number fluctuations were eliminated as illustrated by CPC data (collected after the repair) shown in Figure 46.

The broken ring was sent to the piston ring manufacturer for magnified (10 and 30x) photographs and analysis of the break (Figure 48). Their analysis suggested that there was nothing from a metallurgical perspective to explain the breakage and that the fracture was free of foundry related porosity. Due the location of the fracture (180º from the ring gap) and the microscopic analysis, it was concluded the fracture occurred because the ring was over-opened during its installation on the piston.

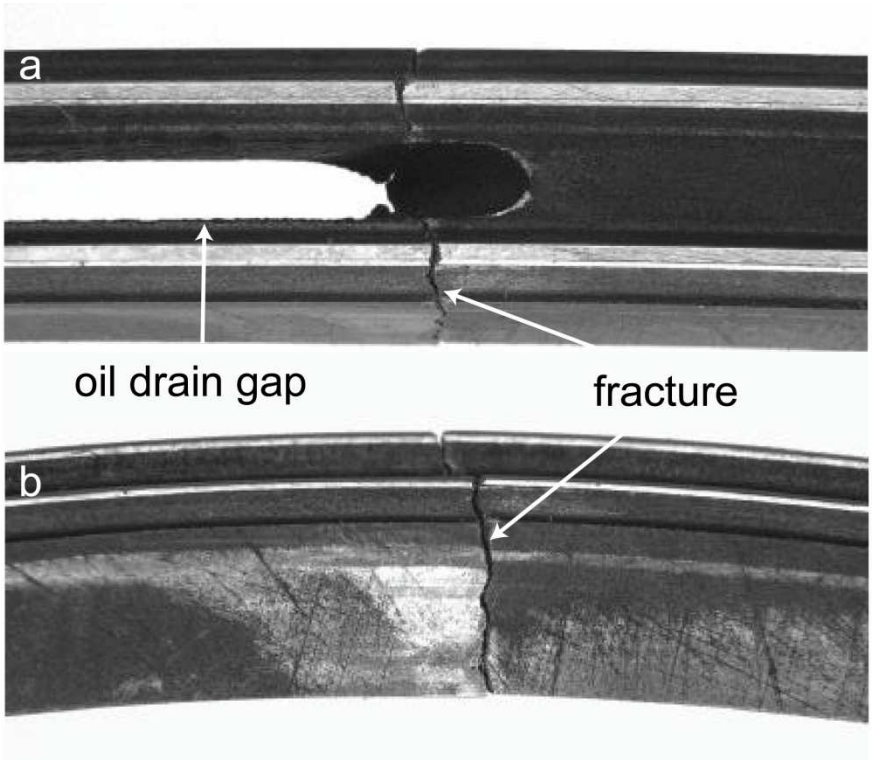

Figure 48. 10x – magnified photographs showing the oil control ring fracture looking at the outer diameter from the side (a) and from the top (b)

Chapter 7: Influence of Storage and Release on Particle Emissions from New and Used CRTs

Introduction

The 2007 heavy-duty Diesel emission standard is 0.01 g/hp-hr. To meet this standard, Diesel engine manufacturers have made significant improvements in Diesel engine design and technology, but further reductions are required to meet current EPA legislation (Johnson, 2008). Additional reductions are achieved by using exhaust filtration systems such as the Continuously Regenerating Trap (CRT) (Cooper and Thoss, 1989; Allansson, et al., 2002). A CRT consists of a Diesel oxidation catalyst (DOC) followed by a ceramic particulate filter . An oxidation catalyst consists of a substrate (the structural element) and a washcoat (high surface area oxide) coated with the catalyst material (platinum, palladium, rhodium, etc). Catalyst application is done by applying a catalyst carrying washcoat to the substrate or by impregnating a bonded washcoat-substrate with a catalyst (Twigg and Wilkins, 1998). In either case, the high surface area of the washcoat allows the catalyst to be highly dispersed, resulting in many reaction sites. The purpose of the catalyst in a CRT application is to oxidize NO to NO_2 but some fraction of SO_2 is oxidized to SO_3, which can lead to an increase in mass emissions in the form of sulfate when high sulfur fuel and lube oils are used (Truex et al., 1980). In some cases, SO_3 is adsorbed at low temperature and stored in the washcoat. Storage in the washcoat is referred to as catalyst "poisoning" because SO_3 reduces the availability of active catalyst sites to participate in chemical reactions with NO (Allansson et al., 2002). This poisoning effect is the main reason EPA requires the use of ultra-low sulfur fuel (<15 ppm sulfur). Sulfate released during some driving cycles and not others contributes to measurement variability. For example, sulfates stored during low temperature portions of a driving cycle can be released during subsequent hot portions (Somers, 1975, Allansson et al., 2002). If a catalyst never experiences high temperature operation, sulfates stored during days or months of low temperature operation may be released only

when an emissions test requires high load driving or when the washcoat has become saturated. Storage and release on this scale has contributed to measurement variability during VERT testing on in-use vehicles with catalyzed aftertreatment (Ulrich et al., 2007).

The University of Minnesota mobile emission lab (MEL) has been used to test the on-road performance of emission control devices, including CRTs (Kittelson et al., 2006b, c, 2008). The MEL enabled the CRTs to be evaluated under real world dilution conditions using a variety of test fuels and lubricants. It was shown that the presence of sulfur in the fuel and in the engine lubricant can lead to significant on-road particle number emissions of sulfate particles <30 nm in size (nanoparticles) when a CRT is used and that number emissions increase with increasing exhaust temperature. The studies suggest the on-road nanoparticle formation observed with the CRT at higher exhaust temperatures results from a combination of two effects: increased oxidation of SO_2 to SO_3 in the DOC section of the CRT and the release of sulfur compounds that were formed and stored at lower temperatures. Evidence supporting these claims can be found in Figure 49 where the temperature dependant emissions from a CRT (Kittelson et al., 2006c) and the calculated apparent sulfur conversion efficiency are plotted. The sulfur conversion is calculated given the fuel sulfur and measured fuel consumption and by assuming nucleation mode particles consist of sulfuric acid with a sulfur mass fraction given by sulfuric acid/water equilibrium data at 25°C and 50 %RH, an approximation of the average MEL test conditions. These data show that at exhaust temperatures of 360°C and higher, the apparent fuel sulfur conversion is greater than 100%. Conversion greater than 100% is not plausible, thus, there must be the release of sulfur compounds. At low temperatures (<300°C) the apparent sulfur conversion efficiencies are <1%. For reference, the SO_2 conversion efficiency of a platinum catalyst measured by Cooper and Thoss (1989) and Wyatt et al. (1993) are also shown in Figure 49. These trends are only representative

because the conversion efficiency depends strongly on the temperature, flowrate or residence time in the catalyst, and catalyst formulation.

Kittelson et al. (2006b, c) also evaluated the on-road performance of *catalyzed* continuously regenerating traps (CCRTs). Whereas emissions from the CRTs increased sharply with increasing temperature due to sulfate release, emissions from the CCRT were not detectable above background for any temperature. Both devices use the same oxidation catalyst but the CCRT has a catalyzed filter that will also oxidize SO_2. Despite having more catalyst material no nucleation mode particles were formed downstream of the CCRT. However, the CCRTs had accumulated fewer miles (5,000 versus 42,000 km) resulting in less time to store material than the CRTs and it is hypothesized that the additional washcoat on the filter allowed for more storage of sulfates. The results suggest that the extent to which a catalyzed surface is saturated with stored sulfur compounds, regardless of temperature, will strongly influence the release of sulfate containing nanoparticles.

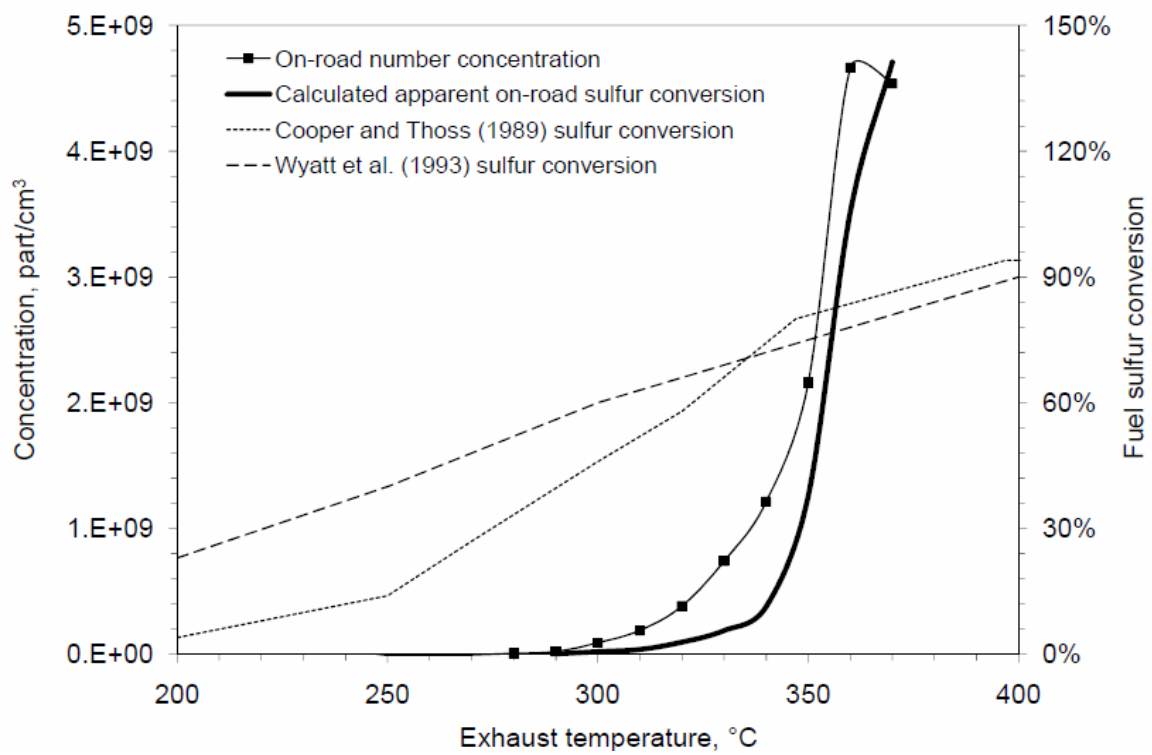

Figure 49. The calculated apparent sulfur conversion efficiency using the on-road data from Kittelson et al. (2006b). Reference platinum SO_2 to SO_3 conversion efficiency curves are also shown

The objective of the current experiments was to test various CRT configurations on an engine dynamometer under controlled laboratory operating and dilution conditions. Three CRT configurations were evaluated. The first configuration was a brand new CRT evaluated using a Diesel engine fueled with near zero sulfur Fischer-Tropsch fuel and specially formulated low sulfur lubricating oil. This configuration allowed us to measure the particle emissions from a CRT-equipped Diesel engine fueled with the lowest practical amount of fuel sulfur. Particle emissions were evaluated at high temperature conditions when the oxidation catalyst is efficiently converting SO_2 to SO_3. Neither the DPF nor the DOC had been previously exposed to sulfur, eliminating the "release" variable on the interpretation of the results. Next, the storage and release effect was evaluated using two used CRT configurations and Fischer-Tropsch fuel. The second

configuration was the MEL CRTs, with used DOCs and used, uncatalyzed DPFs. The third configuration included the used DOCs from the second configuration and new DPFs from the first configuration.

These experiments are relevant to upcoming not-to-exceed (NTE) Diesel particulate matter (DPM) standards. The NTE procedure defines the engine operating regions (i.e., speed and torque) and ambient conditions (i.e., altitude, temperature, and humidity) which are subject to the NTE emission standards. Details of these regions can be found in the Code of Federal Regulations (40 CFR 1065) but in brief, the NTE requirements are intended to ensure that DPM emissions are controlled over a large range of speed and load combinations and environmental conditions commonly experienced during the everyday use of the vehicle. DPM emissions measured during this test procedure must be less than or equal to 1.5 times the FTP standard (0.015 g/hp-hr) when the vehicle is operating in the NTE zone and never be greater than 2 times the NTE standard (0.03 g/hp-hr). Demonstrating compliance with the NTE standards requires measurements that are accurate and sensitive to emissions changes occurring on 30 s time scales. The DPM NTE initially designed to commence in 2007 has been delayed to improve the on-board Portable Emission Measurement System or PEMS (Spears, 2005). In the absence of a standard method, the Engine Exhaust Particle Sizer (EEPS, Johnson et al., 2004) was used to measure DPM during the transient conditions observed in this work.

Experimental Section

Particle/gas measurement instrumentation

Particles were measured with four TSI instruments: a 3934 scanning mobility particle sizer (SMPS, size range: 8 – 300 nm), an EEPS (5.6 – 560 nm), a 3775 condensation particle counter (CPC, limit of detection: 4 nm, concentration limit: 1×10^7 part/cm^3) and a 3025 CPC (3 nm, 1×10^5). The CPC provides a measure of total number concentration,

which can be made NIST traceable (Fletcher et al., 2009). The EEPS and SMPS are used to measure particle number distributions, which are then converted to estimate mass distributions and the total mass concentrations. Some assumptions are required for the mass calculations. In the used CRT experiments, the particles are likely freshly formed sulfuric acid droplets with a small mass fraction of organic material (Schneider et al., 2005; Grose et al., 2006). Such particles are spherical and have well defined properties. For example, under ambient conditions, sulfuric acid forms an equilibrium mixture with water where the acid content and particle density are functions of relative humidity (Seinfeld and Pandis, 1998). Thus, the mass concentration is obtained by multiplying the estimated volume concentration determined by assuming spherical particles by the particle density. A diffusion loss correction (Ayala et al., 2003) was used for all SMPS calculations, as the interest was in determining the absolute emission levels. A California Analytical Instruments NO/NO_x analyzer was used to measure raw NO concentrations and an EcoPhysics CLD 700 AL chemiluminescence analyzer was used to measure dilute exhaust NO concentrations.

Dilution system

Engine exhaust downstream of the CRTs was diluted using a two-stage micro-dilution tunnel similar to the one described elsewhere (Khalek et al., 1999). A pressure swing adsorption (PSA) system was used to provide ultra-clean dilution air, eliminating the possibility of nucleation or growth induced by dilution air species. The PSA reduces contaminant concentrations in compressed air to <1 ppb HC, <1 ppb NOx, <1 part/cm^3, and reduces the dewpoint to -70°C (Swanson et al., 2007). The cleaned air was cooled and mixed with engine exhaust using air ejectors. Primary dilution ratios ranged from 5 – 50:1. A primary dilution ratio within this range typically maximizes particle formation (Kittelson et al., 1999). After the first dilution stage, the mixture passed through a residence time chamber where the aerosol aged for ~1 s. For some engine conditions, the sample was diluted a second time using an air ejector. The primary and secondary

dilution ratios were determined by measuring the NO concentration before and after the primary and secondary air ejectors and total dilution ratios ranged from 16-700:1. Exhaust temperatures were measured using thermocouples and were manually recorded while other sensors and NO concentrations were recorded continuously with a data logger. The SMPS and CPC were controlled and data were analyzed using software provided by TSI. At least three SMPS scans were taken for every condition. NIST traceable gases were used daily to zero and span the NO analyzers. The consistency of the CPCs, SMPS, and EEPS was checked on a daily basis by challenging them with a laboratory-generated aerosol. This aerosol was atomized dioctyl sebacate (DOS) (100 ppm diluted in isopropyl alcohol) that was dried with a molecular sieve to form a semi-volatile aerosol with a mean diameter of 60 nm.

Engine setup

The test engine was a 1995, 12 L, 6-cyinder, turbocharged, and aftercooled Caterpillar 3176, C-12 Diesel engine, modified to meet 1998 EPA post consent decree emissions standards. The C-12 series engines have high pressure, electronically controlled direct injection. The engine was derated to 265-kW (355 hp) for use in the laboratory. For the first experiment, the engine was fueled with a Fischer-Tropsch fuel containing 2.3 ppm sulfur and the engine oil was specially formulated oil containing 420 ppm sulfur (details of formulation are found in Kittelson et al., 2008). The used CRT experiments used fuel with <1 ppm sulfur and the same lube oil (420 ppm). Lube oil sulfur is an important variable because when fuel sulfur levels are <15 ppm the contribution of lubricating oil to nanoparticle formation is significant (Andersson et al., 2004b, Vaaraslahti et al., 2005, Kittelson et al., 2008). Previous work indicates that 420 ppm lube oil sulfur is equivalent to ~ 2 ppm fuel sulfur assuming a lube oil consumption of 0.15% fuel consumption and the propensity of oil sulfur to form nanoparticles downstream of a CRT reported by Kittelson et al. (2008). Each experiment used two CRTs that were sized for the dual exhaust system on the mobile laboratory. For these experiments, they were mounted in

parallel in a split exhaust system to provide flows through the CRTs similar to when they are installed in the mobile lab. The used CRTs have accumulated about 42,000 km during the MEL on-road testing. The MEL has been fueled with commercial fuels and specially formulated lubricating oils with sulfur levels ranging from 4 to 45 ppm and 420 to 6200 ppm, respectively (Kittelson et al., 2008). Based on the amount of each fuel and oil consumed, the total sulfur exposure was 220 g.

CRT conditioning

New CRTs were conditioned using a break-in schedule recommended by the manufacturer to “set” the binding ceramic mat that holds the monolith in place while protecting it from cracking due to engine vibration and thermal expansion. After the device was installed, the engine was run for 8 hr at 1600 rpm, 400 Nm, and 300°C exhaust temperature.

Sampling procedures

New CRT

Particles were continuously sampled from engine exhaust downstream of the CRTs using the two-stage micro-dilution system. Emissions were evaluated at 8 engine conditions covering a range of exhaust temperatures. Exhaust temperature was measured immediately before the CRT. The operating and dilution conditions are shown in Table 19.

Table 19. Engine operating and dilution conditions averaged for each test condition

	Load (Nm)	Sampling time (min)	CRT temp (°C)	Dilution air temp (°C)	Tunnel temp (°C)	Primary DR	Total DR
New CRT	250	20	224	16	24	8	88
	300	20	238	16	27	6	67
	350	20	272	16	25	5	55
	400	20	286	17	27	7	58
	450	20	304	17	28	7	59
	700	20	350	16	20	16	16
	900	30	380	16	18	16	16
	1000	15	395	16	20	16	16
Used DOC, used DPF	350	8	260	12	15	33	33
	450	13	296	13	18	33	33
	700	9	349	13	18	30	30
	990	15	400	14	19	34	584
	1400	60	426	15	20	49	681
Used DOC, new DPF	warm-up	30	n/a	13	19	n/a	n/a
	1150	75	414	14	24	18	502

For all tests, engine speed was 1600 rpm.

Used CRT

The engine was started, warmed up, and stabilized at 1600 rpm. This condition produced an exhaust temperature entering the CRTs of about 250°C. The exhaust temperature was allowed to stabilize for 10 – 15 min while particles were sampled continuously. This was repeated for 4 CRT inlet exhaust temperatures. The experiment was run continuously for 1 hr after the exhaust temperature reached its maximum value of 426°C.

Used DOC and new DPF

The used DPFs from the used CRT experiment were removed and replaced by the new DPFs from the new CRT experiments. The engine was warmed up and the modified CRT inlet temperature was quickly raised to 414°C. The experiment was run continuously for 1.25 hr. This configuration allowed for the evaluation of any material stored on the DOC alone.

Results

New CRT

Figure 50 shows the SMPS particle size distributions for representative steady-state operating conditions. At the lowest temperatures, there is a hint of bimodality with a

nucleation mode at about 30 nm that disappears as the temperature increases. The disappearance is primarily due to the increase in efficiency of the catalyst to oxidize and eliminate organic particle growth species and formation precursors. The absence of a nucleation mode at high exhaust temperatures contrasts with the findings of Vaaraslahti et al. (2004). They found that a significant nucleation mode was present at high load when using 2 ppm sulfur fuel, which was attributed to the high sulfate conversion efficiency at 500°C. Vaaraslahti et al. (2005) suggested that past results might be due to the release of stored sulfate. The on-road data (pooled EEPS and CPC data, Figure 49) from Kittelson et al. (2006c) showed that CRT total particle concentrations at 370°C were ~1 x 10^9 part/cm^3 (based on CPC). The current results show that new CRT emissions at the same temperature are ~1 x 10^6 part/cm^3 (based on CPC), a 99.9% decrease.

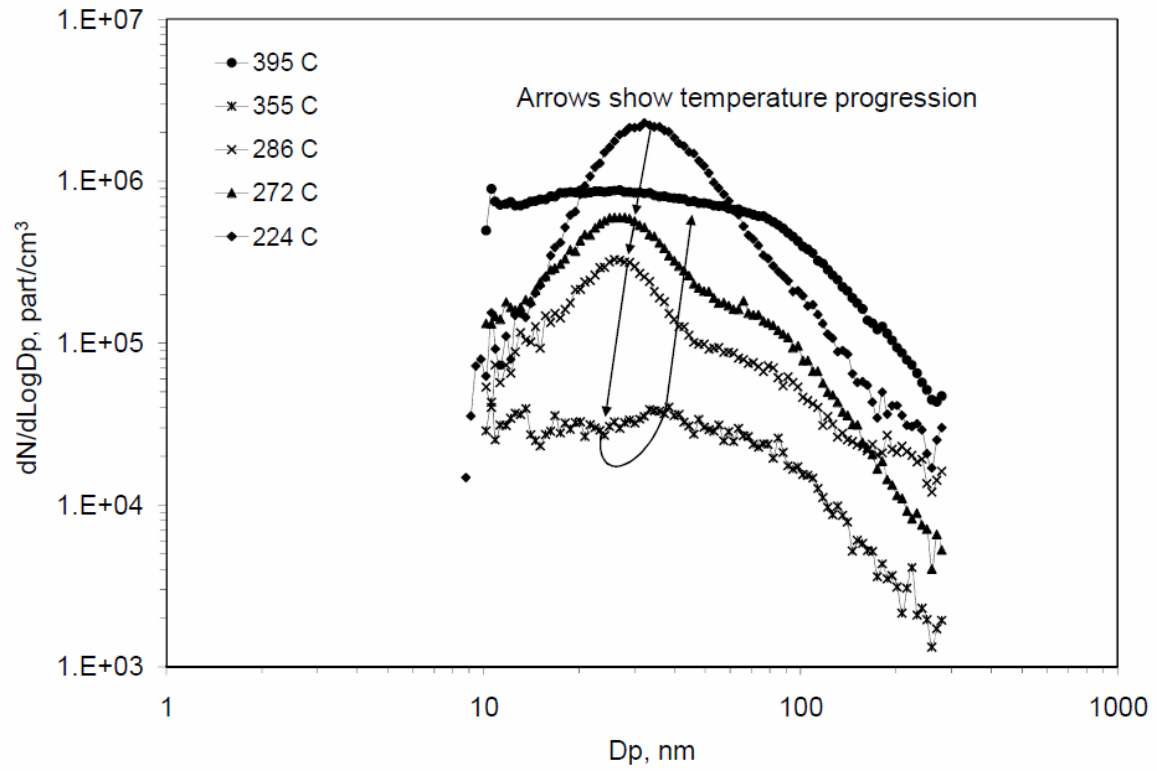

Figure 50. Averaged particle size distributions measured at different exhaust temperatures for the new CRTs. For clarity, not all distributions from Table 19 are shown and the distributions that partially captured spiking events were omitted from the averages

SMPS total concentrations, averaged for each condition and corrected for dilution, ranged from 3.4 x 10^4 to 9.6 x 10^5 part/cm^3. Averaged CPC concentrations ranged from 4.5 x 10^5 to 2.1 x 10^6 part/cm^3 for the new CRTs. The discrepancy in SMPS and CPC number concentration is most likely due to the fact that the CPC is a near real-time instrument that captures large spikes in number concentration while the slower SMPS steps through the size distribution and misses transient events. Large spikes in number concentration are discussed next.

A semi-regular release of high concentrations of particles is illustrated in the time series plot shown in Figure 51. The spikes occurred when the new CRT temperature was

between 355 – 380°C and was at times three orders of magnitude higher in total concentration than the baseline. These spiking events stopped after approximately 1 hr of high temperature operation. The duration of each spike was ~1 – 10 s and they occurred roughly every few minutes. Roughly half of the particles emitted between 355 – 380°C were contained in a spike. It appears that the spikes stopped as the source was eliminated and similar spiking behavior that was observed during the evaluation of used CRTs will be discussed later.

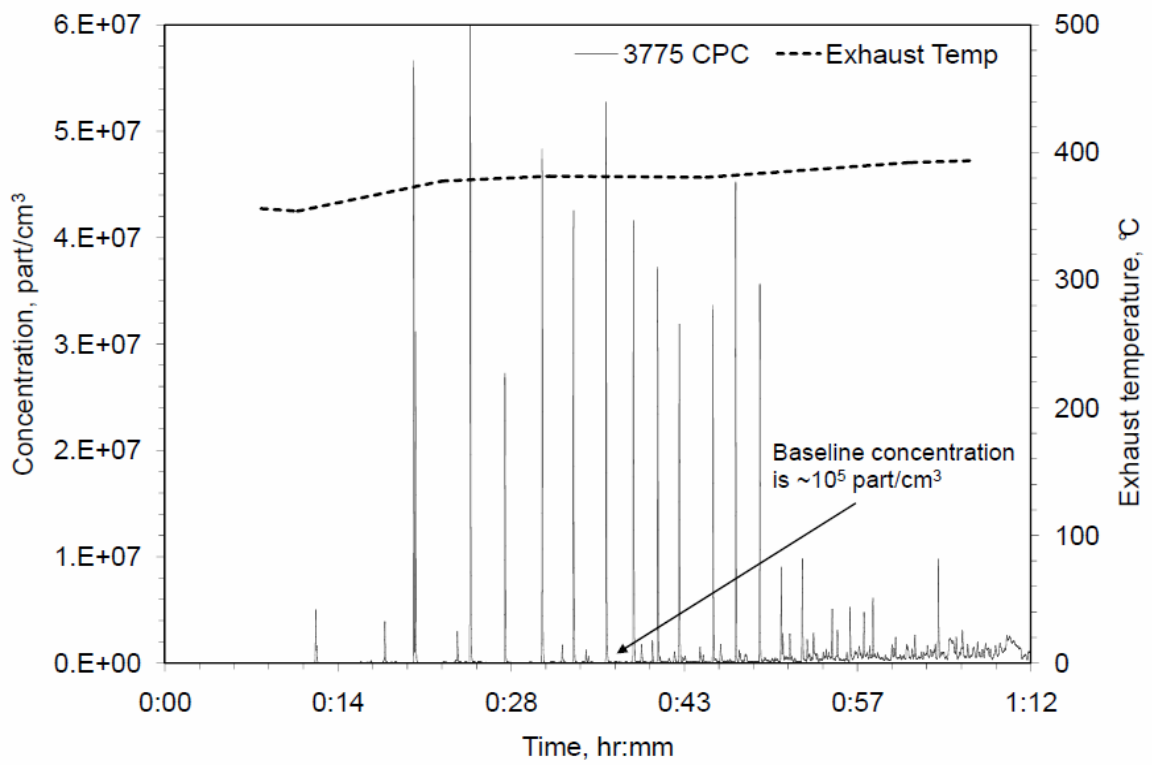

Figure 51. A time-series plot illustrating semi-regular large spikes in particle concentration for the new CRT evaluation measured with the 3775 CPC

Used CRT and used DOC + new DPF

Particle number emissions

Figure 52 shows the results from the used CRT and used DOC + new DPF evaluations in two time series graphs that are combined because the second experiment is a continuation of the first. The total number concentration measured by the 3775 CPC and the exhaust temperature are plotted. Particle number concentrations during the first 30 min were low for the used CRT evaluation (left side). Once the exhaust temperature reached 380°C, the emissions increased sharply and then stabilized. The engine load was increased and there was another sharp increase in particle concentration. Total concentrations as measured by the SMPS and EEPS, averaged for each test condition ranged from 9×10^4 to 9.9×10^8 part/cm^3 and 5.3×10^4 to 1.1×10^9, respectively, after the dilution correction. Similarly, the averaged CPC concentration ranged from 4×10^5 to 2×10^9 part/cm^3. CPC concentrations were, at times, 2 times higher than the integrated EEPS total number concentration due to the large number of particles below the EEPS effective sizing range.

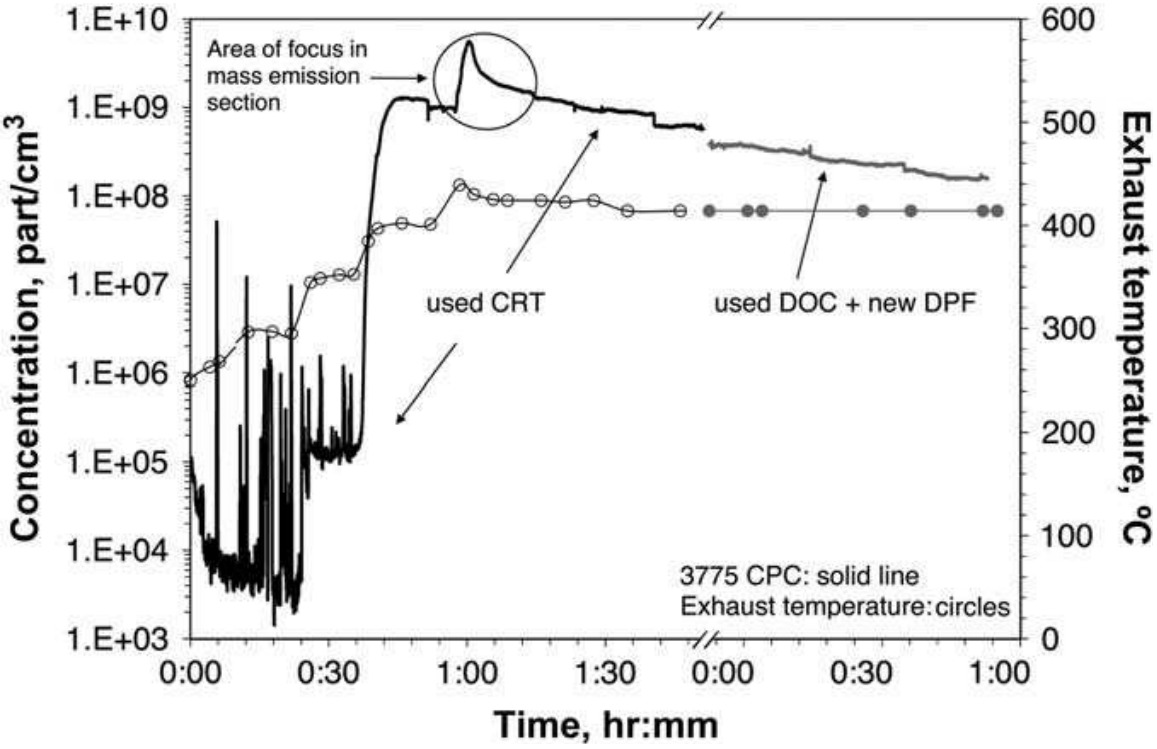

Figure 52. Time-series summary of the used CRT and used DOC and new DPF experiments. The switch between the used CRT and used DOC and new DPF configurations is shown by breaks in the graph

After an hour of observing a slow decline in the total number concentration, the engine was stopped, the used DPFs were replaced by new DPFs, and the experiment resumed. The location of the switch is indicated in Figure 52 by the breaks in the plot. Data from the 30 min warm up period is omitted for clarity. Remarkably, the total number concentration downstream of the used DOC + new DPF system, with a slight decrease, continues the trendline of the used CRT evaluation. The implication is that most of the sulfate storage and release is associated with the DOC, not the uncatalyzed DPF. The ~30% initial difference in number concentration compared to the used CRT test is likely due to the release of sulfates during the used-system warm up. This decrease is consistent with the rate of decrease in total number concentration at the end of the used CRT test

(~3%/min) and the time the used DOC + new DPF system was at high temperature (>400°C) during the omitted warm up (10 min).

Averaged SMPS and EEPS particle size distributions for both used CRT configurations at an exhaust temperature of ~415°C are shown in Figure 53 without error bars to increase clarity. A large nucleation mode spanning 3 orders of magnitude was measured. The only difference between the size distributions was a slight decrease in the nucleation mode for the used DOC + new DPF system because some of the precursor material had already been released. In some cases, the EEPS gave an unexpected response with a large fluctuation in concentration for particles larger than 30 nm. The size distributions span a concentration range of 5 orders of magnitude. The steep slope of the distribution between the nucleation and accumulation modes (~60 nm) presents a problem for the EEPS inversion algorithm (Wang, 2008). In some cases, the middle of the size distribution drops out (the software gives “0s”) because a negative concentration value in the solution is clipped to zero. Figure 53 shows a large oscillation in the EEPS size distribution for the used CRT that is attenuated in the size distribution for the used DOC + new DPF system where the slope of the size distribution is less severe. While this experiment pushed the EEPS’ dynamic range to near its limits, the nucleation and accumulation mode concentrations were within its specified concentration requirements.

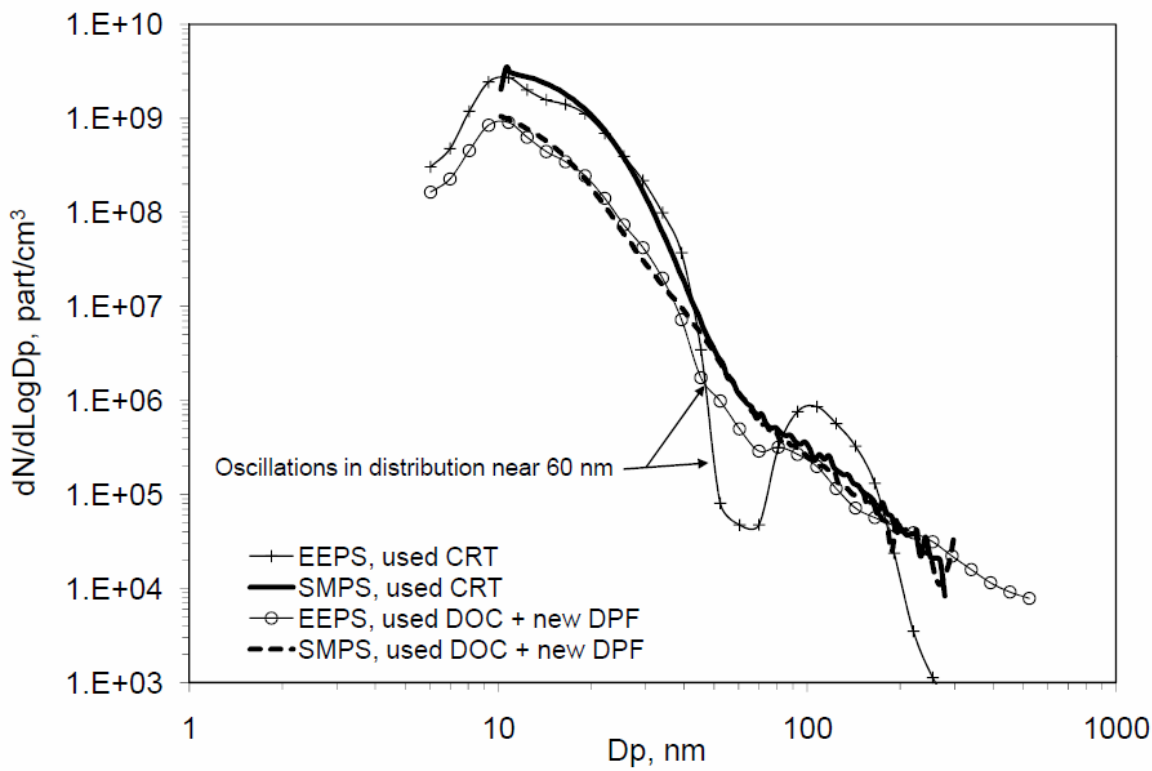

Figure 53. SMPS and EEPS particle size distributions for the used CRT and used DOC and new DPF evaluations

Occasional spikes in particle concentration were observed during the first 30 min of the used CRT evaluation as shown on the left side of Figure 52. These spikes range from seconds to minutes in duration and were at times three orders of magnitude higher in total concentration than the baseline. Similar behavior was observed with the new CRTs, described earlier, although the onset of the new CRT spikes occurred at 350°C whereas the used CRT spikes started at a lower temperature, 280°C. This result is consistent with the observations of Stratakis et al. (2003) who observed that soot particles containing a high volatile hydrocarbon fraction stochastically regenerated at lower temperatures than did drier soot. Figure 54 shows the baseline size distribution measured at an exhaust temperature of 350°C for the used CRT configuration. Additionally, size distributions taken during representatives “spikes” are shown (each representing 1 s of EEPS data).

The size distributions are consistent with previous measurements of solid accumulation particles present in C12 engine out exhaust (Kittelson et al. 2005). If the spikes had been due to the release of volatile material, the size distributions would have a smaller mean size and narrower distribution (Kittelson, 1998). Thus, it is possible that the spikes are the result of the breakthrough or release of solid, carbonaceous, soot particles during discrete, localized regeneration events. However, the similarity of the spiking size distributions to engine out distributions suggests another possible explanation - that the spikes result from micro-cracks in the soot bed that lead to a short term decrease in filtration efficiency which persists until the crack heals itself as it fills with particles. Johnson et al. (2009) observed large spikes in solid particle number concentration downstream of DPFs using the Particulate Measurement Programme's methodology (ECE/TRANS/WP.29/2008/62). Their observations appear to be consistent with ours. These results contrast work by Campbell et al. (2006) and Hall and Dickens (2003) who observed spikes in volatile number concentration that resulted primarily from the release of sulfur compounds. Further investigation is needed to determine the nature of these emissions.

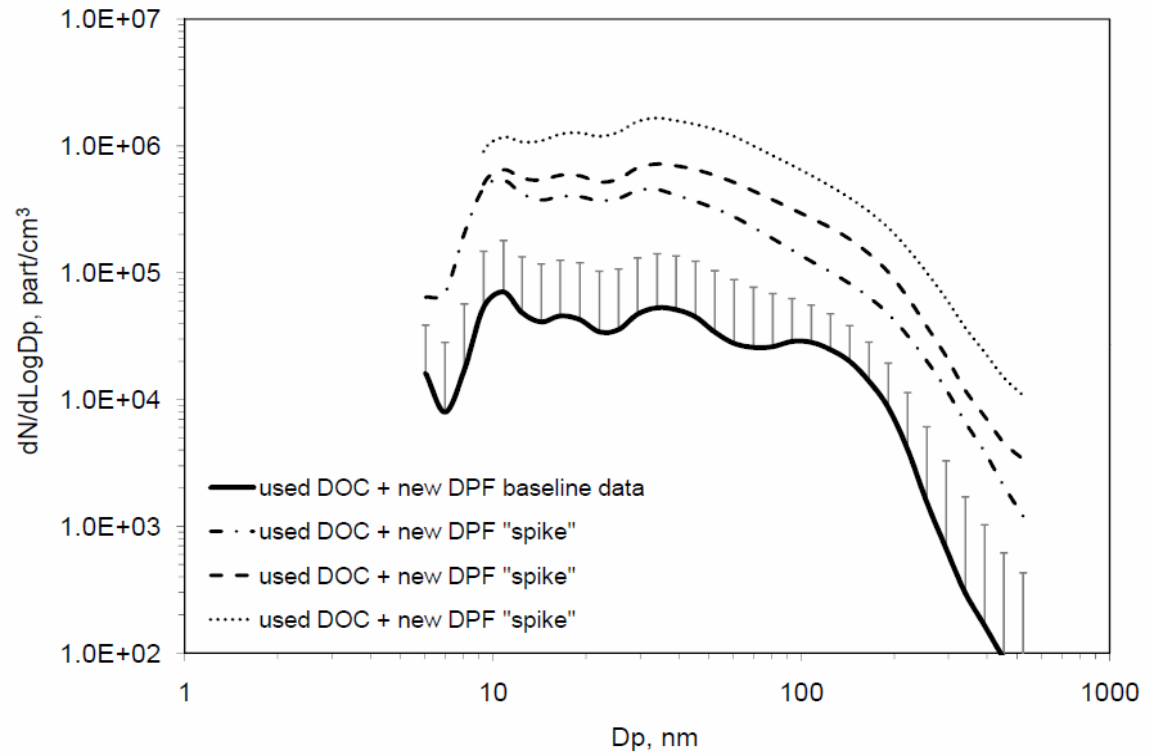

Figure 54. Size distributions showing the average baseline size distribution downstream of the used CRT system (error bars are standard deviations). Also shown are 3 representative size distributions during ‘‘spiking events’’ that are only a few seconds in duration

Particle mass emissions

Table 20 presents the calculated average mass concentration ($\mu g/m^3$), brake specific PM emissions (g/hp-hr), PM emissions rate (g/hr), and sulfur emissions rate (g/hr) for each test condition, as defined in Table 1. Particle mass emission rates are calculated by multiplying the calculated particle mass concentration by the volumetric exhaust flow and brake specific particle emissions (BSPM) are calculated by dividing emission rate by power. High dilution ratios and dry dilution air was used so the relative humidity in the dilution tunnel was 0.3 %RH, corresponding to sulfuric acid particle density of 1.7 g/cm^3 at 25°C. The mass calculation is based upon the EEPS or SMPS diameter and yields the mass concentration at 0.3 %RH. Emission standards or on-road compliance

measurements are based on measurements made with a filter or PEMS and both measurements are made at approximately 50% RH. This increases particle mass by a factor of 1.8 due to water uptake by the sulfuric acid. To make these results comparable with on-road compliance measurements, the measured results are corrected for the theoretical particle mass increase. The dynamic nature of these experiments is best viewed in the graph that follows and not as averages.

Table 20. Mass emissions (calculated from EEPS)

avg. interval (min)	engine load (Nm)	exh. temp (°C)	mass concentration ($\mu g\ m^{-3}$)	PM emission rate ($g\ hr^{-1}$)	BSPM (g hp-hr^{-1})	S emission rate ($g\ hr^{-1}$)
8	350	260	21	0.01	1.4E-4	<0.01
13	450	296	11	<0.01	6.4E-5	<0.01
9	700	349	7	0.03	3.2E-5	<0.01
15	990	400	5942	4.45	2.0E-2	0.66
60	1400	426	11866	10.1	3.2E-2	1.50
20	1150	414	2011	1.59	6.0E-3	0.42
20	1150	414	1028	0.81	3.0E-3	0.22
20	1150	414	1026	0.81	3.0E-3	0.22

Figure 55 shows the circled area in Figure 52 where the total number concentration is converted to BSPM. When the temperature reached 400°C, the BSPM is at 1 to 2 times the on-road standard. As the temperature is increased to 426°C the emissions rise sharply, exceeding the standard by a factor of 15 before decreasing slowly. The emissions are above 0.01 g/hp-hr for about 35 min. The calculated mass emissions rate (not shown) follows the same pattern with a peak at 48 g/hr. For reference, the NTE standard of 0.015 g/hp-hr and the never-to-exceed standard of 0.03 g/hp-hr are also shown on the graph. If the PM mass emission rate is integrated over the time of the experiment and multiplied

by the fraction sulfur expected in the sulfuric acid water droplets the result is about 1.2 g. This is only about 0.5% of the total sulfur exposure (220 g).

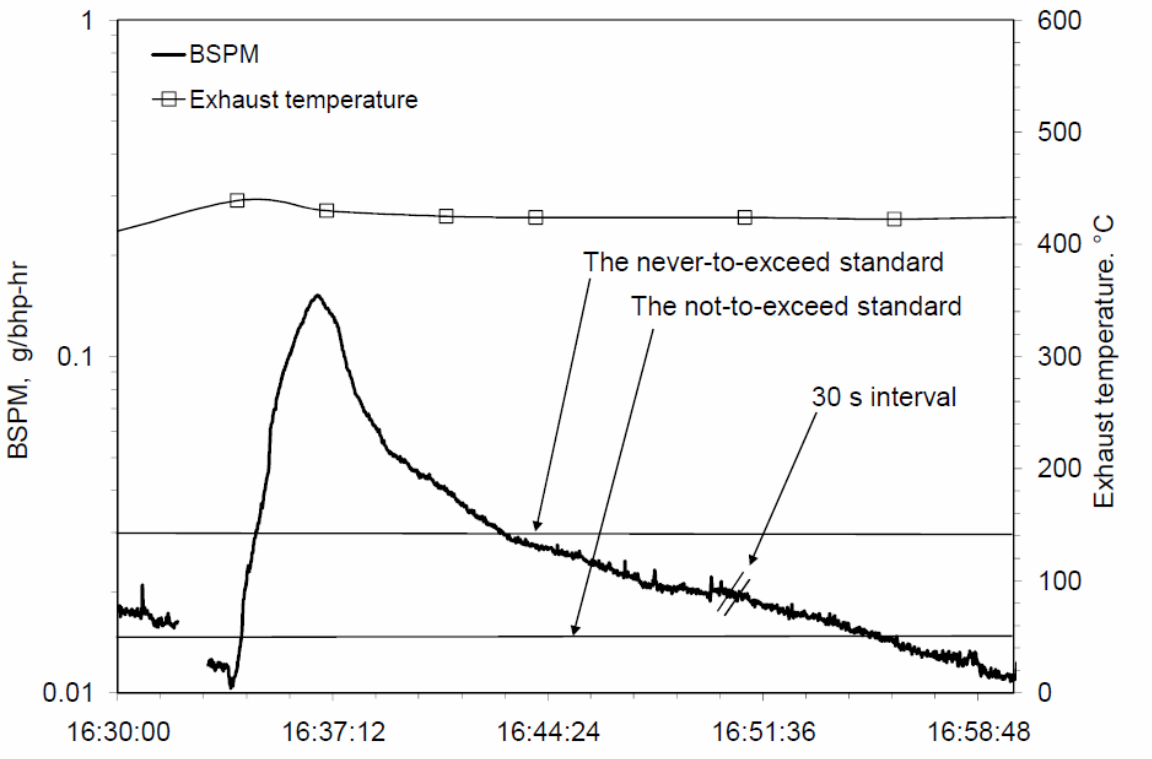

Figure 55. Particle mass emissions calculated from the integrated EEPS size distributions assuming the particles are sulfuric acid particles at 25 °C and 47 %RH. This plot is a snapshot of the experiment as indicated in Figure 54 that was converted to mass

Figure 56 shows the mass concentration distributions from the used CRT and used DOC + new DPF configurations, averaged over the highest temperature sampling interval shown in Table 1. The DOC + new DPF results are much lower because these measurements were made well after the peak release had occurred. The mass distributions are dominated by nucleation modes with mean diameters of only 15 – 30 nm, representing a substantial deviation from a typical engine-out exhaust particle mass distribution (Kittelson, 1998) where most of the mass is found in the accumulation mode above 100 nm. The small but visible accumulation mode is due to a decrease in filtration

efficiency (only the bare substrate material is filtering) at high exhaust temperatures. In addition, the SMPS and EEPS calculated mass distributions are in good agreement. For example, for the used CRT, total concentration is within 6%.

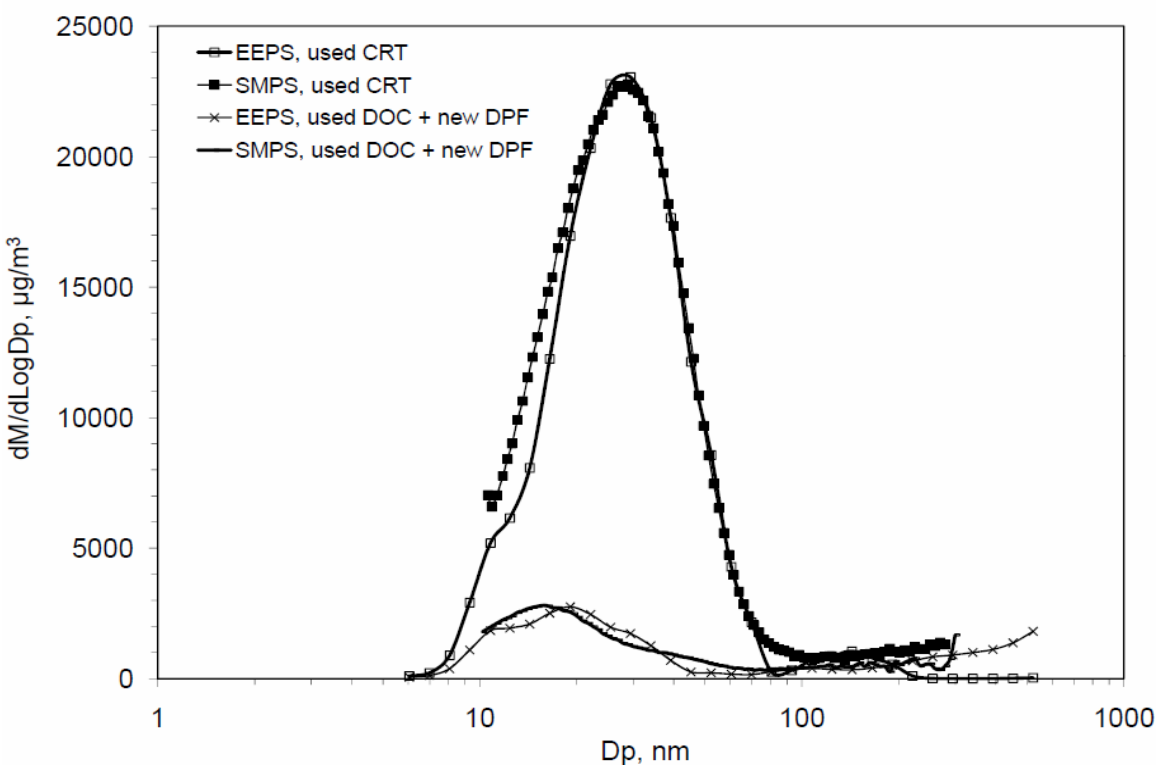

Figure 56. Particle mass distributions from the used CRT and used DOC and new DPF evaluations

Chapter 8: Conclusions

Chapter 2 described current and emerging combustion aerosol measurement technologies that are used to measure particle volatility, number, size, mass, and surface area. The physical metrics are all widely used, but issues remain. The findings are briefly reviewed in the context of, "what metric and methods used to measure it shows the most promise to meeting the need of engine manufacturers trying to develop technology to reduce DPM emissions now and in the future?" The analysis suggests a new metric is needed that is real-time and more sensitive and specific than the current gravimetric method. Cost is now also a consideration. Manufacturers with 10 or more engine development test cells all requiring instrumentation and upcoming regulations that require instruments to be placed on-board multiple vehicles leads one to favor instruments with expense in mind.

Particle number measured by CPCs has many benefits and the measurement is relatively simple and cost effective. The EU PMP method used to regulate solid particle number >23 nm effectively requires the use of particulate filters but it does not prevent emissions of high concentrations of semi-volatile nanoparticles that may be produced. Extending the lower limit to include these particles is feasible but using this metric alone would result in a measurement that was strongly weighted by nanoparticles. This is not particularly desirable because the measurement would be very sensitive to sampling conditions, added variability of CPC D_{50} cutpoints due to particle composition and CPC performance variations, and high mass emissions might result.

The active surface area metric is relatively new. However, preliminary evidence suggests that diffusion-charging techniques used to measure active surface perform well in ultra-low emission environments (Mohr et al., 2005). Known issues in general include different sensitivities for spheres and aggregates, difficulty in predicting response to a bimodal distribution, and sensitivity of unipolar charging to charging geometry. Further

theoretical and experimental study is required to resolve these issues. “Calibration factors” will be required. On the other hand, active surface is a quantity that can be measured quickly and easily, interpreted physically, and is of possible health relevance.

Special emphasis was given to evaluating alternative methods used to improve mass concentration estimates for non-spherical particles. However, the fact that DPM emitted by post-2007 engines typically contains <20% elemental carbon (Spears, 2002, Burtscher, 2005, Khalek et al., 2009) calls into question the need for highly accurate aggregate mass measurements because their mass may not dominate. Emission control systems are prone to emissions of high levels of semi-volatile material during regeneration or storage and release events. In an extreme case, Swanson et al. (2009b) measured emissions of 20 nm sulfuric acid particles downstream of a Diesel oxidation catalyst filter at levels as high as 0.1 g/hp-hr. The effective density of these particles is ~5 times higher than that of 300 nm aggregate particles. Because it is not fully clear how to account for these effects, mass concentrations based on integrated size distributions applied across a range of engines and conditions may differ from the true value by at least a factor of 2. On the other hand, if emission standards are met by partial or open particulate filters that are much less efficient than the best available technologies, elemental carbon may dominate emissions. Until a method to resolve the effective density issue is developed, this is not the most sensitive and specific method. Additionally, the already very low mass emissions of current technology engines suggests that mass is no longer the most appropriate metric for evaluating new technologies.

To conclude this chapter, a metric and methodology that utilizes the technology that shows the most promise to meeting the need of engine manufacturers trying to develop technology to reduce DPM emissions now and in the future is suggested. There may be other choices that satisfy these and other requirements. Thus, the recommendation is only

intended as a first step in a process of research, development, and consolidation of all choices that will help to move forward.

The recommendation is the diffusion charging technique combined with an electrometer operated with and without a catalytic stripper. The combination provides semi-volatile and total solid surface area concentrations on one second time scales. The analysis in the "Surface Area" section described an example of the information and analysis that could result from this technique. Furthermore, in addition to meeting the criteria outlined in the introduction, the method has the following characteristics.

1. It measures particles in a broad dynamic range (10 to 1000 nm). This range encompasses where the majority of particle number, surface area, and mass reside.
2. The active surface area weighting in the transition regime where the Diesel accumulation mode resides is proportional to $\sim d_m^{1.4}$ and other weightings are possible. However specific calibration issues remain. Active surface weighting allows for changes in the accumulation mode to be identified, providing information for engine manufacturers trying to measure and improve DPF and engine performance. It also allows for the detection of high concentrations of nanoparticles, which allows phenomena like DPF regenerations, storage and release effects, and emissions due to metal additives to be better elucidated.
3. The lower size detection limit is not critical and variability due to varying losses of very tiny particles is less of an issue.
4. A degree of chemical specificity is included in the measurement, because semi-volatile and solid fractions are measured.
5. It is adaptable to "add-ons" such as adding a CPC, PAS, or diffusion battery in parallel with the diffusion charger to increase the specificity.

6. Without the CS, the measurement will exhibit less sensitivity to dilution conditions than total number concentration measurements and with the CS there is little to no sensitivity to dilution conditions.
7. It is compact and economical ($10 – 20,000) and robust enough to be used in research laboratories, certification test cells, or on-board vehicles for continuous emissions monitoring.
8. Recent research has suggested that the adverse health effects caused by DPM are most associated with DPM surface area (Oberdorester, 2005).

In **Chapter 3** a de facto standard air-ejector dilutor and typical dilution conditions were used to establish the baseline sensitivity to dilution conditions for the given engine operating condition. The findings were consistent with previous studies that have shown that the number and size of nanoparticles formed is strongly dependent on the conditions in the first stage of dilution. Low temperatures, low dilution ratios, long residence times favor nanoparticle formation and growth. For example, a 10x change in DR (55 to 5) lead to a 2 order of magnitude increase in total particle concentration. Conversely, higher dilution temperatures favor nanoparticle growth but not particle formation. It is critical that exhaust samples be taken in such a way that the growth precursors are not lost in sample lines from the tailpipe to the dilution system. The sample line was designed for low heat and mass transfer rates.

Both the porous tube and ejector dilutor sampling strategies proved to be repeatable laboratory methods that produced representative results while incorporating accepted particle technology principles. The results showed that size distributions downstream of the porous tube and ejector dilutor were qualitatively similar in shape. However, particle number concentrations were consistently higher and the geometric mean diameter was generally 1 to 5 nm larger downstream of the porous tube dilutor. Neither system can exactly duplicate on-road size distributions due to the high variability of plumes, engine

conditions, fuels, environmental conditions and other parameters. Thus, it is not clear which technique is most appropriate for laboratory measurements and both systems have their virtues. In the porous tube system, the DR can be changed rather easily with the mass flow controller system. With a well-calibrated flow system, DRs could even be determined without gas analyzers; this is a considerable time and effort savings. However, the system is more complicated and the under-pressure operating scheme may be problematic for some instruments. The ejector dilutor system works very well when soot concentrations are low enough where orifice plugging is not a major problem and gas analyzers are available. Other studies have shown there is a large loss of particles >300 nm in ejector dilutors, although this was not clearly seen in these experiments. Thus, this study recommends both the porous tube and ejector dilutor systems for representative engine exhaust aerosol measurements so long as the dilution conditions, including the transfer line, are steady, well characterized, and controlled. The final choice is left to the user based on their particular application.

Data presented in **Chapter 4** showed that the TD method as evaluated introduces measurement artifacts. These artifacts can be categorized as volatile particle artifacts due to nucleation or condensation of vapors that is greatly enhanced by low or zero levels of pre-existing solid particles or solid particle artifacts that may be due to charring or pyrolysis reactions within semi-volatile particles and that appear to be catalyzed by sulfuric acid. No such artifacts were observed with the CS, which suggests superior methods exist. However, additional research is warranted before the complex physical phenomena that are responsible for the observations are fully understood.

Future evaluations of solid particle measurements need to account for the fact that Diesel exhaust is a complex mixture that includes DPM and vapors that influence the result. Diesel particles are chemically complex and dependent upon fuel, operating conditions, and other parameters. With the introduction and wider use of alternative fuels such as

biodiesel produced from various feedstocks, the impact of these fuels on nucleation mode particles is less well understood compared to petroleum-based ultra-low sulfur diesel fuel. These variables will contribute to difficulty in applying real – time, online analysis methods to the solid and semi-volatile carbon, organic carbon, and sulfur – containing particles found in Diesel exhaust.

Chapter 5 described the measurement of particle and gaseous emissions from a uniquely modified formula SAE race car engine fueled with E85 and 100 octane. A number of conclusions were reached regarding the ability of E85 to reduce CO and PM emissions that were consistent with trends seen by others testing more traditional spark ignition engines. CO, NO, PM and nanoparticle emissions were extraordinarily high—this is partially due to the forced rich operation but may be representative of spark ignition engines running at high load or fast acceleration conditions. More specific summaries are as follows.

Engine performance—

- The SAE race car engine was ~5-11% more thermally efficient when fueled with E85 compared with 100 octane. For a given throttle position, more torque and power were produced with E85.

Gaseous emissions—

- There was a significant reduction in brake specific CO emissions with E85 compared to 100 octane gasoline. Brake specific CO_2 and NO emissions were no different between fuels.

Particle emissions—

- E85 reduced particle number and volume emissions compared to 100 octane gasoline

- For both fuels and all test conditions, 95% of the particle number concentration was contained in the nucleation mode. On average, these nanoparticles contributed 40% to the total mass emissions.

In **Chapter 6**, an engine fault was detected using aerosol measurement instrumentation and was ultimately diagnosed as an oil control ring failure. This fault would not have likely been detected by traditional filter samples analyzed gravimetrically, by opacity measures, or other routine diagnostic procedures, because the amount of mass emitted would have been below the level of detection and engine performance was not degraded. This study suggests that sophisticated particle measurements have the potential to be used for detection of otherwise masked engine faults that lead to increased emissions. On the other hand, particle number based measurements are relatively costly, show strong sensitivity to sampling conditions, and require trained personal. These factors make particle number based measurements far from routine and these measurements will be best used for research purposes until further advances are made.

The objective of the first experiment in **Chapter 7** was to characterize particle emissions from a new CRT with very low levels of sulfur input. Nucleation mode emissions at high exhaust temperature are eliminated when the sulfur in the fuel and lubricating oil is reduced to 2 and 420 ppm, respectively, and the CRT has not been previously exposed to sulfur. The number distributions observed in the tests are quite different from what Kittelson et al. (2006a, b) observed during on-road testing using fuels and lubricants with higher sulfur contents. There a dramatic increase in very small (below 15 to 20 nm), nucleation mode particles occurs as the temperature rises above about 300°C. In these laboratory tests, there is no indication of such a mode. In addition, the total number concentration is 99.9% lower than on-road measurements. Both the reduction in fuel and oil sulfur content and the lack of sulfate release contribute to this large decrease in

particle concentration, although the importance of these effects cannot be individually quantified.

The objective of the used CRT measurements was to explicitly evaluate the effects of sulfate storage and release on particle formation by testing used CRTs that had previously stored material. The results suggest the strong increase in nanoparticle emissions with increasing exhaust temperature seen in the on-road testing by Kittelson et al. (2006a, b) is at least partly due to storage and release effects. It also raises questions about compliance with the NTE standard for PM emissions when using aftertreatment systems that operate mainly in a passive regeneration mode. It is unclear if this issue was considered during the development of the NTE and these results raise questions about the methods used to enforce the standard. Prior to these laboratory tests, the CRTs were operated for thousands of kilometers although the on-road duty cycle infrequently encountered sustained high load conditions with high exhaust temperatures. This may have allowed storage of atypical amounts of sulfur. Catalyzed DPF systems that use active regeneration would be unlikely to experience this problem because regular regeneration at high temperature would minimize long-term sulfur storage.

Semi-regular large spikes in number concentration were observed when evaluating both the new and used CRTs at exhaust temperatures below 380°C. This behavior appears to be a previously unidentified mode of operation for the CRTs and more research is needed. For the new CRT spikes, the oxidation catalyst has been exposed to minute amounts of sulfur, suggesting that it is unlikely that the particles occurred because of the nucleation of precursors released by the CRT, although precursor release may have played a minor role with the used CRT spikes. The size distributions revealed accumulation mode sized particles. Possible explanations of the spiking phenomena are soot emissions or soot breakthrough associated with the break up or cracking of the soot layer during passive regeneration.

Bibliography

Abdul-Khalek I. S., Kittelson, D. B, Graskow B. R., and Wei Q. “Diesel Exhaust Particle Size: Measurement Issues and Trends.” *SAE Tech. Pap. Ser*. 1998, 980525.

Abdul-Khalek, I. S., and Kittelson, D. B. “Real Time Measurement Of Volatile and Solid Exhaust Particles Using a Catalytic Stripper.” *SAE Tech. Pap. Ser.* 1995, 950236.

Abu-Qudais, M., and Kittelson, D. B. “Experimental and Theoretical Study of Particulate. Re-entrainment from the Combustion Chamber Walls of a Diesel Engine.” *Proc. Instn. Mech. Engnrs*. 1997, 211, 49–57.

Adachi, M., Kousaka,Y., and Okuyama, K. “Unipolar and Bipolar Diffusion Charging of Ultrafine Aerosol Particles.” *J. Aerosol Sci*. 1985, 16, 109–123.

Agarwal, J. K., and Sem, G. J. Continuous Flow, “Single-Particle-Counting Condensation Nucleus Counter.” *J. Aerosol Sci.* 1980, 11, 343-357.

Allansson, R., Blakeman, P. G., Cooper, B. J., Phillips, P. R., Thoss J. E., and Walker, A. P. “The Use of the Continuously Regenerating Trap (CRT®) to Control Particulate Emissions: Minimizing the Impact of Sulfur Poisoning.” *SAE Tech. Pap. Ser.* 2002, 2002-01-1271.

Andersson, J. D., Clark, D. P., and Watson, J. A. “UK Particulate Measurement Programme (PMP): a Near U.S. 2007 Approach to Heavy Duty Diesel Particulate Measurements-Comparison with the Standard European Method.” *SAE Tech. Pap. Ser*. 2004, 2004-01-1990.

Andersson, J. D., Preston, H., Warrens, C., Brett, P., and Payne, M., 2004. “Lubricant Composition Impact on the Emissions from a European Heavy Duty Engine Equipped with a Diesel Particulate Filter.” *SAE Tech. Pap. Ser*. 2004, 2004-01-3012.

Andrews, G. E., Rojas, N., Clarke, A. G., Sale, T., and Gregory, D. “The Transient Storage and Blow-Out of Diesel Particulate in Practical Exhaust Systems.” *SAE Tech. Pap. Ser*. 2001, 2001-01-0204.

Andrews, G. E., Xu, J., and Sale, T. “Influence of Catalyst and Exhaust System on Particulate Deposition and Release from an Idi Diesel Passenger Car Under Real-World Driving.” *SAE Tech. Pap. Ser*. 2002, 2002-01-1006.

Anyon, P. “Managing Diesel Particle Emissions through Engine Maintenance - an Australian Perspective.” 12th U.S./North American Mine Ventilation Symposium 2008. Wallace (ed) ISBN 978-0-615-20009-5.

Asbach, C., John, A. C., Pagels, J., Isaxon, C., Gudmundsson, A., Karlsson, J. E., Kammer, R., Tinnerberg, H., Kuhlbusch, T. A. J., and Boghard, M. *Particle Size Distribution and Lung Deposited Surface Area Concentration in Welding Fumes Measured in Real Workplaces with High Time Resolution*, Thessaloniki, Greece: European Aerosol Conference, August 25th, 2008.

Ayala, A., Olson, B., Cantrell, B., Drayton, M., and Barsic, N. “Estimation of Diffusion Losses When Sampling Diesel Aerosol: a Quality Assurance Measure.” *SAE Tech. Pap. Ser*. 2003, 2003-01-1896.

Bagely, S. T., Baumgard, K. J. Gratz, L. D., Johnson, J. H., and Leddy, D. G. “Characterization of Fuel and Aftertreatment Device Effects on Diesel Emissions.” Health Effect Institute, Research Report Number 76, 1996.

Baltensperger, U. “Real-Time Characterization of Ultrafine and Accumulation Mode Particles in Ambient Combustion Aerosols.” *J. Aerosol Sci*. 2002, 33, 1139-1154.

Bardasz, E. A., Antoon, F., Elizabeth, A., Schiferl, E. A., Wang, J., Totten, W. “The Impact of Lubricant and Fuel-derived Sulfur Species on Efficiency and Durability of Diesel NOx Adsorbers.” *SAE Tech. Pap. Ser.* 2004, 2004-01-3011.

Baumgard, K. J., and Johnson, J. H. “The Effect of Fuel and Engine Design on Diesel Exhaust Particle Size Distribution.” *SAE Tech. Pap. Ser.* 1996, 960131.

Bickel, K. “Biodiesel and Other Biofuels.” Home grown energy conference, Morse, MN. 2006.

Biskos, G. K., Reavell, K., and Collings, N. “Unipolar Diffusion Charging of Particles in the Transition Regime.” *J. Aerosol Sci.* 2005, 36, 247-265.

Biskos, G., Mastorakos, E., and Collings, N. “Monte-Carlo Simulation of Unipolar Diffusion Charging for Spherical and Non-Spherical Particles.” *J. Aerosol Sci.* 2004, 35, 707-730.

Biswas, P., and Wu, C-Y. “Nanoparticles and the Environment.” *J. Air Waste Manage. Assoc.* 2005, 55, 708-746.

Black, F. “An Overview of the Technical Implications of Methanol and Ethanol as Highway Motor Vehicle Fuels.” *SAE Tech. Pap. Ser*. 912413.

Branstetter, R., Burrahm, R., and Dietzmann, H. “Relationship of Underground Diesel Engine Maintenance to Emissions.” Volume I of II, Pages 25-26, 45, U.S. Department of the Interior, Bureau of Mines, 1983, USBM Contract No. H0292009.

Brown, R. C., and Hemingway, M. A. “Electric Charge Distribution and Capacitance of Agglomerates of Spherical Particles: Theory and Experimental Simulation.” *J. Aerosol Sci.* 1995, 26, 1197-1206.

Brunauer, S., Emmett, P. H., and Teller, E. “Adsorption of Gases in Multimolecular Layers.” *J. Am. Chem. Soc.* 1938, 60, 309-319.

Brusstar, M., and Bakenhsu, M. “Economical, High Efficiency Engine Technologies for Alcohol Fuels.” San Diego, CA: U.S. EPA, International Symposia on Alcohol Fuels, 2002, EPA-FEV-ISAF-No55.

Brusstar, M., and Gray, C. “High Efficiency with Future Alcohol Fuels in a Stoichiometric Medium Duty Spark Ignition Engine.” *SAE Tech. Pap. Ser*. 2007-01-3993.

Bukowiecki, N., Kittelson, D. B., Watts, W.F., Burtscher, H., Weingartner, E., Baltensperger, U. “Real-time Characterization of Ultrafine and Accumulation Mode Particles in Ambient Combustion Aerosols.” *J. Aerosol Sci.* 2002, 33, 1139–1154.

Burtscher H. “Measurements and Characteristics of Combustion Aerosols with Special Consideration of Photoelectric Charging and Charging by Flame Ions.” *J. Aerosol Sci*., 1992, 23, 549-595.

Burtscher, H. “Measurements and Characteristics of Combustion Aerosols with Special Consideration of Photoelectric Charging and Charging by Flame Ions.” *J. Aerosol Sci*. 1992, 23, 549-595.

Burtscher, H. “Physical Characterization of Particulate Emissions from Diesel Engines: A Review.” *J. Aerosol Sci.* 2005, 36, 896-932.

Burtscher, H., Baltensperger, U., Bukowiecki, N., Hüglin, C., Mohr, M., Matter, U., Nyeki, S., Streit, N., and Weingartner, E. “Separation of Volatile and Non-Volatile Aerosol Fractions by Thermodesorption: Instrumental Development and Applications.” *J. Aerosol Sci.* 2001, 32, 427-442.

California Air Resources Board. Fuels Report: Appendix to the Diesel Risk Reduction Plan, Appendix IV. 2000.

Campbell, B., Peckham, M., Symonds, J., Parkinson, J., and Finch, A. “Transient Gaseous and Particulate Emissions Measurements on a Diesel Passenger Car Including a DPF Regeneration Event.” Warrendale, PA: Society of Automotive Engineers, 2006. 2006-01-1079.

Carlson D., Osborne, M., and Johnson, J. “The Development and Application to Detector Tubes of a Laboratory Method to Assess Accuracy of Occupational Pollutant Concentration Measurements.” *AIHA J*. 1982, 43, 285.

Casati, R., Volker Scheer, V., Vogt, R., and Benter, T. “Measurement of Nucleation and Soot Mode Particle Emission from a Diesel Passenger Car in Real World and Laboratory In-Situ Dilution.” *Atmos. Environ.* 2007, 41, 2125-2135.

Chan, L., Carlson, D., and Johnson, J. “Evaluation and Application of a Portable Tailpipe Emissions Measurement Apparatus for Field Use.” *SAE Tech. Pap. Ser.* 1992, 921647.

Chan, P., and Dahneke, B. “Free Molecule Drag on Straight Chains of Uniform Spheres.” *J. Applied Phys*. 1981, 52, 3106-3110.

Chang, J.-S. “Theory of Diffusion Charging of Arbitrarily Shaped Conductive Aerosol Particles by Unipolar Ions.” *J Aerosol Sci*. 1981, *12*, 19-26.

Chase, R. E., Duszkiewicz, G.J., Rickert, J. F. O., Lewis, D., Maricq, M. M., and Zing, Xu. “PM Measurement Artifact: Organic Vapor Deposition on Different Filter Media.” *SAE Tech. Pap. Ser.* 2004, 2004-01-0967.

Chernich, D. J. “Development of a Chassis Based Inspection and Maintenance Program for Heavy-Duty Diesel Powered Vehicles.” San Diego, CA: 13th CRC On-Road Vehicle Emissions Workshop, April 2003.

Code of Federal Regulations. “Protection of Environment, Control of Emissions from New and in-Use Highway Vehicles and Engines.”40 CFR, Pt.86 2007). (Current through July, 2010). available from http://ecfr.gpoaccess.gov/cgi/t/text/text-idx?c=ecfr&tpl=/ecfrbrowse/Title40/40cfr86_main_02.tpl.

Cooper, B. J., and Thoss, J. E. “Role of NO in Diesel Particulate Emission Control.” *SAE Tech. Pap. Ser.* 1989, 890404.

de Hartog, J. J., Hoek, G., Peters, A., Timonen, K.L., Ibald-Mulli, A., Brunekreef, B., Heinrich, J., Tiittanen, P., van Wijnen, J. H., Kreyling, W., Kulmala, M., and Pekkanen, J. “Effects of Fine and Ultrafine Particles on Cardiorespiratory Symptoms in Elderly Subjects with Coronary Heart Disease-The ULTRA Study.” *Am. J. Epidemiol.* 2003, 157, 613- 623.

Dockery, D. W., Pope III, A., Xu, X., Spengler, J. D., Ware, J. H., Fay, M. E., Ferris, Jr. B. G., and Speizer, F. E. “An Association Between Air Pollution and Mortality in Six U.S. Cities.” *J. Medicine,* 1993, 329, 1753-1759.

Donaldson, K., and Beswick, P.H., Gilmour, P.S. “Free Radical Activity Associated with the Surface of Particles: a Unifying Factor in Determining Biological Activity.” *Toxicol, Lett*. 1996, 88, 293-298.

Du, H., and Yu, F. “Nanoparticle Formation in the Exhaust of Vehicles Running on Ultra-low Sulfur Fuel.” *Atmos. Chem. Phys.* 2008, 8, 4729–4739.

Ehara, K., Hagwoodt, C., and Coakley, K. J. “Novel Method to Classify Aerosol Particles According to Their Mass-to-Charge Ratio – Aerosol Particle Mass Analyser.” *J. Aerosol Sci*. 1996, 27, 217–234.

Environmental Protection Agency, "Regulatory Announcement." December 2003. U.S. Environmental Protection Agency. Accessed September 30, 2008: available from http://www.epa.gov/OMS/roadbike.htm.

Environmental Protection Agency. “A Comprehensive Analysis of Biodiesel Impacts on Exhaust Emissions.” EPA420-P-02-001, 2002. available at: http://www.epa.gov/otaq/models/analysis/biodsl/p02001.pdf.

Environmental Protection Agency. “Alternative Fuels: Biodiesel.” 2006. EPA420-F-06-044.

Ericsson, P., and M. Holmström, A. Amberntsson-Carlsson, C. Ohlson, M. Skoglundh, B. Andersson and P.-A. Carlsson. “Characterization of Particulate from Non-Diesel Combustion Systems.” *SAE Tech. Pap. Ser*. 2008-01-1746.

Fierz, M., Vernooij, M., and Burtscher, H. (2007). “An Improved Low-Flow Thermodenuder.” *J Aerosol Sci*. 38, 1163–1168.

Fierz, M., Burtscher, H., Steigmeier, P., and Kasper, M. “Field Measurement of Particle Size and Number Concentration with the Diffusion Size Classifier (Disc).” *SAE Tech. Pap. Ser.* 2008, 2008-01-1179.

Filho, O. V., F. Rheunissen, G. B. Colli, X. Liu, L. Shi and J. Priestley. “Flex Fuel Engine Management for Small Motorcycles.” SAE Pap. 2007-01-2729.

Filippo, A. D., and Maricq, M. M. (2008). “Diesel Nucleation Mode Particles: Semivolatile or Solid?” *Envir. Sci, and Tech.* 42, 7957–7962.

Fissan, H., Neumann, S., Trampe, A., Pui, D.Y. H., and Shin, W. G. “Rationale and Principle of an Instrument Measuring Lung Deposited Nanoparticle Surface Area.” *J. Nanoparticle Res*. 2007, *9*, 53–59.

Flanner, M. G., Zender, C. S., Randerson, J. T., and Rasch, P. J. “Present-Day Climate Forcing and Response from Black Carbon Snow.” *J. Geo Phys. Res*. D21201, 2007, 112, D11202.

Fletcher, R. A., Mulholland, G. W., Winchester, M. R., King, R. L., and Klinedinst, D. B. “Calibration of a Condensation Particle Counter Using a NIST Traceable Method.”*Aerosol Sci. Technol.* 2009, 43, 425–441.

Franklin, L., Bika, A., Watts, W. F., and Kittelson, D. B. “Comparison of Water and Butanol Based CPCs for Examining Diesel Combustion Aerosols.” in press, 2010. *Aerosol Sci. Technol.*

French, T. “Advanced Collaborative Emissions Study—ACES.” Initial ACES Workshop, Aurora, CO: November 2003.

Friedlander S. K. Smoke Dust and Haze, 2nd ed. New York: John Wiley and Sons. 2002.

Fuchs, N. A. “On the Stationary Charge Distribution on Aerosol Particles in a Bipolar Ionic Atmosphere.” *Geofis. Pura Appl.* 1963, 56, 185–193.

Gentry, J. W. “Charging of Aerosol by Unipolar Diffusion of Ions.” *J. Aerosol Sci.* 1972, 3, 65–76.

Gibson, J. D., Dudgeon, D. Dureno, S. Roseborsky, J. Woodiwiss, E. Barbour, K. Roth, D. McBride, R., Doiron, G. Panzera, M. Veccera, A. Sobiesiak, G.W. Rankin, B. Maskary and D. Vincent. “The University of Windsor—St. Clair College E85 Silverado.” *SAE Tech. Pap.Ser.* 2001-01-0680.

Giechaskiel, B., Dilara, P., Sandbach, E., and Andersson, J. (2008). “Particle Measurement Programme (PMP) Light-Duty Inter-Laboratory Exercise: Comparison of Different Particle Number Measurement Systems.” *Measurement Sci. and Tech.* 19, 1–16.

Giechaskiel, B., Ntziachristos, L., Samaras, Z., Scheer, V., Casati, R., and Vogt, R. “Formation Potential of Vehicle Exhaust Nucleation Mode Particles on-Road and in the Laboratory.” *Atmos. Environ.* 2005, 39, 3191-3198.

Giechaskiel, B., Dilara, P, and Andersson, J. “Particle Measurement Programme (PMP) Light-Duty Inter-Laboratory Exercise: Repeatability and Reproducibility of the Particle Number Method.” *Aerosol Sci. Technol.* 2008, *42*, 528–543.

Girshick, S. L. Nucleation and Growth of Particles from the Gas Phase. in press; Cambridge University Press.

Gold, D. R., Litonjua, A., Schwartz, J, Lovett, E., Larson, A., Nearing, B., Allen, G., Verrier, M., Cherry, R., and Verrier, R. “Ambient Pollution and Heart Rate Variability.” *Circulation* 2000, 101, 1267–1273.

Graskow, B. R., Kittelson, D. B., Abdul-Khalek, I. S., Ahmadi, M. R., and Morris, J. E. “Characterization of Exhaust Particulate Emissions from a Spark Ignition Engine.” *SAE Tech. Pap. Ser.* 1998. 980528.

Grose, M., Sakurai, H., Savstrom, J., Stolzenburg, M. R., Watts, W. F., Morgan, C. G. et al. “Chemical and Physical Properties of Ultrafine Diesel Exhaust Particles Sampled Downstream of a Catalytic Trap.” *Envi. Sc.and Tec.* 2006, 40, 5502–5507.

Gunn, R. “Diffusion Charging of Atmospheric Droplets by Ions and the Resulting Combination Coefficients.” *J. of Meteorology*. 1954, 11, 339–347.

Gwinn, M. R., and Vallyathan, V. “Nanoparticles: Health Effects—Pros and Cons.” *Environ Health Perspect* 2006, 114, 1818–1825.

Hall, D., and Dickens, C. “The Effect of Sulpher-Free Diesel Fuel on the Measurement of the Number and Size Distribution of Particle Emitted from a Heavy-Duty Diesel Engine Equipped with a Catalyzed Particulate Filter.” *SAE Tech. Pap. Ser.* 2003, 2003-01-3167.

Hall, D. E., Stradling, R. J., Rickeard, D. J., Martini, G., Meco-Morato, A., Hagemann, R., Szendefi, J., and Rantanen, L. “Measurement of the Number and Mass Weighted Size Distributions of Exhaust Particles Emitted from European Heavy Duty Engines.” CONCAWE report, 2001.

Hansen, J, and Nazarenko, L. “Soot Climate Forcing Via Snow and Ice Albedos.” *Proc. Natl. Acad. Sci*, 2003, 101, 2, 423–428.

Harris, S. J., and Maricq, M. M. “Signature Size Distributions for Diesel and Gasoline Engine Exhaust Particulate Matter.” *J. Aerosol Sci.* 2001, 32, 749–764.

Hawker, P., Hüthwohl, G., Henn, J., Koch, W., Lüders, H., Lüders, B., and Stommel, P. “Effect of a Continuously Regenerating Diesel Particulate Filter on Non-Regulated Emissions and Particle Size Distribution.” *SAE Tech. Pap. Ser.* 1998, 980189.

Heejung, J., and Kittelson, D. B. “Characterization of Aerosol Surface Instruments in Transition Regime.” *Aerosol Sci. Technol*. 2005, 39, 902–911.

Hering, S. V., and Stolzenburg, M. R. “Online Determination of Particle Size and Density in Nanometer Size Range.” *Aerosol Sci. Technol.* 1995, 23, 155–173.

Hering, S.V., Stolzenburg, M. R., Quant, F. R., O'Berreit, D. R., and Keady, P. B. “A Laminar-Flow, Water-based Condensation Particle Counter (WCPC).” *Aerosol Sci. Technol. 2005,* 39, 659-672.

Heywood, J. S. Internal Combustion Engine Fundamentals. New York: McGraw-Hill Publishing, 1988.

Hill, P. H., Zhang, D., and Li, G. “Direct Injection Combustion Cylinder Geometry.” U.S. Patent 7213564. May 8, 2007.

Hinds, W. C. Aerosol Technology. 2nd ed. New York: John Wiley and Sons, Inc., 1999.

Hiranuma, S., Takeda, Y., Kawatani, T., Doumeki, R., and Nagasaki, K. “Development of DPF System for Commercial Vehicle-Basic Characteristic and Active Regenerating Performance.” *SAE Tech. Pap. Ser.* 2003, 2003-01-3182.

Holmén, B. A., and Ayala, A. “Ultrafine PM Emissions from Natural Gas, Oxidation-Catalyst Diesel, and Particle-Trap Diesel Heavy-Duty Transit Buses.” *Environ. Sci. Technol.* 2002, 36, 5041–5050.

Human D. M and Ullman, T. L. ‘Development of an I/M Short Emissions Test for Buses.’ *SAE Tech. Pap. Ser.* 1992, 920727.

Hüthwohl, G., Pischinger, F., and Lepperhoff, G. “Self-Supporting Regeneration of Diesel Particulate Traps.” *SAE Tech. Pap. Ser.* 1987, 870017.

Ibald-Mulli, A., Wichmann, H. E., Kreyling, W., and Peters, A. “Epidemiological Evidence on Health Effects of Ultrafine Particles.” *J. Aerosol Med.* 2002, 15, 189–201.

International Commission on Radiological Protection. Human Respiratory Tract Model for Radiological Protection. A Report of Committee 2 of the ICRP. Oxford, England: Pergamon Press. 1994.

Jacobson, M. Z. “The Climate Response of Fossil-Fuel and Biofuel Soot, Accounting for Soot’s Feedback to Snow and Sea Ice Albedo and Emissivity.” *J. Geophys*. Res. 109, 2004, D21201.

Jaroonjitsathian, S., Akarapanjavit N., Sa-norh, S. S. and Chanchaona, S. “Investigation of 2-Wheeler Performance, Emissions, Driveability and Durability: Effect of Ethanol-blended Gasoline.” *SAE Tech. Pap. Ser.* 2007, 2007-01-2034.

Johnson, J. E., and Kittelson, D. B. (1996). “Deposition, Diffusion, and Adsorption in the Diesel Oxidation Catalyst.” *Applied Catalysis B: Environ.*1996, 10, 117–137.

Johnson, J. H., and Baumgard, K. H. “The Effect of Fuel and Engine Design on Diesel Exhaust Particle Size Distributions.” *SAE Tech. Pap. Ser.*1996, 960131.

Johnson, K. C., Durbin, T. D., Jung, H., Chaudhary, A., Cocker, D. R., Herner, J. D., Robertson, W. H., Huai, T., Ayala, A., and Kittelson, D. B. “Evaluation of the European PMP Methodologies During on-Road and Chassis Dynamometer Testing for DPF Equipped Heavy Duty Diesel Vehicles.” *Aerosol Sci. Technol*. 2009, 43, 962–969.

Johnson, T. “Diesel Emission Control in Review.” *SAE Tech. Pap. Ser.* 2008, 2008-01-0069.

Johnson, T., Caldow, R., Pöcher, A., Mirme, A., and Kittelson, D. B. “A New Electrical Mobility Particle Sizer Spectrometer for Engine Exhaust Particle Measurements.” *SAE Tech. Pap. Ser.* 2004, 2004-01-1341.

Jones, T. J., and Kittelson, D. B. “Experiments Performed on the Caterpillar C12 Test Stand: January 1st through May 1st 2002.”Report submitted to Caterpillar, Inc. 2002.

Joshi, A., Chatterjee, S., Sawant, A., Akerlund, C., Andersson, S., Blomquist, M., Brooks, J., and Kattan, S. “Development of an Actively Regenerating DPF System for Retrofit Applications.” *SAE Tech. Pap. Ser.* 2006, 2006-01-3553.

Jung, H., and Durbin, T.D. (2008). “Measurement of Diesel Solid Nanoparticle Emissions Using a Catalytic Stripper for Comparison to Europe’s PMP Protocol.” Proposal funded by CARB, 2008.

Jung, H. and Kittelson, D. B. “Measurement of Electrical Charge on Diesel Particles.” *Aerosol Sci. Techol.* 2005a, 39, 1129–1135.

Jung, H. and Kittelson, D. B. “Characterization of Aerosol Surface Instruments in Transition Regime.” *Aerosol Sci. Technol.* 2005b, *39*, 902–911.

Kasper, G. “Dynamics and Measurement of Smokes.” *Aerosol Sci. Technol.* 1982, 1, 187–199.

Kasper, M. “Sampling and Measurement of Nanoparticle Emissions for Type Approval and Field Control.” *SAE Tech. Pap. Ser.* 2005, 2005-26-013.

Kawai, T., Goto, Y., and Odaka, M. “Influence of Dilution Process on Engine Exhaust Nano-Particles.” *SAE Tech. Pap. Ser.* 2004, 2004-01-0963

Kelly, W. P., and McMurry, P. H. “Measurement of Particle Density by Inertial Classification of Differential Mobility Analyzer-Generated Monodisperse Aerosols.” *Aerosol Sci. Technol.* 1992, 17,199–212.

Keskinen, J., Pietarinen, K., and Lehtimäki, M. “Electrical Low Pressure Impactor.” *J. Aerosol Sci.* 1992, 23, 353–360.

Khalek, I. A. “Diesel Particulate Matter Research.” CRC Project E-66, Phase 1, 2005.

Khalek, I. A. “Diesel Particulate Matter Research.” CRC Project E-66, Phase 2, 2006.

Khalek, I. A. “Diesel Particulate Matter Research.” CRC Project E-66, Phase 3, 2007.

Khalek, I. A., Bougher, T., Merritt, P., Tennant, C., and Costantini, M. “Phase 1 of the Advanced Collaborative Emissions Study (ACES): Highlights of Project Findings.” San Diego, CA: Nineteenth CRC On-road Vehicle Emissions Workshop, March 23–25, 2009.

Khalek, I. A., Kittelson, D. B., and Brear, F. “The Influence of Dilution Conditions on Diesel Exhaust Particle Size Distribution Measurements.” *SAE Tech. Pap. Ser.* 1999, 1999-01-1142.

Khalek, I. A., Spears, M., and Charmley W. “Particle Size Distribution from a Heavy-Duty Diesel Engine: Steady-State and Transient Emission Measurement Using Two Dilution Systems and Two Fuels.” *SAE Tech. Pap. Ser.* 2003, 2003-01-0285.

Khalek, I. A., Kittelson, D. B., and Brear, F. “Nanoparticle Growth During Dilution and Cooling of Diesel Exhaust: Experimental Investigation and Theoretical Assessment.” *SAE Tech. Pap. Ser.* 2000, 2000-01-0515.

Kim, D., Gautam, M., and Gera, D. “Modeling Nucleation and Coagulation Modes in the Formation of Particulate Matter Inside a Turbulent Exhaust Plume of a Diesel Engine.” *J. Colloid Interface Sci.* 2002b, 249, 96–103.

Kim, D., Gautam, M., and Gera, D. “Parametric Studies on the Formation of Diesel Particulate Matter Via Nucleation and Coagulation Modes.” *J. Aerosol Sci.* 2002a, 33, 12, 1609–1621.

Kim, S. C., Wang, J., Emery, M. S., Shin, W. G., Mulholland, G. W., and Pui, D. Y. H. “Structural Property Effect of Nanoparticle Agglomerates on Particle Penetration Through Fibrous Filter.” *Aerosol Sci. Technol.* 2009, 43, 344–355.

Kinney P. K., Pui, D. Y. H., Mulholland, G. W., and Bryner, N. P. “Use of the Electrostatic Classification Method to Size 0.1-μm SRM Particles—a Feasibility Study.” *J. Res. Natl. Inst. Stand. Technol*. 1991, 96,147–176.

Kittelson, D. B. “Engines and Nanoparticles: A Review.” *J. Aerosol Sci.* 1998, 29, 575–588.

Kittelson, D. B., Arnold, M., and Watts, W. F. “Review of Diesel Particulate Matter Sampling Methods. Final Report.” 1999, available at: http://www.me.umn.edu/centers/cdr/Proj_EPA.html.

Kittelson, D. B., Dolan, D. F., Diver, R. B., and Aufderheide E. “Diesel Exhaust Particle Size Distributions: Fuel and Additive Effects." *SAE Tech. Pap. Ser.* 1978, 780787.

Kittelson D. B., and Johnson, J. H. “Variability in Particle Emissions Measurements in the Heavy-Duty Transient Test.” *SAE Tech. Pap. Ser*. 1991, 910738.

Kittelson, D. B., Moon, K. C., and Pui, D. Y. H. “Diesel Particle Control with a Simple Electrostatic Trap.” *SAE Tech. Pap. Ser*. 1986, 860009.

Kittelson, D. B., and Stenitzer, M. “A New Catalytic Stripper for Removal of Volatile Particles.” Zurich : Proceedings of the 7th ETH Conference on Combustion Generated Particles, 2003.

Kittelson, D. B., Watts, W. F. and Johnson, J. P. “Diesel aerosol sampling methodology.” CRC E-42 Final Report, 2002.

Kittelson, D. B., Watts, W. F., and Johnson, J. P. “On-Road and Laboratory Evaluation of Combustion Aerosols-Part1: Summary of Diesel Engine Results.” *J. Aerosol Sci.* 2006a, 37, 913–930.

Kittelson, D. B., Watts, W. F., Johnson, J. P., Rowntree, C., Payne, M., Goodier, S., Warrens, C., Preston, H., Zink, U., Ortiz, M., Görsmann, C., Twigg, M. V., Walker, A. P., and Caldow, R. “On-Road Evaluation of Two Diesel Exhaust Aftertreatment Devices.” *J. Aerosol Sci.* 2006c, 37, 1140–1151.

Kittelson, D. B., Watts, W. F., Johnson, J., Schauer, J., and Lawson, D., “On-Road and Laboratory Evaluation of Combustion Aerosols—Part 2: Summary of Spark Ignition Engine Results.” *J. Aerosol Sci*. 2006, 37, 931– 949.

Kittelson, D. B., Watts, W. F., Johnson, J. P., Thorne, C., McCann, C., Payne, M., Goodier, S., Warrens, C., Preston, H., Zink, U., Pickles, D., Goersmann, C., Twigg, M. V., Walker, A. P., and Boddy, R. “Driving Down on-Highway Particulate Emissions.” *SAE Tech. Pap. Ser.* 2006b, 2006-01-0916.

Kittelson, D. B., Watts, W. F., Johnson, J. P., Thorne, C., McCann, C., Payne, M., Goodier, S., Warrens, C., Preston, H., Zink, U., Pickles, D., Goersmann, C., Twigg, M.V., Walker, A.P., and Boddy, R. “Effect of Fuel and Lube Oil Sulfur on the Performance of a Diesel Exhaust Gas Continuously Regenerating Trap.” *Environ. Sci. and Tech.* 2008, 42, 9276–9282.

Kittelson, D. B., Watts, W. F., Ramachandran, G., Paulsen, D. and Kreager, C. "Measurement of Diesel Aerosol Exposure: A Feasibility Study. in Health Effects Institute Report Research Directions to Improve Estimates of Human Exposure and Risk from Diesel Exhaust A Special Report of the Institute's Diesel Epidemiology Working Group." April 2002, Health Effects Institute, Boston, MA, 2002, pp. 153–179. available from www.healtheffects.org.

Kittelson, D. B., Watts, W. F., Savstrom, J. C., and Johnson J. P. "Influence of Catalytic Stripper on Response of PAS and DC." *J. Aerosol Sci.* 2005, 36, 1089–1107.

Kittelson, D. B., Watts, W. F., and Johnson, J. P. Ragatz, A. C. "A New Method for the Real-Time Measurement of Diesel Aerosol." Contract Final Report for Grant 1 R01 OH8676-01, 2010. available from www.me.umn.edu/centers/cdr/.

Knothe, G., Sharp, C. A., and Ryan, T. W., III. "Exhaust Emissions of Biodiesel, Petrodiesel, Neat Methyl Esters, and Alkanes in a New Technology Engine." *Energy Fuels*. 2006, 20, 403–408.

Knutson, E. O., and Whitby, K. T. "Aerosol Classification by Electric Mobility: Apparatus, Theory, and Applications." *J. Aerosol Sci.* 1975, 6, 443–451.

Ku, B. K., and Maynard, A. D. "Comparing Aerosol Surface-area Measurements of Monodisperse Ultrafine Silver Agglomerates by Mobility Analysis, Transmission Electron Microscopy and Diffusion Charging," *J. Aerosol Sci.* 2005, 36, 1108–1124.

Laframboise, J. G., and Chang, J. "Theory of Charge Deposition on Charged Aerosol Particles of Arbitrary Shape." *J Aerosol Sci*. 1977, 8, 331–338.

Lahaye, J., and Prado, G. “Morphology and Internal Structure of Soot and Carbon Blacks,” in Particulate Carbon Formation during Combustion, ed. Donald Siegla, New York: Springer, 1981.

Lahde, T., Rönkkö, T., Virtanen, A., Solla, A., Kyto, M., Soderstrom, C. et al. “Dependence between nonvolatile nucleation mode particle and soot number concentrations in an EGR equipped heavy-duty Diesel engine exhaust.” In press, *Environ. Sci. Technol.* DOI: 10.1021/es903428y.

Lahde, T., Ronkko, T., Virtanen, A., Schuck, T., Pirjola, L., Hameri, K., Kulmala, M., Arnold, F., Rothe, D., and Keskinen, J. “Heavy Duty Diesel Engine Exhaust Aerosol Particle and Ion Measurements.” *Environ. Sci. Technol*. 2009, 43, 163–168.

Lall, A. A., and Friedlander, S. K. “On-line Measurements of Ultrafine Aggregate Surface Area and Volume Distributions by Electrical Mobility Analysis: I. Theoretical Analysis.” *J. Aerosol Sci.* 2006a, 37, 260–271.

Lall, A. A., Rong, W., and Madler, L., Friedlander, S. K. “Nanoparticle Aggregate Volume Determination by Electrical Mobility Analysis: Test of Idealized Aggregate Theory Using Aerosol Particle Mass Analyzer Measurements.” *J. Aerosol Sci.* 2008, 39, 403-417.

Lall, A. A., Seipenbusch, M., Rong, W., and Friedlander, S. K. “On-line Measurements of Ultrafine Aggregate Surface Area and Volume Distributions by Electrical Mobility Analysis: II. Comparison of Measurements and Theory.” *J. Aerosol Sci.* 2006b, 37, 260–271.

Lapuerta, M., Martos, F. J., and Herreros, J. M., “Effect of Engine Operating Conditions on the Size of Primary Particles Composing Diesel Soot Agglomerates.” *J. Aerosol Sci*. 2007, 38, 455–466.

Laresgoiti, A., and Springer, G. S. “Sulfate and Particulate Emissions from an Oxidation Catalyst Equipped Engine.” *Environ. Sci. Technol.*1977, 11, 285–292.

Lee, D., Miller, A., Kittelson, D. B., and Zachariah, M. R. “Characterization of Metal-Bearing Diesel Nanoparticles Using Single-Particle Mass Spectrometry.” *J. Aerosol Sci.* 2006, 37, 88–110.

Lehmann, U., Niemela, V., and Mohr, M. “New Method for Time-Resolved Diesel Engine Exhaust Particle Mass Measurement.” *Environ. Sci. Technol.* 2004, 38, 5704–5711.

Lemmetty, M., Pirjola, L., Makela, J. M., Ronkko, T., and Keskinen, J. “Computation of Maximum Rate of Water-Sulphuric Acid Nucleation in Diesel Exhaust.” *J. Aerosol Sci.* 2006, 37, 1596–604.

Leonhard, R., and Projahn, U. (Robert Bosch Gmbh). “Device for Removing Soot from Diesel Exhaust.” U.S. Patent 4,989,408. February 5, 1991.

Li, L., Liu, Z., Wang, H., Deng, B., Xiao, Z., Wang, Z., Gong, C. and Y. Su. “Combustion and Emissions of Ethanol Fuel (E100) in a Small SI Engine.” *SAE Tech. Pap. Ser.* 2003-01-3262.

Liang, C. Y., Baumgard, K. J., Gorse, R. A. Jr., Orban, J. E., Storey, J. M. E., and Tan, J. C.,

Liao, D. P., Creason, J., Shy, C., Williams, R., Watts, R., and Zweidinger, R. “Daily Variation of Particulate Air Pollution and Poor Cardiac Autonomic Control in the Elderly.” *Environ. Health Perspect.* 1999, 107, 521–525.

Lighty, J. S., Veranth, J. M., and Sarofim, A. F. “Combustion Aerosols: Factors Governing Their Size and Composition and Implications to Human Health,” *Air Waste Manage. Assoc*. 2000, 50, 1565–1618.

Litzinger, T., Stoner, M., Hess, H.and Boehman, A. “Effects of Oxygenated Blending Compounds on Emissions from a Turbocharged Direct Injection Diesel Engine.” *Int. J. Engine Research*, 1999, 1, No. 1, 57–70.

Liu, B. Y. H., and Pui, D. Y. H. “A Submicron Aerosol Standard and the Primary, Absolute Calibration of the Condensation Nuclei Counter.” *J. Colloid Interface Sci.* 1974a, 47, 155–171.

Liu, B. Y. H., and Pui, D. Y. H. “Electrical Neutralization of Aerosols.” *J. Aerosol Sci.* 1974b, 5, 465–472.

Liu, B. Y. H., and Pui, D. Y. H. “On the Performance of the Electrical Aerosol Analyser.” *J. Aerosol Sci.* 1975, 6, 249–264.

Liu, B. Y. H., and Pui, D. Y. H. “On Unipolar Diffusion Charging of Aerosols in the Continuum Regime,” *J. Colloid Interface Sci.* 1977, 58, 142–149.

Liu, B. Y. H., Whitby, K. T., and Yu, H. H. S. “On the Theory of Charging of Aerosol Particles by Unipolar Ions in the Absence of an Applied Electric Field,” *J. Colloid Interface Sci.* 1967, 23, 367–378.

Liu, G. Z., Ford, D. C., Vasys, V. N., Chan, D-R., and Johnson, T. R. “Influence of Engine Operating Conditions on Diesel Particulate Matter Emissions in Relation to Transient and Steady-State Conditions.” *Environ. Sci. Technol.* 2007, 41, 4593–4599.

Liu, J., Vasys, V., Dettmann, M., Schauer, J., Kittelson, D. B., and Swanson, J. “Comparison of Strategies for the Measurement of Mass Emissions from Diesel Engines Emitting Ultra-Low Levels of Particulate Matter.” *Aerosol Sci. Technol.* 2009, *43*, 1150–1160.

Liu, W., Kaufman, S.L., Osmondson, B. L., Sem, G.J., Quant, F. R., and Oberreit, D. R. “Water-based Condensation Particle Counters for Environmental Monitoring of Ultrafine Particles.” *J Air Waste Management Assoc*. 2006, 56, 444–455.

Liu, W., Osmondson, B., Bischof, O., and Sem, G. “Calibration of Condensation Particle Counters.” *SAE Tech. Pap. Ser.* 2005, 2005-01-0189.

Lowenthal, D. H., Zielinska, B., Chow, J.C., Watson, J. G., Mridui, G., Ferguson, D. H., Neuroth, G.R ., and Stevens, K. D. “Characterization of Heavy Duty Diesel Vehicle Emissions.” *Atmos Environ*. 1994, *28*, 731–743.

Ludecke, O. A., and Dimick, D. L. “Diesel Exhaust Particulate Control System Development.” *SAE Tech. Pap. Ser.* 1983, 830085.

Lyyränen, J., Jokiniemi, J., Kauppinen, E. I., Vesala, H., and Backman, U. “Comparison of Different Dilution Methods for Measuring Diesel Particle Emissions.” *Aerosol Sci. Technol*. 2004, 38, 12–23.

Maricq, M. M. “Chemical Characterization of Particulate Emissions from Diesel Engines: A Review,” *J. Aerosol Sci.* 2007, 38, 1079–1118.

Maricq M. M. “Exhaust Composition and Sampling Artifacts.” Denver: CO: ACES Workshop, November 2003.

Maricq, M. M., Chase, R. E., Xu, N., and Laing, P. M. “The Effects of the Catalytic Converter and Fuel Sulfur Level on Motor Vehicle Particulate Matter Emissions: Light Duty Diesel Vehicles.” *Environ. Sci. Technol.* 2002, 36, 283–289.

Maricq M. M., and Xu N. “The Effective Density and Fractal Dimension of Soot Particles from Premixed Flames and Motor Vehicle Exhaust.” *J. Aerosol Sci.* 2004, 35, 1251-1274.

Mathis, U., Ristimaki, J., Mohr, M., Keskinen, J., Ntziachristos, L., Samaras, Z., and Mikkanen, P. “Sampling Conditions for the Measurement of Nucleation Mode Particles in the Exhaust of a Diesel Vehicle.” *Aerosol Sci. Technol*. 2004a, 38, 1149-1160.

Mayer, A. “VERT: Diesel Nano-Particles Emissions: Properties and Reduction Strategies.” *SAE Tech. Pap. Ser.* 1998, 980539.

Mayer, A., Czerwinski, J., and Scheideggeret, P. “Trapping Efficiency Depending on Particulate Size.” *SAE Tech. Pap. Ser.*1996, 960472.

McCawley, M. A. “Should Dust Samples Mimic Human Lung Deposition? Counterpoint.” *Appl. Occup. Environ. Hyg*., 1990, 5, No. 12, 829–835.

McDow, S. R., and Huntzicker, J. J. “Vapor Adsorption Artifact in the Sampling of Organic Aerosol: Face Velocity Effects.” *Atmos. Environ.* 1990, 24, 2563–2571.

McGinn, S. “The Relationship Between Diesel Engine Maintenance and Exhaust Emissions. Diesel Emissions Evaluation Program (DEEP). available at http://www.deep.org/reports/mtce_report.pdf.

McMurry, P. H., and Friendlander, S. K. “New Particle Formation in the Presence of an Aerosol.” *Atmos. Environ.* 1979, 13, 1635–1651.

McMurry, P. H., Wang, X., Park, K., and Ehara, K. “The Relationship between Mass and Mobility for Atmospheric Particles: A New Technique for Measuring Particle Density.” *Aerosol Sci. Technol.* 2002, 36, 227–238.

Mikkanen, P., Moisio, M., Keskinen, J., Ristimäki, J., and Marjamäki, M. “Sampling Method for Particle Measurements of Vehicle Exhaust.” *SAE Tech. Pap. Ser.* 2001, 2001-01-0219.

Miller, A., Stipe, C., Habjan, M., and Alstrand, G. “Role of Lubrication Oil in Particulate Emissions from A Hydrogen-Powered Internal Combustion Engine.” *Environ. Sci. Technol*. 2007, 41, 6828–6835.

Min, B.-S., Kim, J.-S., Oh, D.-Y., Choi, J.-K., and Jin, J.-H. “Dynamic Characteristics of Oil Consumption- Relationship between the Instantaneous Oil Consumption and the Location of Piston Ring Gap.” *SAE Tech. Pap. Ser.* 1998, 982442.

Mirabel, P., and Katz, J. L. “Binary Homogenous Nucleation As a Mechanism for the Formation of Aerosols.” *J. Chem. Phys.* 1974, 60, 1138–1144.

Mohr, M., Lehmann, U., and Margaria, G.”ACEA Programme, Part 2: Effect of Sampling Conditions and Fuel Sulphur Content on the Particle Emission.” *SAE Tech. Pap. Ser.* 2003, 2003-01-1890.

Mohr, M., Lehmann, U., and Rutter, J. “Comparison of Mass-Based and Non-Mass-Based Particle Measurement Systems for Ultra-Low Emissions from Automotive Sources.” *Environ. Sci. Technol.* 2005, 39, 2229–2238.

Monahan, P., and Friedman, D. “The Diesel Dilemma: Diesel’s Role in the Race for Clean Cars.” Union of Concerned Scientists, January, 2004. available at: http://www.ucsusa.org/assets/documents/clean_vehicles/dieseldilemma_fullreport.pdf Internet

Morgan, R. E., Gold, M. R., and Laguitton, O. “Characterization of the Soot Formation Processes in a High Pressure Combusting Diesel Fuel Spray.” *SAE Tech. Pap. Ser.* 2003, 2003-01-3086.

Mulawa, P., Cradle, S., Knapp, K., Zweidinger, R., Snow, R., Lucus, R., and Goldbach, J. “Effect of Ambient Temperature and E-10 Fuel on Primary Exhaust Particulate Matter Emission from Lights Duty Vehicles.” *Environ. Sci. Technol*. 1997, 31, 1302-1307.

Newton G. J., Carpenter, R. L., Yeh, H-C., and Peele, E. R. “Respirable Aerosols from Fluidized Bed Coal Combustion. 1. Sampling Methodology for an 18-inch Experimental Fluidized Bed Coal Combustor.” *Environ. Sci. Technol.* 1980, 14, 849-853.

Ni, T., S. B. Gupta and Santoro, R. J. “Suppression of Soot Formation in Ethene Laminar Diffusion Flames by Chemical Additives.” Twenty-Fifth Symposium (International) on Combustion, the Combustion Institute. 1994, pp. 585–592.

Ntziachristos, L., Giechaskiel, B., Pistikopoulos, P., and Samaras, Z. (2005a). "Comparative Assessment of Two Different Sampling Systems for Particle Emission Type-Approval Measurements." *Society of Automotive Engineers*, 2005-01-0198.

Ntziachristos, L., Samaras, Z., Mohr, M., Mathis, U., Keskinen, J, Ristmäki, J. et al. "Performance and Evaluation of a Novel Sampling System for Exhaust Particle Characterization." *SAE Tech. Pap. Ser.* 2004, 2004-01-1439.

Ntziachristos, L., Giechaskiel, B., Pistikopoulos, P., Samaras, Z., Mathis, U., Mohr, M., Ristimäki, J., Keskinen, J., and Mikkanen, P. "Performance Evaluation of a Novel Sampling and Measurement System for Exhaust Characterization." *SAE Tech. Pap. Ser.* 2004a, 2004-01-1439.

Ntziachristos, L., Tzamkiozis, T., Mamakos, A., and Samaras, Z. "A New Constant Dilution Ratio Concept for Vehicle and Engine Exhaust Particle Sampling." *SAE Tech. Pap. Ser.* 2008, 2008-01-0762.

Ntziachristos, L., Giechaskiel, B., and Samaras, Z. "Calibration of Dekati's Automotive Surface Monitor-'ASMO'", 2001, *LAT Report, No: 0117.* Thessaloniki School of Engineering, Aristotle University.

Oberdörster, G. "Pulmonary Effects of Inhaled Ultrafine Particles." *Internat. Arch. Occupat. Environ. Health* 2001, 74, 1–8.

Oberdörster G., Oberdörster E., and Oberdörster J. "Nanotoxicology: An Emerging Discipline Evolving from Studies of Ultrafine Particles." *Environ. Health Perspect.* 2005, 113, 823–839.

Oh, H., Park, H., and Kim, S. “Effects of Particle Shape on the Unipolar Diffusion Charging of Non-spherical Particles.” *Aerosol Sci. Technol.* 2004, 38, 1045–1053.

Olfert, J. S., and Collings, N. “New Method for Particle Mass Classification—the Couette Centrifugal Particle Mass Analyzer.” *J. Aerosol Sci*. 2005, 36, 1338–1352.

Olfert, J. S., and Collings, N. “The Effective Density and Fractal Dimension of Particles Emitted from a Light-duty Diesel Vehicle with a Diesel Oxidation Catalyst.” *J. Aerosol Sci*. 2007, 38, 69–82.

Osunsanya, T., Prescott, G., and Seaton, A. “Acute Respiratory Effects of Particles: Mass or Number?” *Occup. Environ. Med.* 2001, 58, 154–159.

Park, K., Cao, F., and Kittelson, D. B., McMurry, P. “Relationship Between Particle Mass and Mobility for Diesel Exhaust Particles.” *Environ Sci Technol.* 2003, 37, 577–583.

Park, K., Kittelson, D. B., and McMurry, P. “Structural Properties of Diesel Exhaust Particles Measured by Transmissions Electron Microscopy (TEM): Relationships to Particle Mass and Mobility.” *Aerosol Sci. Technol.* 2004, 38, 881–889.

Pekkanen, J., Peters, A., Hoek, G., Tiittanen, P., Brunekreef, B., de Hartog, J., Heinrich, J., Ibald-Mulli, A., Kreyling, W.G., Lanki, T., Timonen, K. L., and Vanninen, E. “Particulate Air Pollution and Risk of ST-Segment Depression During Repeated Submaximal Exercise Tests Among Subjects with Coronary Heart Disease - the Exposure and Risk Assessment for Fine and Ultrafine Particles in Ambient Air (ULTRA) Study.” *Circulation* 2002, 106, 933–938.

Pekkanen, J., Timonen, K. L., Ruuskanen, J., Reponen, A., and Mirme, A. “Effects of Ultrafine and Fine Particles in Urban Air on Peak Expiratory Flow Among Children with Asthmatic Symptoms.” *Environ. Res.* 1997, 74, 24–33.

Penttinen, P., Timonen, K. L., Tiittanen, P., Mirme, A., Ruuskanen, J., and Pekkanen, J. “Ultrafine Particles in Urban Air and Respiratory Health Among Adult Asthmatics.” *J. Eur. Respir.* 2001, 17, 428–435.

Peters, A., Dockery, D. W., Muller, J. E., and Mittleman, M. A. “Increased Particulate Air Pollution and the Triggering of Myocardial Infarction.” *Circulation* 2001, 103, 2810-2815.

Peters, A., Wichmann, H.E., Tuch, T., Heinrich, J., and Heyder, J. “Respiratory Effects Are Associated with the Number of Ultrafine Particles.” *American J. Respir. Crit. Care Med.* 1997, 155, 1376–1383.

Pope III, C. A., Thun, M. J., Namboodiri, M. M., Dockery, D. W., Evans, J. S., Speizer, F. E., and Heath, Jr. C. W. “Particulate Air Pollution As a Predictor of Mortality in a Prospective Study of U.S. Adults.” *Am. J. Respir. Crit. Care Med.* 1995, 151, 669-674.

Preining, O. “The Physical Nature of Very, Very Small Particles and Its Impact on Their Behavior.” *J. Aerosol Sci.* 1998, 29, 481–495.

Price, P., Twiney, B., Stone, R., Kar, K., and Walmsley, H. “Particulate and Hydrocarbon Emissions from a Spray Guided Direct Injection Spark Ignition Engine with Oxygenate Fuel Blends.” *SAE Tech. Pap. Ser.* 2007, 2007-01-0472.

Pui, D. Y. H. “Experimental Study of Diffusion Charging of Aerosols.” Ph.D> diss., University of Minnesota, 1976.

Pui, D. Y. H., Fruin, S., and McMurry, P. H. “Unipolar Diffusion Charging of Ultrafine Aerosols.” *Aerosol Sci. Technol.* 1988, 8, 173–187.

Pyykönen, J., Miettinen, M., Sippula, O., Leskinen, A., Raunemaa, T., and Jokiniemi, J. “Nucleation in a Perforated Tube Dilutor.” *J. Aerosol Sci.* 2007, 38, 172–191.

Qi, C., Asbach, C., Shin, W. G., Fissan, H., and Pui, D. Y. H. “The Effect of Particle Pre-existing Charge on Unipolar Charging and its Implication on Electrical Aerosol Measurements.” *Aerosol Sci. Technol*. 2009, 43, 232–240.

Ragazzi, R., and Nelson, K. “The Impact of 10% Ethanol Blended Fuel on Exhaust Emissions of Tier 0 and Tier 1 Light Duty Vehicles at 35 Degrees.” CO DPHE 1999, available from www.cdphe.state.co.us/ap/down/oxyfuelstudy.pdf.

Rakovec, N., Olenski, B., Maney, M. and Bower, G. R. “Improving Upon Best Available Technology: A Clean Flex Fuel Snowmobile.” *SAE Tech. Pap. Ser*. 2008, 2008-32-0049.

Rao, V. D., White, J. E., Wade, W. R., Aimone, M. G., and Cikanek, H. A. “Advanced Techniques For Thermal And Catalytic Diesel Particulate Trap Regeneration.” *SAE Tech. Pap. Ser.* 1985, 850014.

Rissler, J., Abdulhamid, H., Pagels, J., Nilsson, P., Sanati, M., and Boghard, M. “Mass-Mobility Relationship of Soot Generator and Diesel Soot.” Karlsruhe, Germany: European Aerosol Conference, 2009. Abstract T083A09.

Ristimäki, J., Vaaraslahti, K., Lappi, M., and Keskinen, J. “Hydrocarbon Condensation in Heavy-Duty Diesel Exhaust.” *Environ. Sci. Technol.* 2007, 41, 6397–6402.

Ristimäki, J., Virtanen, A., Marjamäki, M., Rostedt, A., and Keskinen, J. “On-line Measurement of Size Distribution and Effective Density of Submicron Aerosol Particles.” *J. Aerosol Sci*. 2002, 33, 1541–1557.

Robertson, W. H., Herner, J. D., Ayala, A., and Durbin, T. D. (2007). “Investigation of the Application of the European PMP Method to Clean Heavy Duty Vehicles.” Detroit, MI: Proceedings of 2007 Diesel Engine-Efficiency and Emissions Research Conference, 2007.

Rogak, S. N., and Flagan, R. C. “Bipolar Diffusion Charging of Spheres and Agglomerate Aerosol Particles.” *J. Aerosol Sci*. 1992, 23, 693–710.

Rönkkö, T., Virtanen, A., Kannosto, J., Keskinen, J., Lappi, M., and Pirjola, L. “Nucleation Mode Particles with a Nonvolatile Core in the Exhaust of a Heavy Duty Diesel Vehicle.” *Environ. Sci. Technol*. 2007, *41,* 6384–6389.

Rönkkö, T., Virtanen, A., Kannosto, J., Keskinen, J., Pirjola, L., and Lappi, M. “Effect of Dilution Conditions and Driving Parameters on Nucleation Mode Particles in Diesel Exhaust: Laboratory and on-Road Study.” *Atmos. Environ.* 2006, 40, 2893–2901.

Rostedt, A., Marjamäki, M., and Keskinen, J. “Modification of ELPI to Measure Mean Particle Effective Density in Real Time.” *J. Aerosol Sci*. 2009, 40, 823–831.

Sakurai, H. “Primary Standard for Aerosol Particle Number Concentration.” Zurich, Switzerland: 11th ETH Conference on Combustion Generated Nanoparticles, August, 2007.

Sakurai, H., Tobias, H. J., Park, K., Zarling, D., Docherty, K. S., Kittelson, D. B., McMurry, P. H., and Ziemann, P. J. “On-Line Measurements of Diesel Nanoparticle Composition and Volatility.” *Atmos. Environ*. 2003, 37, 1199–1210.

Sakurai, H., Saito, K., and Ehara, K. “Japan's National Standard for Aerosol Particle Number Concentration.” Orlando, FL: 27th AAAR Conference, 2008.

Sakurai, H., Tobias H.J ., Park, K., Zarling, D., Docherty, K. S., Kittelson, D. B., McMurry, P. H., and Ziemann, P. J. “On-line Measurements of Diesel Nanoparticle Composition and Volatility.” *Atmos. Environ.* 2003, 37, 1199–1210.

Salvat, O., Marez, P., and Belot, G. “Passenger Car Serial Application of a Particulate Filter System on a Common Rail Direct Injection Diesel Engine.” *SAE Tech. Pap. Ser.* 2000, 2000-01-0473.

Samet, J. M., Dominici, F., Curriero, F. C., Coursac, I., and Zeger, S. L. “Fine Particulate Air Pollution and Mortality in 20 U.S. Cities, 1987–1994.” *N. Engl. J. Med.* 2000, 343, 1742–1749.

Sandbach, E. “Volatile Particle Remover Calibration Procedure. Working Chapter No. GRPE-PMP-18-118th.” Geneva: PMP Working Group Meeting, January 10, 2007.

Schauer, J. J., Kleeman, M. J., Cass, G. R., and Simoneit, B. R. T. “Measurement of Emission from Air Pollution Sources. 2. C1 through C30 Organic Compounds from Medium Duty Diesel Trucks.” *Environ Sci. Technol.* 1999, 33, 1578–1587.

Schmid, O., Karg, E., Hagen, D. E., Whitefield, P. D., and Ferron G. A. “On the Effective Density of Non-spherical Particles as Derived from Combined Measurements of Aerodynamic and Mobility Equivalent Size.” *J. Aerosol Sci.* 2007, *38*, 431–443

Schmitz, T., Hassel, D., and Weber, F-J. “Determination of VOC-Components in the Exhaust of Gasoline and Diesel Passenger Cars.” *Atmos. Environ.* 2000, 34, 4639–4647.

Schneider, E. W., and Blossfeld, D. H. “Method for Measurement of Piston Ring Rotation in an Operating Engine.” *SAE Tech. Pap. Ser.* 1990, 900224.

Schneider, E. W., Blossfeld, D. H., Lechman, D. C., Hill, R. F., Reising, R. F., and Brevick, J. E. “Effect of Cylinder Bore Out-of-Roundness on Piston Ring Rotation and Engine Oil Consumption.” *SAE Tech. Pap. Ser.* 1993, 930796.

Schneider, J., Hock, N., Weimer, S., Borrmann, S., Kirchner, U., Vogt, R., and Scheer, V. “Nucleation particles in Diesel exhaust: Composition Inferred from in Situ Mass Spectrometric Analysis.” *Environ Sci. Technol.* 2005, 39, 6153–6161.

Seaton, A. “Particles in the Air: the Enigma of Urban Air Pollution.” *J. Royal Soc. Med.* 1996, 89, 604-607.

Seaton, A., and Macnee, W., Donaldson, K., Godden, D”. Particulate Air-Pollution and Acute Health-Effects.” *Lancet* 1995, 345, 176–178.

Seinfeld, J. H., and Pandis, S. N. Atmospheric Chemistry and Physics, from Air Pollution to Climate Change. New York: John Wiley, 1998.

Shakhashiri, B. Z. Chemical Demonstrations: A Handbook for Teachers of Chemistry. Vol. 1. Madison, WI: University of Wisconsin Press, 1983.

Shi, J. P., and Harrison, R. M. “Investigation of Ultrafine Particle Formation During Diesel Exhaust Dilution.” *Environ. Sci. Technol.* 1999, 33, 3730–3736.

Shin, W. G. Pui, D. Y. H., Fissan, H., Neumann, S., and Trampe, "A. Calibration and Numerical Simulation of Nanoparticle Surface Area Monitor (TSI model 3550 NSAM)." *J. Nanoparticle Res*. 2007, 9, 61–69.

Shin, W. G., Qi, C., Wang, J., Fissan, H., and Pui, D. Y. H. "The Effect of Dielectric Constant of Materials on Unipolar Diffusion Charging of Nanoparticles." *J. Aerosol Sci*. 2009, 40, 463 – 468.

Siegl, W. O., Hammerle, R. H., Herrmann, H. M., Wenclawiak, B. W., and Luers-Jongen, B. "Organic Emissions Profile for a Light-Duty Diesel Vehicle." *Atmospheric Environment*, 1999, 33, 797–805.

Siegmann, K., and Siegmann, H. C. "Fast and Reliable 'In Situ' Evaluation of Particles and Their Surfaces with Special Reference to Diesel Exhaust." *SAE Tech. Pap. Ser.* 2000, 2000-01-1995.

Skillas, G., Künzel, S., Burtscher, H., Baltensperger, U., and Siegman, K. "High Fractal-Like Dimension of Diesel Soot Agglomerates." *J. Aerosol Sci.* 1998, 29, 411–419.

Smith, O. I. "Fundamentals of Soot Formation in Flames with Applications to Diesel Engine Particulate Emissions." *Prog. Energy Combust. Sci.* 1981, 7, 229–291.

Sommers, J. H. "Automotive Sulfate Emission Data." *Environ Health Per.* 1975, 10, 15-28.

Spears, M. 2005. “Overview of U.S. EPA’s Programs Utilizing PEMS with a Focus on Compliance Testing. Office of Transportation and Air Quality, U.S. Environmental Protection Agency. available at http://transportenv07.jrc.it/pdf/C/C_1_19_Spears_M_PEMS%20in%20On-road%20and%20Off-road%20legislation%20in%20US.pdf.

Spears, M. An Emissions-Assisted Maintenance Procedure for Diesel-Powered Equipment. University of Minnesota Contract report #: USDI/1432 C0369004

Spears, M. EPA’s Recent Heavy-Duty Diesel PM Test Procedure Changes and Other PM Mass Measurement Research, Washington, DC: U.S. Government Printing Office:, 2002.

Spears, M., “Overview of U.S. EPA’s Programs Utilizing PEMS with a Focus on Compliance Testing.” 2005. available at : http://transportenv07.jrc.it/pdf/C/C_1_19_Spears_M_PEMS%20in%20On-road%20and%20Off-road%20legislation%20in%20US.pdf.

Stenitzer, M. Nano Particle Formation in the Exhaust of Internal Combustion Engines. *Diplom-Ingenieurs, Technischen UniversitätWien, Fakultät für Maschinenbau* (in English), 2003.

Stratakis, G. A., Konstantas, G. S., and Stamatelos, A. M. “Experimental Investigation of the Role of Soot Volatile Organic Fraction in the Regeneration of Diesel Filters.” *Proc. IMechE Part D, J. Automotive Engineering*. 2003, 217, 307–317.

Swanson, J., and Kittelson, D. B. “Factors Influencing Mass Collected During 2007 Diesel PM Filter Sampling.” *SAE Int. J. Fuels Lubr.* 2009, 2:1, 718–729.

Swanson, J., and Kittelson, D. B. “Fundamental Investigation of Methods for “Solid” Particle Measurements.” Minneapolis, MN: 28th AAAR Conference, Oct 26–30th, 2009.

Swanson, J., Kittelson, D. B., and Dallas, A. “An Alternative Method for Generating Ultra-Clean Dilution Air for Engine Emissions Measurements.” *SAE Tech. Pap. Ser.* 2007, 2007-01-1111.

Swanson, J., Kittelson, D. B., and Dikken, D. “Uncertainties in Filter Mass Measurements Made to Determine Compliance with the 2007 Diesel PM Standard.” *SAE Int. J. Fuels Lubr.* 2009a, 2:1, 708–717.

Swanson, J., Kittelson, D.B, Watts, W., Gladis, D., and Twigg, M. “Influence of Storage and Release on Particle Emissions from New and Used CRTs.” *Atmos. Environ*. 2009b, 43, 3998–4004.

Thoss, J. E., and Clark, W., “Effects of Diesel Fuel Sulfur Level on Performance of a Continuously Regenerating Diesel Particulate Filter and Catalyzed Particulate Filter. *SAE Tech. Pap. Ser.* 2000, 2000-01-1875.

Tilman, D., Hill, J., and Lehman, C. “Carbon-Negative Biofuels from Low-Input High Diversity Grassland Biomass.” *Science* 2006, 314, 1598–1600.

Tobias, H . J., Beving, D. E., Ziemann, P. J., Sakurai, H., Zuk, M., McMurry, P. H., Zarling, D., Waytulonis, R., and Kittelson, D. B. “Chemical Analysis of Diesel Engine Nanoparticles Using a Nano-DMA/Thermal Desorption Particle Beam Mass Spectrometer.” *Environ. Sci. Technol.* 2001, 35, 2233–2243.

"Tracktek 100 Racing Fuel," accessed September 13, 2004. Information available from http://www.cpchem.com/bl/specchem/en-us/Pages/TrackTekFuelsApplications.aspx.

Truex, T. J., Pierson, W. R., and McKee, D. E., "Sulfate in Diesel Exhaust." *Environ. Sci. Technol.* 1980, 14, 1118–1121.

Twigg, M. V., and Wilkins, A. J. J. "Autocatalysts—Past, Present, Future." in: Structured Catalysts and Reactors, ed. A, Cybulski, et al., 91–120. New York: Marcel Dekker, Inc., 1998.

Ullman, T. L., and Human, D. M. "Fuel and Maladjustment Effects on Emissions from a Diesel Bus Engine." *SAE Tech. Pap. Ser.* 1991, 910735.

Ullman, T. L., and Hare, C. T. "Influence of Maladjustment on Emissions from Two Heavy-Duty Diesel Bus Engines." *SAE Tech. Pap. Ser.* 1984, 840416.

Ulrich, A., Wicher, A., Figi, R., Heeb, N., Neubert, T., Czerwinski, J., and Mayer, A., "Identification of Storage and Release Effects of SOx Artifacts on DPF Systems After Long Term Use." Zurich, Switzerland: 11th ETH Conference on Combustion Generated Nanoparticles, August, 2007.

Vaaraslahti, K., Keskinen, J., Giechaskiel, B., Solla, A., Murtonen, T., and Vesala, H. "Effect of Lubricant on the Formation of Heavy-Duty Diesel Exhaust Nanoparticles." *Environ. Sci. Technol.* 2005, 39, 8497–8504.

Vaaraslahti, K., Virtanen, A., Ristimaki, J., and Keskinen, J. "Nucleation Mode Formation in Heavy-Duty Diesel Exhaust with and Without a Particulate Filter." *Environ. Sci. Technol.* 2004, 38, 4884–4890.

Van Gulijk, C., Marijnissen, J. C. M., Makkee, M., Moulijn, J. A., and Schmidt-Ott, A. "Measuring Diesel Soot with a Scanning Mobility Particle Sizer and an Electrical Low-Pressure Impactor: Performance Assessment with a Model for Fractal-Like Aggregates." *J. Aerosol Sci.* 2004, 35, 633–655.

Van Setten, B. A. A. L., Makkee., M., and Moulijn, J. A. "The Science and Technology of Catalytic Diesel Particulate Filters." *Catal. Rev.* 2001, 43, 489–564.

Veranth, J. M., Gelein, R., and Oberdörster, G. (2003). "Vaporization – Condensation Generator of Ultrafine Hydrocarbon Particulate Matter for Inhalation Toxicology Studies." *Aerosol Science Technol.* 37, 603–609.

Virtanen, A., Ristimaki, J., and Keskinen, J. "Method for Measuring Effective Density and Fractal Dimension of Aerosol Aggregates." *Aerosol Sci. Technol.* 2004, 35, 1251–1274.

Virtanen, A., Ristimaki, J., Marjamaki, M., Vaaraslahti, K., Keskinen, J., and Lappi, M. "Effective Density of Diesel Exhaust Particles as a Function of Size." *SAE Tech. Pap. Ser.* 2002, 2002-01-0056.

Vogt, R., Scheer, V., Casati, R., and Benter, T. "On-Road Measurement of Particle Emissions in the Exhaust Plume of a Diesel Passenger Car." *Environ. Sci. Technol.* 2003, 37, 4070–4076.

Vouitsis, E., Ntziachristos, L., and Samaras, Z. "Modeling of Diesel Exhaust Aerosol during Laboratory Sampling." *Atmos. Environ.* 2005, 39, 1335–1245.

Vouitsis, E., Ntziachristos, L., and Samaras, Z. “Particulate Matter Mass Measurements for Low Emitting Diesel Powered Vehicles: What’s Next?” *Progr. Energy Combust. Sci.* 2003, 29, 635–672.

Vouitsis, E., Ntziachristos, L., and Samaras, Z. “Theoretical Investigation of Nucleation Mode Formation Downstream of Diesel After-Treatment Devices.” *Aerosol and Air Quality Research* 2008, 8, 37–53.

Wall, J. C., Shimpi, S. A., and Yu, M. L. “Fuel Sulfur Reduction for Control of Diesel Particulate Emissions.” *SAE Tech. Pap. Ser.* 1987, 872139.

Wang, Xiaolong with TSI Incorporated. Interview by author, 2008.

Wang, J., Shin, W. G., Mertler, M., Sachweh, B., Fissan, H., and Pui, D. Y. H. “Measurement of Nanoparticle Agglomerates by Combined Measurement of Electrical Mobility and Unipolar Charging Properties.” *Aerosol Sci. Technol.* 2010, 44, 97-108.

Wang, S. C., and Flagen, R. C. “Scanning Electrical Mobility Spectrometer.” *Aerosol Sci. Technol.* 1990, 12, 230–240.

Wehner, B., Philippin, S., and Wiedensohler, A. “Design and Calibration of a Thermodenuder with an Improved Heating Unit to Measure the Size-Dependent Volatile Fraction of Aerosol Particles.” *J. Aerosol Sci.* 2002, 33, 1087–1093.

Wei, Q., Kittelson, D. B., and Watts, W. F. “Single-Stage Dilution Tunnel Design.” *SAE Tech. Pap. Ser.* 2001, 2001-01-0207.

Wei, Q., Kittelson, D. B., and Watts, W. F. “Single-Stage Dilution Tunnel Performance.” *SAE Tech. Pap. Ser.* 2001, 2001-01-0201.

Wen, H. Y., Reischl, G. P., and Kasper, G. “Bipolar Diffusion Charging of Fibrous Aerosol Particles—I. Charging Theory.” *J Aerosol Sci.* 1984, 15, 89–101.

Whitby, K. T., Cantrell, B.K. *Atmospheric aerosols: Characteristics and measurement.* Washington, DC: Proceedings of the International Conference on Environmental Sensing and Assessment (ICESA). Institute of Electrical and Electronic Engineers (IEEE). IEEE #75-CH 1004-1, ICESA chapter 29-1, 1976.

Whitby, K. T., Husar, R. B., and Liu, B. Y. H. “The Aerosol Size Distribution of Los Angeles Smog.” *J. Colloid Interface Sci.* 1972, 39, 211.

White, H. J. Particle “Charging in Electrostatic Precipitation.”, *Transactions of Am. Inst. of Elect.l Engineers*, 1951, 70, 1186–1191.

Wittmaack, K. “Search of the Most Relevant Parameter for Quantifying Lung Inflammatory Response to Nanoparticle Exposure: Particle Number, Surface Area or What?” *Environ. Health Perspect.* 2007, 115, 187–194.

Wong, C. P., Chan, T. L., and Leung, C. W. “Characterization of Diesel Exhaust Particle Number and Size Distributions Using Mini-Dilution Tunnel and Ejector-Diluter Measurement Techniques.” *Atmos. Environ.* 2003, 37, 4435–4446.

World Health Organization, International Program on Chemical Safety. Diesel Fuel and Exhaust Emissions. Geneva, Switzerland: WHO, 1996.

Wyatt, M., Manning, W. A., Roth, S. A., D'Aniello, M. J., Andersson, E. S., and Fredholm, S. C. G. "The Design of Flow-Through Diesel Oxidation Catalysts." *SAE Tech. Pap. Ser.* 1993, 930130.

Yu, J. Z., Xu, J., and Yang, H. "Charring Characteristics of Atmospheric Organic Particulate Matter in Thermal Analysis." *Environ. Sci. Technol*, 2002, 36, 754-761.

Zeller, W. Fuel Additive and Engine Operation Effects on Diesel Soot Emissions. Bureau of Mines IC, 9238, 1992, 5–9.

Zhang, X., and McMurry, P. H." Evaporative Loss of Fine Particulate Nitrates During Sampling." *Atmos. Environ.* 1992, 26, 3305–3312.

Zhang X., and McMurry, P. H. "Theoretical Analysis of Evaporative Losses from Impactor and Filter Deposits." *Atmos. Environ.* 1987, 21, 1779–1789.

Zhang X., and McMurry, P. H. "Theoretical Analysis of Evaporative Losses of Adsorbed or Absorbed Species during Atmospheric Aerosol Sampling." *Environ Sci. Technol.* 1991, 25, 456–459.

Zielinska, B., Sagebiel, J., Arnott, W. P., Rogers, C. F., Kelly, K. E., Wagner, D. A., Lightly, J. S., Sarofim, A. F., and Palmer, G. "Phase and Size Distribution of Polycyclic Aromatic Hydrocarbons in Diesel and Gasoline Vehicle Emissions." *Environ. Sci. Technol.* 2004, 38, 2557–2567.

Appendix

This appendix contains copies of the copyright permissions granted by the owners of the journals where this work is published.

Powered by RIGHTSLINK

Home | Account Info | Help

Title: Influence of storage and release on particle emissions from new and used CRTs

Author: Jacob J. Swanson, David B. Kittelson, Winthrop F. Watts, David D. Gladis, Martyn V. Twigg

Publication: Atmospheric Environment

Publisher: Elsevier

Date: August 2009

Copyright © 2009, Elsevier

Logged in as: Jacob Swanson

LOGOUT

Order Completed

Thank you very much for your order.

This is a License Agreement between Jacob J Swanson ("You") and Elsevier ("Elsevier"). The license consists of your order details, the terms and conditions provided by Elsevier, and the payment terms and conditions.

Get the printable license.

License Number	2473100920604
License date	Jul 20, 2010
Licensed content publisher	Elsevier
Licensed content publication	Atmospheric Environment
Licensed content title	Influence of storage and release on particle emissions from new and used CRTs
Licensed content author	Jacob J. Swanson, David B. Kittelson, Winthrop F. Watts, David D. Gladis, Martyn V. Twigg
Licensed content date	August 2009
Licensed content volume number	43
Licensed content issue number	26
Number of pages	7
Type of Use	reuse in a thesis/dissertation
Requestor type	Not specified
Intended publisher of new work	n/a
Portion	full article
Format	both print and electronic
Are you the author of this Elsevier article?	Yes
Will you be translating?	No
Order reference number	
Title of your thesis/dissertation	Development and Application of Emerging Engine Exhaust Aerosol Measurement Technologies
Expected completion date	Aug 2010
Estimated size (number of pages)	200
Elsevier VAT number	GB 494 6272 12
Permissions price	0.00 USD
Value added tax 0.0%	0.00 USD
Total	0.00 USD

ORDER MORE... | CLOSE WINDOW

Jacob Swanson

From: Nancy Bernheisel [nbernheisel@awma.org]
Sent: Tuesday, July 20, 2010 6:33 AM
To: Jacob Swanson
Subject: RE: copyrights

Dear Jacob,

Thank you for your message. Yes, you may use the paper or parts of its content in your thesis. Will this e-mail message suffice, or do you need for me to print permission on our letterhead?

Best wishes,

Nancy

Nancy E. Bernheisel
Publications Coordinator
Air & Waste Management Association
One Gateway Center, Third Floor
420 Fort Duquesne Blvd.
Pittsburgh, PA 15222 USA
P: +1-412-232-3444, ext. 3179
F: +1-412-232-3450
email: nbernheisel@awma.org

From: Jacob Swanson [mailto:jswanson@me.umn.edu]
Sent: Mon 7/19/2010 7:34 PM
To: Nancy Bernheisel
Subject: RE: copyrights

Dear Nancy,

I am the corresponding author of a paper that will be published by your Journal. Material from this paper is included as part of my PhD thesis completed at the University of Minnesota with a degree conferral date of August 2010. I plan to delay publication of the thesis for 1 year.

Swanson, J. Kittelson, D.; Pui, D.; Watts, W. (2010). Alternatives to the Gravimetric Method for Quantification Of Diesel Particulate Matter Near the Lower Level Of Detection. In press, *J. Air Waste Management Association*.

I am requesting that you authorize the use of graphs and text included in the above paper in my thesis, which will eventually be published and distributed by the University of Minnesota Library in print and online through ProQuest (http://www.proquest.com/en-US/). In order for ProQuest to achieve the thesis, they must receive written confirmation that the copyright owner (you) must be aware that ProQuest may supply single copies of my thesis on demand.

Thank you for considering my request and authorizing publication.

Jacob Swanson

Jacob Swanson

From: copyright [copyright@sae.org]
Sent: Thursday, July 29, 2010 3:36 PM
To: jswanson@me.umn.edu
Subject: RE: sae copyright question

Dear Jacob,
Thank you for your correspondence requesting permission to reprint SAE material from SAE paper number 2009-01-1400 – which you co-authored – in your doctoral dissertation for the University of Minnesota.

Permission is hereby granted, and subject to the following conditions:

- Permission is for this one time use only. New requests are required for further use of the material.
- The following credit statement must appear below the figures: "Reprinted with permission from SAE Paper No. 2009-01-1400* © 2009* SAE International." *please insert the paper number and **year of publication

Permission is for this one-time use only, and does not cover any third party copyrighted work which may appear in the material requested.

Again, thank you for contacting SAE for this permission.

Regards,
Terri Kelly
Intellectual Property Rights Administrator
SAE International
Phone: 001.724.772.4095; Fax: 001.724.776.9765
E-mail: terri@sae.org

Jacob Swanson

From: Peter Williams [peterw@pepublishing.com]
Sent: Monday, August 09, 2010 9:49 AM
To: jswanson@me.umn.edu
Cc: Gertrud Gustafsson
Subject: RE: Permission to use material from JAUTO1164

Dear Jacob

Thank you for your Email of 20th July detailed below seeking permission to use material published in one of our journals within your PhD Thesis that will be made available by ProQuest. I am pleased to inform you that permission is granted.

Could you please ensure that a full reference is given:

Article	Nanoparticle measurements used to detect an engine oil control ring failure
Authors	Swanson, J.; Ragatz, A.; Kittelson, D.; Watts, W.; Winsor, R.
Journal	Proceedings of the Institution of Mechanical Engineers, Part D: Journal of Automobile Engineering
Publisher	Professional Engineering Publishing
ISSN	0954-4070 (Print) 2041-2991 (Online)
Issue	Volume 223, Number 8 / 2009
DOI	10.1243/09544070JAUTO1164
Pages	1071-1076

With kind regards

Peter

Peter Williams
Academic Director
Professional Engineering Publishing
1 Birdcage Walk
London SW1H 9JJ
UK
Registered in England No. 1103638

Tel: +44 (0) 207 304 6852
Fax: +44 (0) 207 304 6926
EMail: peterw@pepublishing.com
Web: www.pepublishing.com

From: Jacob Swanson [mailto:jswanson@me.umn.edu]
Sent: 20 July 2010 00:40